

Tracer Studies of River-Groundwater Interaction under Hydropeaking Conditions

Dissertation Markus W. Fette



Dissertation ETH Nr. 16103

Tracer Studies of River-Groundwater Interaction under Hydropeaking Conditions

A dissertation submitted to the

SWISS FEDERAL INSTITUTE OF TECHNOLOGY ZURICH

for the degree of

DOCTOR OF NATURAL SCIENCES

presented by

MARKUS WOLFGANG FETTE

Dipl.-Ing., University of Stuttgart

born on September 12, 1973

citizen of Germany

accepted on recommendation of

Prof. Dr. Bernhard Wehrli, examiner

Prof. Dr. Pierre Perrochet, co-examiner

Prof. Dr. Anton Schleiss, co-examiner

Zürich 2005

Was den Menschen angeht, so glaube ich an das Individuum,
nicht aber an den Individualismus.

Was die Natur angeht, so glaube ich an das sinnvolle Zusammenspiel ihrer
schöpferischen und zerstörerischen Kräfte, nicht aber an deren Manipulierbarkeit zu
eigennützigen Zwecken.

Was die Musik angeht, so glaube ich an die Töne, nicht aber an die Noten.

Was das Geld angeht, so glaube ich an Münzen und Noten und sonst an gar nichts.

Was die ewige Liebe angeht, so glaube ich an ihre fortdauernde Renovierbarkeit,
nicht aber an ihre Konservierbarkeit.

Was die Religion angeht, so glaube ich an Erfahrung, nicht aber an Überzeugungen.

Was Antworten auf die letzten Fragen angeht, so glaube ich an den Gedankenstrich,
nicht aber an das Ausrufezeichen.

Balts Nill, Musiker (Stiller Has)

T Table of Contents

T.	Table of Contents	7
A.	Acknowledgements	10
S.	Summary	12
Z	Zusammenfassung	13
1.	Introduction.....	14
1.1	River Rehabilitation	15
1.2	Hydropeaking.....	16
1.3	Outline and Goal of the Thesis	18
2.	Stable Isotope Analysis.....	20
2.1	General	21
2.2	The δ -Notation.....	21
2.3	Fractionation During Evaporation and Condensation of Meteoric Water.....	22
2.4	Meteoric Water Line.....	23
2.5	Geological interactions	25
2.5.1	Analytical Procedures	26
2.5.2	Accuracy and Precision	28

3.	Assessing River- Groundwater Exchange in the Regulated Rhone River (Switzerland) Using Stable Isotopes and Geochemical Tracers.....	31
3.1	Abstract	32
3.2	Introduction	32
3.3	Methods and Study Site	35
3.4	Results.....	37
3.4.1	Seasonality of Isotopic Signature in Precipitation	37
3.4.2	Seasonality in River Water	40
3.4.3	River- Groundwater Interactions.....	42
3.5	Discussion	46
3.5.1	Seasonality of Tracer Signals	46
3.5.2	$\delta^{18}\text{O}$ as a Tracer for the Altitude of Water Origin	47
3.5.3	Identification of Lateral Groundwater Sources in the Alluvial Floodplain ...	49
3.5.4	What is the Longitudinal Travel Velocity of the Groundwater	51
3.6	Conclusions	52
3.7	Acknowledgement	54
4.	Temperature Fluctuations as Natural Tracer for River-Groundwater Interaction under Hydropeaking Conditions....	55
4.1	Abstract	56
4.2	Key Words.....	56
4.3	Introduction.....	56
4.3.1	Hydropower and Channelling of Rivers	57
4.4	Methods	59
4.4.1	Study Area	59
4.4.2	Acquisition and Evaluation of Data	62
4.4.3	Interpretation of Data	63
4.5	Results.....	66
4.5.1	Time Series of Water Level and Temperature	66
4.5.2	Hydraulic Conductivity Estimated from Temperature Data	73
4.6	Discussion	75
4.6.1	Comparison with literature data	75
4.6.2	Clogging	77

4.6.3	Temporal and Spatial Variations in Clogging	78
4.6.4	Quantification of the Seepage Rate	80
4.6.5	Consequences for River Rehabilitation.....	81
4.7	Conclusion	81
4.8	Acknowledgement	82
5.	Seasonal Variability in the Chemical and Isotopic Composition of Alluvial Groundwaters in Rhone Valley	83
5.1	Introduction	84
5.2	Study Site and Methods	85
5.3	Results and Discussion	88
5.3.1	Lateral Recharge	88
5.3.2	Spatial Variability in Aquifer Geochemistry	90
5.3.3	Temporal Variations in Aquifer Geochemistry	92
5.3.4	Conclusion	94
6.	Ecological Consequences of Hydropeaking.....	96
6.1	A Difficult Situation for Ecology	97
6.1.1	Reduced Benthic Diversity due to Hydropeaking Effects.....	98
6.1.2	Fish Ecology	99
6.2	Possible Solutions	100
6.2.1	Longitudinal	100
6.2.2	Lateral.....	101
6.2.3	Possible Solutions	102
6.3	Conclusion and Outlook	103
R.	References	106
C.	Curriculum Vitae	109
A.	Annexes	113

A

Acknowledgements

Herzlichen Dank an alle Menschen in Kastanienbaum und Dübendorf, denen ich neben einer wundervollen Zeit noch viel mehr zu verdanken habe. Ich habe vieles lernen dürfen – insbesondere von.....

Christian Dinkel, der mir beigebracht hat, wie man einen anständigen „Topf“ kocht. *Hans- Jürg Meng*, der mich von Linux überzeugen wollte, aber auch immer da war, wenn mal wieder ein „Blue Screen“ im Kopf das Leben schwer gemacht hat. *Michael Schurter*, der für die Buchführung meines Plus- und Minuskontos verantwortlich war und mich gelehrt hat, Schäkel immer fest anzuziehen. *Scott Tiegs* und *Daniel McGinnis*, die immer spontan für Korrekturen meines Englisch zur Stelle standen und mir die Erkenntnis brachten, dass ich Germanismen wohl nie loswerden werde. *Christine Weber*, die fast nie „bärndütsch“ mit mir reden wollte (äuä...), aber mir die Fische bei der Erstellung einer Publikation näher gebracht hat. *Bia Mbuemo*, der mir gezeigt hat, wie man Plankton fängt und Fische ausnimmt (halleluja...) und *Daniel Steiner*, der mir den Umgang mit Illustrator gelehrt hat. Nicht zu vergessen *Francisco Vazquez*, der mir immer wieder erklären musste, welche Gasflasche denn nun ein Links- und wann ein Rechtsgewinde hat und *Ruth Stierli*, die mir alles beigebracht hat, was es denn sonst so im Labor braucht. Bedanken möchte ich mich weiterhin bei *Sabine Siblinger*, die Audi A4 auch im Schlaf sagen kann und bei *Alois Zwysig* der mich hautnah spüren liess, wie es denn dem alten Tell damals so bei Föhnsturm am Axen gegangen sein muss. Den Tanz auf dem Parkett hat mir *Kornelia Konrad* beigebracht und vieles für den Tanz im Leben konnte ich von *André Steffen* lernen. *Doris Hohmann* brachte mir bei, was „E3“ im Display des pH-Messgerätes bedeutet und dass es hierzulande keinen Unterschied zwischen „lehren“ und „lernen“ gibt.

Von *Johny Wüest* habe ich gelernt, dass der „Tessiner Hof“ in Zürich früher die „Räuberhöhle“ war. Unterricht in Navigation bekam ich von *Armin Peter*, der als Kapitän des Rhone-Thur Projektes erfolgreich alle Untiefen umschiffte hat. Und natürlich herzlichen Dank an *Luzia Fuchs*, *Eliane Scharmin* (Erdbeertörtle...), *Patricia Achleitner* und *Michelle Sidler*, die Crew im Sekretariat in Kastanienbaum, die bis in alle Ewigkeit einen Ehrenplatz in meiner Nachtgebetsliste haben werden. Danke an *Jürg Beer* und *Eduard Höhn* für die unermüdliche Hilfe beim Schreiben meiner Publikationen. Das gleiche gilt auch für *Rolf Kipfer*, der mich zudem den Zusammenhang zwischen Magnetismus und Rinderzucht gelehrt hat und *Olaf Cirpka* für Einblicke in die tiefen Sphären der Grundwassermodellierung.

Anton Schleiss sowie *Pierre Perrochet* danke ich sehr für die Übernahme des Co-Referates. Von meinem Doktorvater *Bernhard Wehrli* durfte ich lernen, dass man auch Professor sein kann, obwohl man "eigentlich gar keiner sein will". Er ist einer der wenigen Menschen in meinem Leben, von denen ich weiss, dass ich genau hinhören muss, wenn er etwas sagt, weil es meist Substanz, Gehalt und Tiefe hat – und das nicht nur in fachlicher Hinsicht... Er besticht dadurch, was er zwischen den Zeilen sagt und nicht durch Sätze, an deren Ende ein Ausrufezeichen steht. Leider waren seine Zeitfenster für mich immer nur sehr klein bemessen und meist von Zeitnot und Hast geprägt. Aber die Erkenntnis, die ich durch ihn erlangt habe, dass es viel wichtiger ist, mit seinem Unwissen gestaltend umzugehen, als scheinbare Sicherheit vorzugaukeln, die wird mir sicherlich niemand mehr nehmen können. Bernhard, herzlicher Dank für die Zeit mit Dir.

Nicht zuletzt möchte ich *meiner Familie* für alle Unterstützung danken. *LU*, *Sigma* und *Cargo* für die Erkenntnis, dass Passstrassen und Luzern von oben ja soooo schön sein können und wie man auch grossen Menschen mit kleinen Dingen unglaublich Freude machen kann. Meine grösste Dankbarkeit gilt aber Lucia, von der ich lernen durfte, dass das zu zweit alles viel mehr Spass macht.

S Summary

The morphology of the Rhone River in the Swiss Canton Wallis is heavily impacted by river training works. The hydrological regime is altered by hydropeaking caused by the tailwaters of huge storage hydropower plants. The Rhone River is currently subject of a river rehabilitation project emphasizing sustainable planning, considering not only social and political concerns, but also ecological values. The planned rehabilitation of the Rhone River will trigger large scale river training works such as the dislocation of levees and a subsequent modification of the geomorphology of the river. If rehabilitation measures increase the permeability of the river bed, the water level in the adjacent aquifer could rise and potentially damage the valley's agriculture, infrastructure and public drinking water supply.

Quantification of river- groundwater exchange is therefore of major importance. Using stable isotopes, sulphate and temperature as tracers, the investigation showed only limited exchange in the hydropower affected lower reach of the Rhone River between Sion and Martigny. Results taken from the chemical parameters revealed slight exfiltration during the winter months ranging between 0 and $5 \text{ m}^3\text{s}^{-1}$. Temperature as a physical parameter focused specifically on the direct river- groundwater interface. Using the amplitude and time shift of temperature maxima and minima in the groundwater with respect to the river allowed the characterisation of the recharge process in summer. Specific infiltration rates for the seasonal investigations vary between $0.1 \text{ m d}^{-1} < q < 1.8 \text{ m d}^{-1}$ and range near the lower end of the known infiltration rates of Swiss rivers which were reported to be between 0.05 m d^{-1} for River Töss and 3 m d^{-1} for River Rhine. Specific infiltration rates under hydropeaking conditions, characterizing the intermittently flooded part of the river bed vary between $0.6 \text{ m d}^{-1} < q < 3.1 \text{ m d}^{-1}$.

Zusammenfassung

Die Rhone im Schweizer Kanton Wallis wurde durch die flussbauliche Hochwasserschutzmassnahmen der Ersten und Zweiten Rhonekorrektur begradigt und kanalisiert, was zu starken morphologischen Beeinträchtigungen führte. Das hydrologische Regime ist durch den Betrieb von Speicherkraftwerken und den dadurch hervorgehobenen Schwall- und Sunkerscheinungen in der Rhone ebenfalls stark beeinträchtigt. Die Hochwasser der letzten Jahre machten erneute Mängel deutlich, die zur 3. Korrektur der Rhone führen werden. Dabei wird insbesondere Wert auf die nachhaltige Umsetzung der durchzuführenden Hochwasserschutzmassnahmen gelegt werden, welche auch sozioökonomische und ökologische Werte mit einbeziehen. Umfassende Umstrukturierungen, wie beispielsweise die Verlagerung von Hochwasserschutzdämmen, werden die geplanten Revitalisierungsarbeiten begleiten. Dadurch verursachte Veränderungen in der Durchlässigkeit der Deichbauwerke können unerwünschte Folgen nach sich ziehen. Mögliche Szenarien bestehen beispielsweise in einer Erhöhung des Grundwasserspiegels - mit unerwünschten Folgen für die Landwirtschaft, Infrastruktur und Trinkwassergewinnung.

Kenntnis der Fluss- Grundwasserinteraktion ist daher von grosser Wichtigkeit. Durch die Verwendung stabiler Isotope, Sulfat und Temperatur als Tracer konnte eine nur sehr eingeschränkte Interaktion zwischen Fluss und Grundwasser im Bereich zwischen Sion und Martigny nachgewiesen werden. Die Ergebnisse der geochemischen Untersuchungen deuten auf leichte Winterexfiltration zwischen 0 und $5 \text{ m}^3 \text{ s}^{-1}$ hin, wohingegen die Auswertungen der Sommertemperaturganglinien leichte Infiltration im Bereich zwischen 0.08 m d^{-1} und 0.95 m d^{-1} belegen. Unter Schwall- und Sunkeinfluss scheint sich diese Infiltrationsrate auf Werte zwischen 0.4 m d^{-1} und 3.2 m d^{-1} zu erhöhen.

1

Introduction

Ignace Mariétan describes the Rhone River in his book « Le Rhone – La lutte contre l'eau en Wallis » from the source to Lake Geneva. He will guide through this thesis introducing each chapter with a citation.

“ A sa sortie du glacier du Rhône, notre jeune fleuve est déjà vigoureux. Il s'élanche joyeusement sur la petite auge glacière de Gletsch, se précipite sur des rochers jusqu'à Oberwald, en vrai torrent de montagne.” (Mariétan, 1953)

For centuries, inhabitants of the Rhone valley have been at the mercy of a river that has produced massive flood events and caused great human loss and material damage. After the dramatic flood of 1860, it was decided to force the river into a rigid structure, which was realized by the (1863 – 1894) and second (1930-1960) Rhone correction. Recent floods revealed major deficiencies in flood protection along the river corridor, which led to the proposed third regulation project of the Rhone (Fette et al., 2002). The project (consecutively called 3RC) will run for 30 years with a total budget of approximately 900 million Swiss Francs. It aims at improving flood protection and enhancing the ecological aspects along the Rhone River.

1.1 River Rehabilitation

At the time of the first and the second Rhone correction, “canalizing” was the method of controlling a river to protect the plain against flooding. This allowed the construction of infrastructure near the river, saved agricultural land and reduced diseases like malaria, which had their origin in the swamp areas of the floodplain. The management of the sediment transport was another goal that had to be faced. Today, river management emphasizes sustainable planning, considering not only economic, social and political concerns, but also ecological values (Willi, 2001). The rehabilitation potential in alpine river systems is very high. In Switzerland, approximately 22'500 km of streams and rivers (37 % of the total stream/ river length) are artificially deepened, dammed, straightened or flow in culverts and require rehabilitation (Peter et al., 2005). To investigate the social and ecological aspects of river rehabilitation projects and to develop tools for success evaluation after the completion, the 3RC in its initial stages is accompanied by an interdisciplinary research project, the “Rhone-Thur Project”.

In contrast to the pragmatic goals of rehabilitation, restoration, i.e., “reverting the river back to a natural, or at least near natural, state” (Bradshaw, 1996), will, to a large extent, remain wishful thinking (Figure 1).

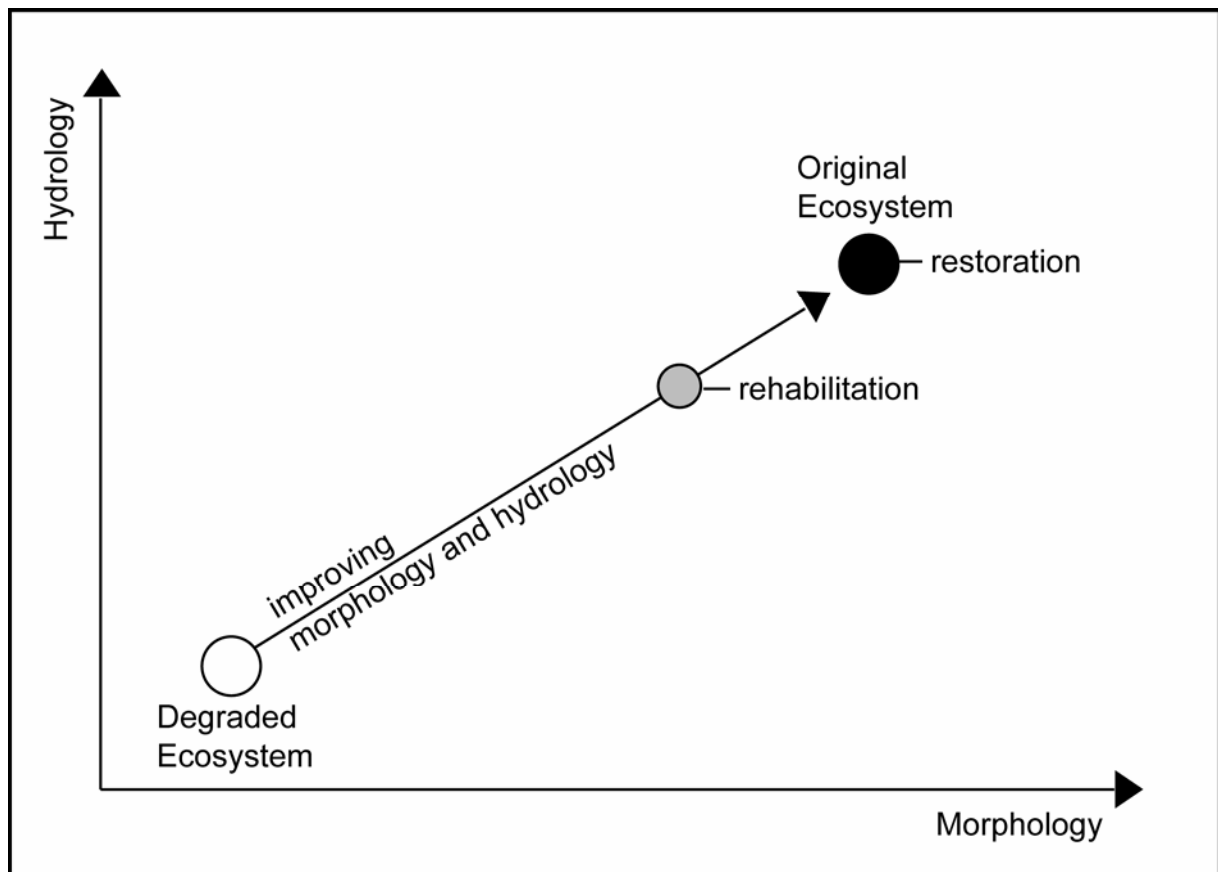


Figure 1: Rehabilitation vs. restoration in remediation work (modified from Bradshaw, 1996)

Instead, the 3RC will rehabilitate selected stretches of the river (Fette et al., 2002) with a focus on the improvement of both, the hydrological and morphological situation of the Rhone River.

As an engineering measure for preventing incision, widenings show significant morphological and hydraulic potentials for the development of gravel banks, channel braiding, increased variability of depth, velocity and ecotone shoreline, and a more diverse aquatic habitat (Truffer et al., 2003). Widenings therefore represent an appropriate rehabilitation measure in formerly braided systems.

1.2 Hydropeaking

The upper Rhone valley upstreams of lake Geneva is called the “Wallis”. Due to its topographical characteristics, it is ideally suited for the operation of hydroelectric power plants.



Figure 2: Variation of water level due to hydropeaking in the Rhone River. The snowline indicates the daily maximum water level fluctuation. Photo: Armin Peter.

Over the last century, several impressive projects were realized, including the largest hydroelectric power plant in Switzerland, Cleuson-Dixence, with an installed capacity of 1200 MW, equivalent to that of a nuclear power plant. The plants produce electricity on demand, brought online almost exclusively during periods of peak consumption. Water from high alpine reservoirs created by dams is transferred by pressure tunnels and shafts to the powerhouses situated in a distance of 5 to 20 km and up to 2000 m lower in the Rhone valley. Hydrological problems result, when the water is discharged into the Rhone where it causes sharp transient fluctuations in water level. This phenomenon is called hydropeaking (Figure 2) and can cause daily variation of water level as much as one meter in some locations (Fette et al., 2002; Meile et al., 2005).

1.3 Outline and Goal of the Thesis

Agricultural uses of the floodplain, river correction and intensive hydroelectric power generation have deprived the River Rhone of its natural character. The construction of dams for flood protection resulted in a narrow channel with limited connection to the adjacent floodplain (Baumann and Meile, 2004; Fette, submitted).

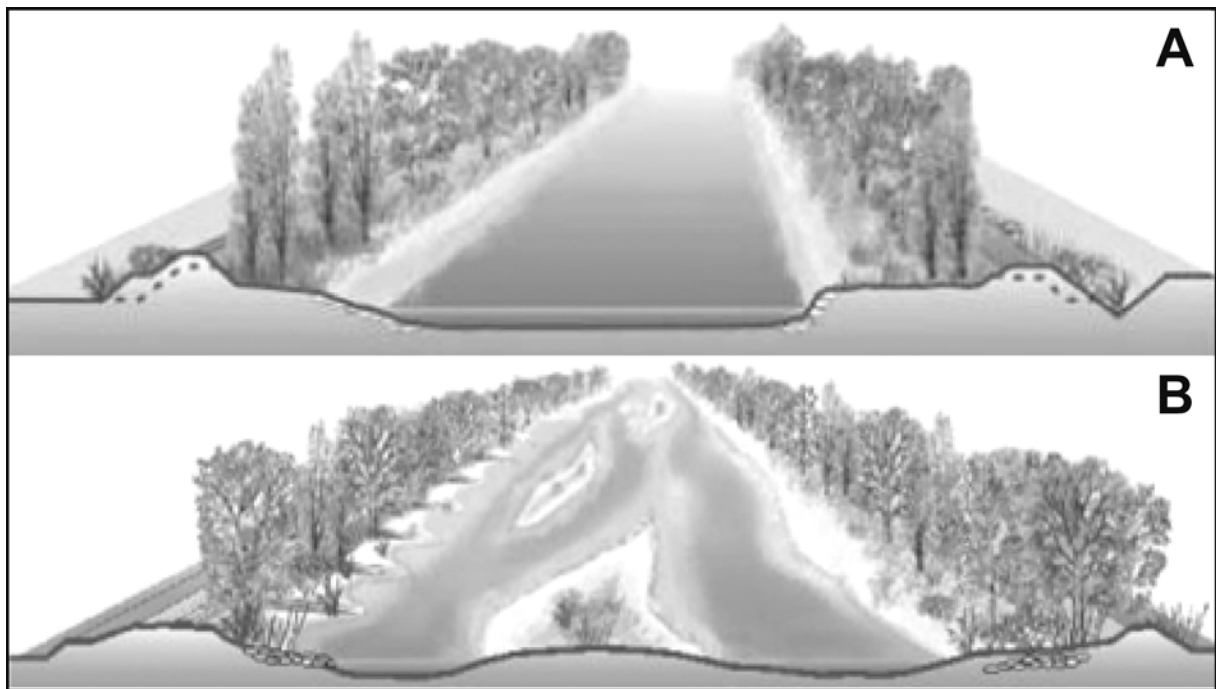


Figure 3: Sketch of river reaches before (A) and after (B) rehabilitation measures. Taken from Canton Wallis (2000)

The planned rehabilitation of the Rhone River will trigger large scale river training works such as the dislocation of levees and a subsequent modification of the geomorphology of the river (Figure 3). If rehabilitation measures increase the permeability of the river bed, the water level in the adjacent aquifer could rise and potentially damage the valley's agriculture, infrastructure (Greco, 2001) and public drinking water supply (Regli et al., 2004). According to an upcoming legislation in Switzerland, the groundwater shall be protected by preventing water pollution and implementing well capture zones (Regli et al., 2003) which will lead to serious trade-offs between groundwater protection and nature conservation.

As a methodological introduction, **Chapter 2** provides background information on stable isotope analysis. Basic features of the hydrology in the Rhone valley are outlined in **Chapter 3**. The study in Chapter 3 reports methods and data to trace the water masses of the high - altitude reservoirs to the river and further into the groundwater. The alpine environment as well as the geological situation in the Rhone valley is well suited for applying a combination of stable isotope analysis with geochemical measurements (SO_4^{2-}) and transient tracer techniques (T^3He). **Chapter 4** discusses a method to trace river-groundwater interaction under hydropeaking conditions. The seasonal temperature regime in the Rhone River is superposed by regular diurnal and weekly temperature variations. These conditions are well suited to apply cross-correlation techniques between temperature records of the river water and adjacent groundwater. The results reveal intense clogging of the permanently flooded riverbed and more permeable conditions in the zones intermittently flooded by hydropower conditions. While **Chapter 5** expands these findings by analyzing seasonal records of geochemical tracers in a wider transect of observation wells in the floodplain **Chapter 6** outlines the importance of the findings for ecological processes.

River-groundwater interaction between the Rhone River and the adjacent groundwater is currently limited caused by clogging of the interface between the river and the adjacent groundwater (Baumann and Meile, 2004; Fette, submitted). The upcoming rehabilitations will create large riverbanks, but in order to secure the valley bottom, flood protection dams will be needed, even if the river corridor is broadened. This work investigated and tested methods to describe river-groundwater interaction using stable isotopes and temperature migration as natural tracers. The results helped to characterize and quantify the infiltration behaviour between surface water and groundwater under different hydrological conditions comprising seasonal and diurnal fluctuations of the water level in the Rhone River. Further research on this topic should focus on the application of the method on other river systems under similar hydrological and morphological conditions to test and improve the proposed techniques.

2

Stable Isotope Analysis

“On se représente sans peine l’attitude des hommes devant le fleuve: ses grandes crues assez fréquentes devaient leur donner l’impression que le Rhône est une force contre laquelle l’homme ne peut rien.” (Mariétan, 1953)

2.1 General

Isotopes are atoms of the same element that differ in their number of neutrons. The possible stable isotopic compositions of water are: H_2^{16}O , HD^{16}O , D_2^{16}O , H_2^{17}O , HD^{17}O , D_2^{17}O , H_2^{18}O , HD^{18}O and D_2^{18}O . All of these occur in natural waters but, considering the natural abundances of the isotopes, it is only the molecules of H_2^{16}O , H_2^{18}O , HD^{16}O and H_2^{17}O which are of analytical relevance (Gat and Gonfiantini, 1981). Differences among the stable isotopic content in snow, rainfall, surface waters and groundwater are therefore used for estimating e.g. flow paths and became an important subset of the larger hydrological use of isotopic tracers.

2.2 The δ -Notation

Measuring an absolute isotope ratio or abundance is not easily done and requires sophisticated mass spectrometric equipment. Further, measuring this ratio on a routine basis would lead to tremendous problems in comparing data sets from different laboratories. However, the main interest is focused on the comparison of the relative variations in stable isotope concentrations rather than absolute abundance. By measuring a known reference on the same machine at the same time, comparison of a sample to a reference is possible. Isotopic concentrations are then expressed as the difference between the measured ratios of the sample and a reference over the measured ratio of the reference. This procedure cancels instrumental measurement errors. This difference is designated by the letter δ and is defined as follows:

$$\delta = \frac{R_{\text{sample}} - R_{\text{reference}}}{R_{\text{reference}}} \quad (\text{Eq 1})$$

where the R's are, in the case of water, for example the $R_{\text{H}_2\text{O}} = \frac{\text{H}_2^{18}\text{O}}{\text{H}_2^{16}\text{O}}$ isotope

concentration ratios. R is always defined as the ratio of the heavier to the lighter isotope.

Obviously, positive values show the samples to be enriched in the heavy isotope with respect to the reference. As the differences between the samples and references are usually quite small, it is convenient to express the delta values in per mille, i.e.

$$\delta(\text{‰}) = \delta * 1000 \quad (\text{Eq 2})$$

For $\delta^{18}\text{O}$, the normal reference standard is VSMOW, an acronym for Vienna Standard Mean Ocean Water. In practice, each laboratory has its own standard or set of standards which have been calibrated against VSMOW. During the measurement, the isotopic ratio of the sample is compared to that of the laboratory standard and the result is recalculated to the SMOW scale (Drever, 1997). Other standards are Greenland Ice Sheet Precipitation (GISP) and Standard Light Antarctic Precipitation (SLAP)

2.3 Fractionation During Evaporation and Condensation of Meteoric Water

The primary source of the water of the hydrological cycle is the ocean, which has an average isotopic composition of 0 ‰ relative to the VSMOW scale. In general, the water vapour of the atmosphere is depleted in heavy stable isotopes because of their lower vapour pressure. Mass dependent rate constants or equilibration processes in the water cycle cause isotopic fractionation in nature. In general, rain becomes progressively lighter in δD and $\delta^{18}\text{O}$ from the equator towards the poles, and from lower to higher altitudes (Drever, 1997). This isotopic differentiation is commonly described by the fractionation factor α . In the case of evaporation processes it is defined as the ratio of the isotope content of the liquid (solid) and of the vapour phase (Araguas-Araguas et al., 2000). When water undergoes evaporation, the residual water becomes progressively enriched in the heavier isotopes ^{18}O and D. This leads to different global and local effects:

Continental Effect: The mean $\delta^{18}\text{O}$ and $\delta^2\text{H}$ composition of precipitation is generally lower at continental stations than at coastal and island stations of comparable

altitudes. However, the gradient for continental stations varies considerably from area to area and during the different seasons of a year (Gat and Gonfiantini, 1981). Snow accumulating on the ice sheets of Greenland and Antarctica – from atmospheric water vapour – is heavily depleted in ^{18}O . Enriched waters are mainly found in warm regions.

Altitude Effect: In a given region, the δ -values of precipitation at higher altitudes will be more negative. The magnitude of the effect depends on local climate and topography, with gradients in $\delta^{18}\text{O}$ of between $0.15 < \delta^{18}\text{O} < 0.5 \text{ ‰ (100m)}^{-1}$ and gradients in $\delta^2\text{H}$ of between $\sim 1.5 < \delta^2\text{H} < 4 \text{ ‰ (100m)}^{-1}$ (Drever, 1997).

2.4 Meteoric Water Line

In general, the water vapour of the atmosphere is depleted in ^{18}O since H_2^{16}O has a higher vapour pressure than H_2^{18}O . The analogous depletion of deuterium in meteoric water leads to a linear relationship between $\delta^{18}\text{O}$ and δD , because H_2O has also a higher water pressure than HDO . This difference accounts for deuterium enrichment in water which is about 8 times greater than for ^{18}O . This relationship is observed in the δD and $\delta^{18}\text{O}$ values of the global precipitation and is called the global meteoric water line GMWL. It may be written as (Craig, 1961):

$$\delta\text{D} = 8\delta^{18}\text{O} + 10 \quad (\text{Eq 3})$$

Craig's line is only global in application, and is actually an average of many Local Meteoric Water Lines (LMWL) which differ in both slope and y-intercept from the global line due to varying climatic and geographic parameters (Clark and Fritz, 1999).

Lakes and other water bodies which lose water by evaporation (which was condensed before from precipitation) are enriched in heavy isotopes. Plotting their isotopic composition in the same $\delta^{18}\text{O}$ - $\delta^2\text{H}$ diagram results in a deviation from the Meteoric Water Line with lower slope which depends largely on the relative humidity.

Low humidities will lead to maximized evaporation resulting in low slopes of the meteoric water line (Figure 4, point A).

The y-intercept value of 10 in the GMWL equation is called Deuterium Excess. The term only applies to the calculated y- intercept for sets of meteoric data “fitted” to a slope of 8. Deuterium excess correlates poorly with latitude but depends primarily on the mean relative humidity of the air masses formed above the ocean surface (Merlivat and Jouzel, 1979). The fact that the intercept of the GMWL is greater than zero means that the line does not intersect with $\delta^{18}\text{O} = \delta^2\text{H} = 0$, which is the composition of average ocean water (VSMOW). It does not intersect the composition of the ocean, the source of most of the water vapour that produces rain, because of the ~ 10 ‰ kinetic enrichment in ^2H of vapour evaporating from the ocean at an average humidity of 85 % (Kendall and Caldwell, 1998).

Values for deuterium intercept range from 0 to 20 ‰ but can vary regionally due to variations in humidity, wind speed and sea surface temperature during primary evaporation (Clark and Fritz, 1999). High values for deuterium intercept are found especially under low relative humidity conditions. The Mediterranean Sea is the classic example of a reservoir producing water vapour with a high deuterium excess, owing to the modification of continental air masses by interaction with the warm Mediterranean sea (Gat and Carmi, 1970). Values lower than 10 ‰ may be indicative of secondary evaporation processes (Figure 4, point A), for instance, the evaporation of falling raindrops in a warm and dry atmosphere (Araguas-Araguas et al., 2000) which is characteristic for inland stations (Figure 4, point B).

Pearson (1991) found that the GMWL is within the 95% confidence interval of the line calculated for northern Switzerland (Figure 4). The slope of the LMWL for Northern Switzerland is lower than 8 and therefore indicative for secondary evaporation processes during rainfall which are characteristic for innercontinental stations.

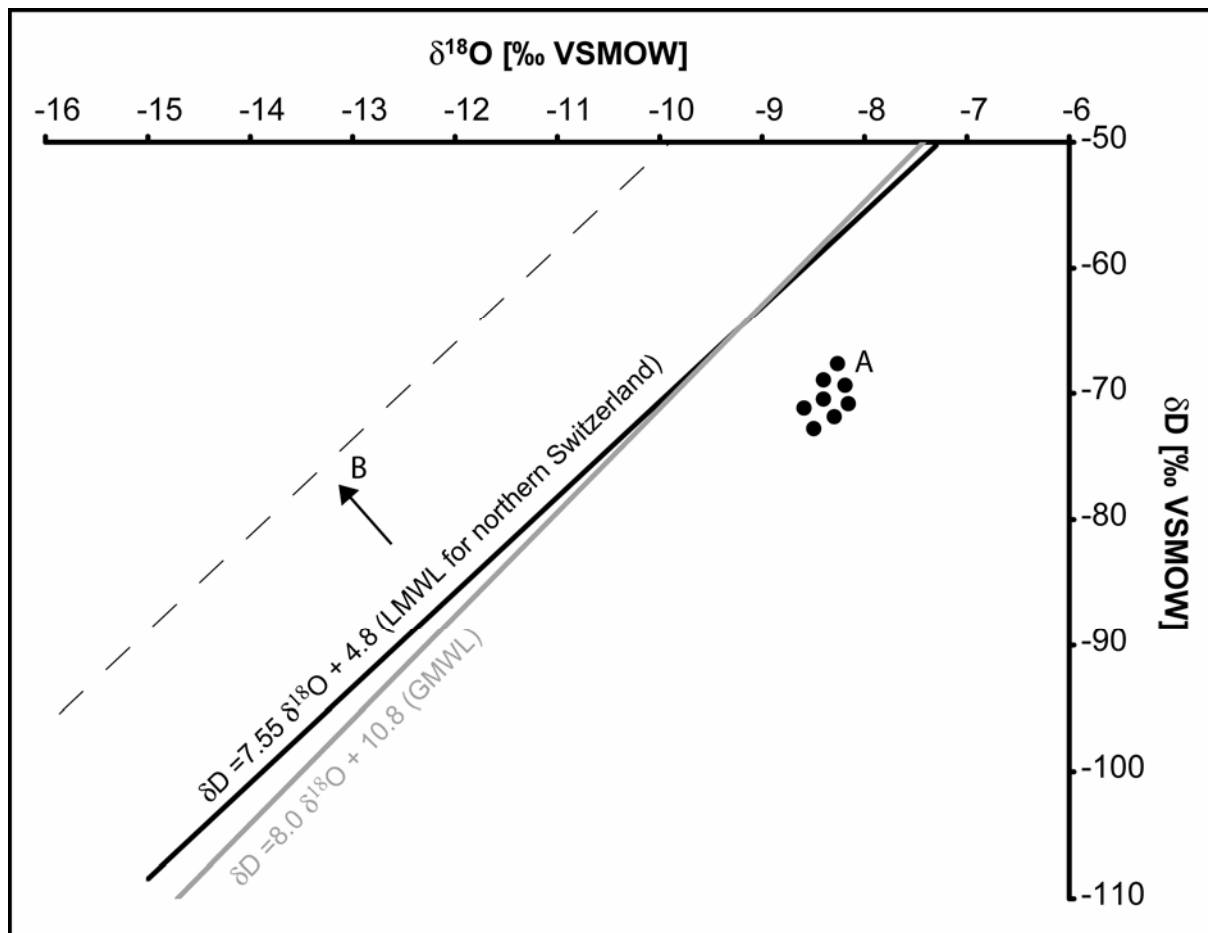


Figure 4: Global Meteoric Water Line GMWL as defined from Craig (1961) in comparison to the Local Meteoric Water Line for northern Switzerland (adapted from Pearson (1991)). (A) water samples affected by secondary evaporation processes are characterized by enrichment in stable isotopes resulting in a decreasing slope of the meteoric water line. (B) the isotopic water line shifted parallel to the LMWL for northern Switzerland is indicative for a decrease in deuterium intercept.

The investigation of meteoric water lines shows that local lines can differ significantly from the global line. A local line can reflect the origin of the water vapour and subsequent modifications by secondary processes of re-evaporation and mixing. Any detailed study of groundwater recharge using stable isotopes of water should therefore attempt to define as best as possible the LMWL

2.5 Geological Interactions

Analyses of δD and $\delta^{18}O$ can also be used to identify the probable source of groundwater. In general, δD is unaffected by reactions with aquifer materials at low

temperatures, whereas $\delta^{18}\text{O}$ exchanges with CaCO_3 in limestone aquifers which may cause a significant shift towards heavier $\delta^{18}\text{O}$ values. If the isotopic composition of groundwater plots close to the meteoric water line in a position similar to the present day precipitation in the same region, the water is almost certainly meteoric. If it has the same δD value as local precipitation, but slightly heavier $\delta^{18}\text{O}$ values, the water is probably meteoric but has been affected by exchange with calcite (Drever, 1997).

2.5.1 Analytical Procedures

Samples for stable isotope analysis were collected in 250 mL polyethylene-bottles, and were analyzed at the EAWAG Kastanienbaum for $^{18}\text{O}/^{16}\text{O}$ and D/H ratios by a Micromass Isoprime isotope ratio mass spectrometer (IRMS) in continuous flow mode. The continuous flow inlet comprises of two silica capillaries which continuously carry helium gas into the ion source of the mass spectrometer. These two capillaries draw helium at two open splits, one fed from a reference gas injector system, the other from the sample gas bench. At user defined times, the reference gas injector pulses rectangular peaks of pure reference gas into the ion source. The sample gases exiting from a gas chromatographic column are carried by a stream of helium towards the sample open split, from where the sample gases also enter the ion source (Micromass, 2003).

To analyse the sample gas its molecules must be ionized, formed into a beam, accelerated by an electric field, and finally detected (Figure 5). These four processes take place in the analyzer of a mass spectrometer, which consists of three separate sections: source, flight tube and collector. Ionisation, beam formation and acceleration all occur in the source, magnetic deflection takes place in the flight tube and in the collector, ions are detected by a Faraday cup.

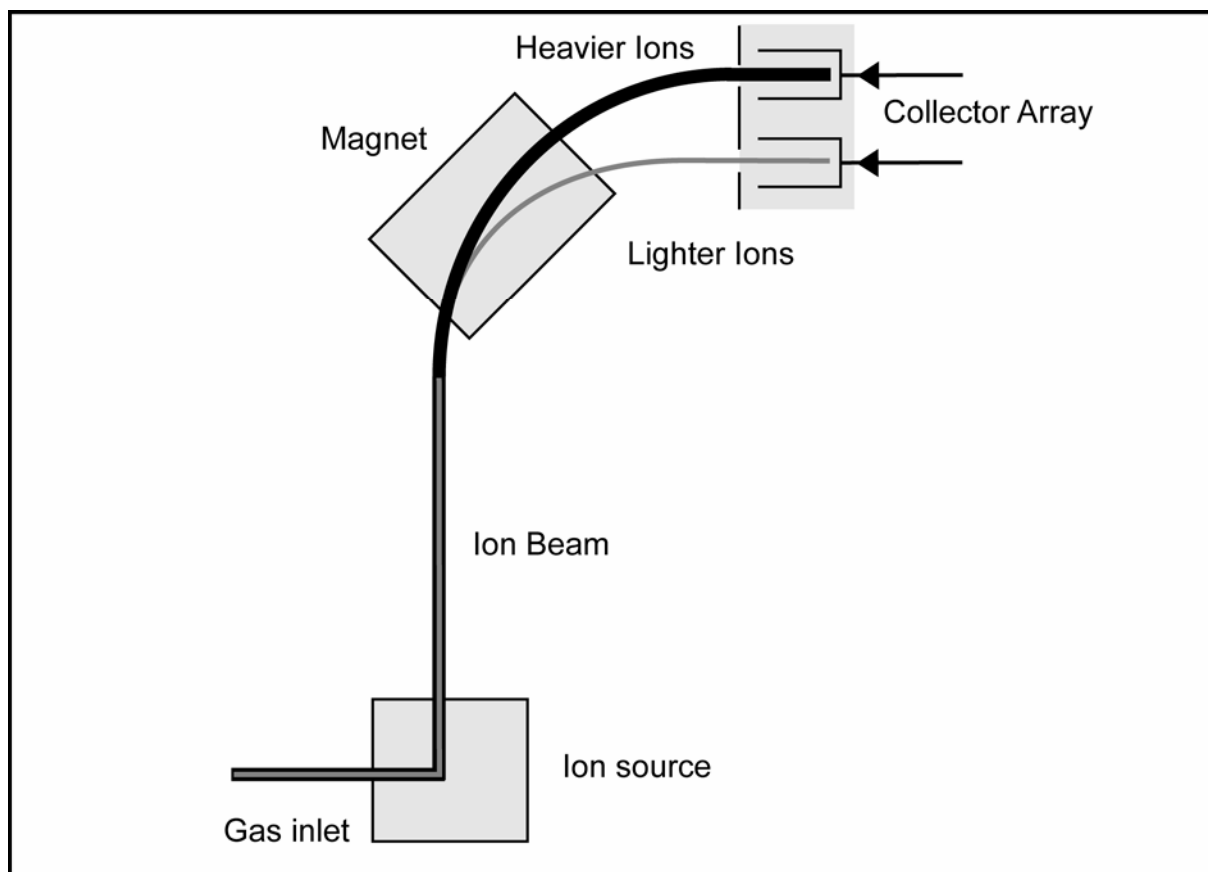


Figure 5: The mass spectrometer used for isotopic analysis generally comprises three basic sections: an ion source, a mass analyzer and an ion collector.

The ion current from the cup is proportional to the number of incident ions and hence to the partial pressure of the corresponding isotopes in the molecular species of sample gas (Micromass, 2003).

For every-day use, the primary reference material like VSMOW of the International Atomic Energy Agency (IAEA) can not be used because of its limited quantity.

Therefore secondary laboratory standards were collected from different locations: outflow of the Grande-Dixence Hydropower plant (EA-1), snow-melt water from the Jungfrauoch (EA-2) and water from the North Sea (EA-3).

For calibration we ran 10 sample vials for each primary standard VSMOW, GISP and SLAP in a sequence with the internal standards EA-1, EA-2 and EA-3. All sample vials were measured in triplets accounting for 180 ^{18}O measurements altogether. For “day-trading” sample measurements, we ran 2 sample vials of each internal standard

in a sequence with the groundwater samples. On these daily measurements, all vials were measured in triplets.

The ^{18}O and D abundance in water samples is measured in the headspace of glass vials with a $\text{CO}_2\text{--He}$ and $\text{H}_2\text{--He}$ mixture atmosphere. With a syringe, 200 μL of water sample were injected in 10 mL glass vials topped with a septum.

After water injection, the glass vials are filled with the headspace gases and equilibrated at 40°C inside a Gilson auto sampler rack. The samples are allowed to equilibrate for at least 12 h (Werner and Brand, 2001). The isotopic fractionation occurring in the isotope transfer reaction from liquid water to gaseous CO_2 is highly temperature dependent. The reference material is subjected to the same reaction conditions. The isotopic fractionation cancels as long as the chemical nature of sample and reference is closely comparable (Werner and Brand, 2001).

Following equilibration, the sample vial is analyzed by piercing the septum with a double wall needle. The needle has a feed (He) and an exit (sample CO_2 in He). The sample gas flows through an injection loop from which the GC run is started (Werner and Brand, 2001). The measurement sequence is then started, following a rigid protocol with a dedicated loading list. After five sample measurements the three standards EA-1, EA-2 and EA-3 are analyzed again.

2.5.2 Accuracy and Precision

Accuracy describes how close a measurement corresponds to the true value which is given by the predefined IAEA-standards respectively the internal standards (EA-1, EA-2, EA-3). Accuracy of measurements is generally determined by intercomparison programmes between different laboratories, which were, however, no subject of the current investigations, because comparison with external data was not attempted.

Precision indicates how close several measurements of the same sample correspond to each other and can be improved by repeated measurements. Internal standards

EA-1, EA-2 and EA-3 were used to monitor precision because of their regularly repeated analysis after five normal water samples. Two results were drawn from this proceeding:

1. The consistent quality of the internal standards was assured by means of control charts (Figure 6). The measuring results of the internal standard analysis were listed in a scatter plot. Any contamination in the internal standard would show up as a step. Slow, long term alteration (e.g. evaporative loss in water standards) would be indicated as a drift (Werner and Brand, 2001). During the first 10 samples increased scattering was observed whereas the following results showed none of these effects.
2. The internal precision of the measurements of each batch was determined by measuring each sample vial in triplets. Precision has been determined by averaging the first and third measurement of each sample before subtracting the value of the second sample. The resulting precision, unique for each internal standard is listed in Table 1 (line 3 and 6). EA-1 and EA-3 show precision values for $\delta^{18}\text{O}$ of 0.18 ‰ and 0.2 ‰, respectively, which are comparable to the IRMS specifications given by the manufacturer (precision for $\delta^{18}\text{O}$ = 0.2 ‰). Precision of EA-2 ($\delta^{18}\text{O}$ = 0.39 ‰) is significantly worse and declines the precision, averaged over EA-1, EA-2 and EA-3 to $\delta^{18}\text{O}$ = 0.26 ‰.

sample number m	$\delta^{18}\text{O}$	EA1 [‰]	EA2 [‰]	EA3 [‰]
m < 10	Average	-15.21	-9.48	-0.67
	Precision	0.18	0.38	0.20
m > 10	Average	-15.19	-9.46	-0.67
	Precision	0.18	0.39	0.20

Table 1: Statistical data for internal standards EA1, EA2 and EA3. Precision has been calculated by averaging the first and the third measurement of each sample before subtracting the value of the second sample. For $m < 10$, the signal is unstable. Therefore, precision was calculated separately for $m < 10$ and $m > 10$.

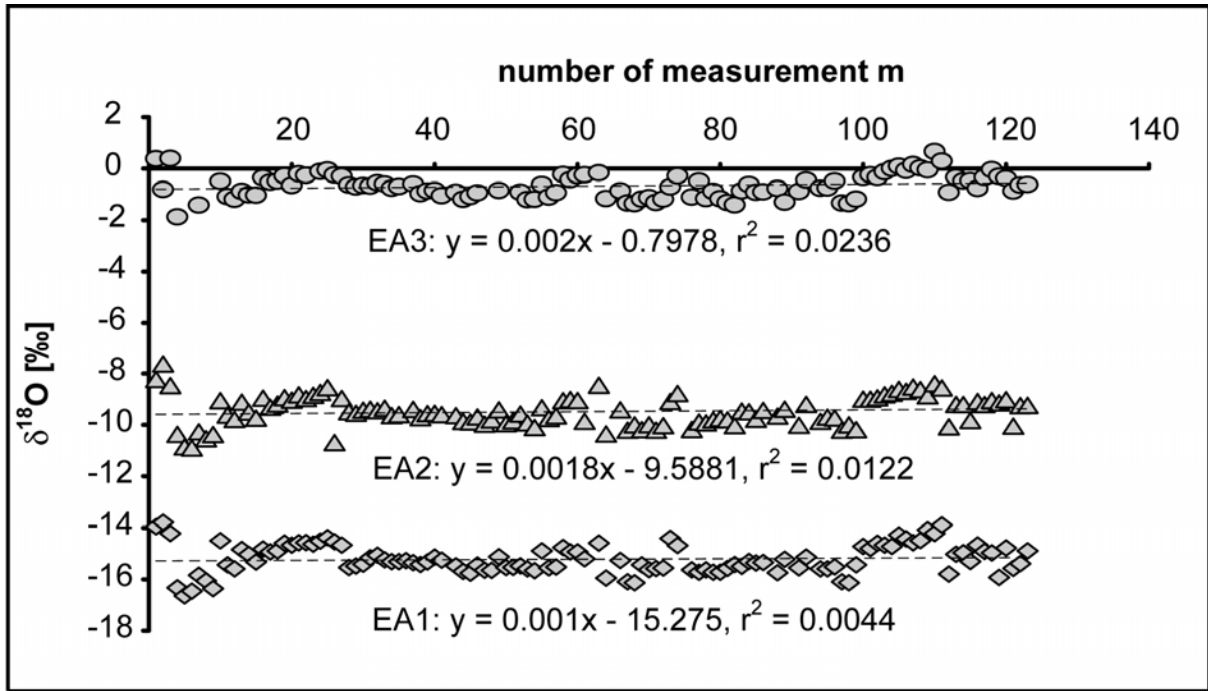


Figure 6: Evolution of internal standard measurements m for $\delta^{18}\text{O}$ with number of samples. Trend lines are plotted as dashed lines. Three of each internal standard were measured together in one batch within 24 h. Time between the batches varied between one day and three weeks, maximum.

3

Assessing River- Groundwater Exchange in the Regulated Rhone River (Switzerland) Using Stable Isotopes and Geochemical Tracers

Fette, M., Kipfer, R., Schubert, C.J., Hoehn, E., Wehrli, B.

Slightly adapted from the version published in:

Journal for Applied Geochemistry (2005), **20** (4), 701-712

“Dès le début du 19^e siècle la lutte se précise, (...). On discute du rétrécissement du lit du fleuve, de sa correction, on constate la difficulté d’entretenir les ponts et les routes. (...) Cependant une lente évolution se produisait dans les esprits, le terrain se préparait pour entreprendre le grand œuvre.” (Mariétan, 1953)

3.1 Abstract

Modern flood protection projects are often combined with measures for river rehabilitation, which enlarge the river bed to improve the flow capacity during peak discharge and to reduce bed erosion. For the planning of such projects it is essential to quantify the river-groundwater exchange. To address this question in the highly regulated upper Rhone River basin, we combined stable isotope techniques with geochemical and transient tracers. The $\delta^{18}\text{O}$ signal in precipitation is decreasing towards more negative values with a slope of 0.34 ‰ per 100 m altitude, precipitation during winter was about 5.5 ‰ more negative than in summer. Since in winter about 55 % of the water in river Rhone comes from high alpine hydropower reservoirs with a known $\delta^{18}\text{O}$ value, this isotopic signature provides direct information of the source region and the seasonality in samples from groundwater wells. On a spatial scale sulphate measurements help to constrain groundwater components, because the tributaries and groundwater sources south of the Rhone are rich in SO_4^{2-} with concentrations of more than 12 mM in spring water. In winter the Rhone water reaches concentrations of up to 1.5 mM, and during snowmelt in summer, this value drops below 0.5 mM. Finally the transient tracer $\text{T}/^3\text{He}$ is used to estimate groundwater inflow in deep gravel pits and to calculate an average travel velocity in the alluvial aquifer of about 1.7 km yr^{-1} .

3.2 Introduction

Alpine rivers are in the midst of a major transition. Over the last two centuries most river systems in Central Europe were regulated to improve flood protection. About 50 years ago, large storage hydropower schemes were developed in the Alps, Scandinavia, the Pacific Northwest and in other mountain regions, which strongly modified the hydrological regimes (Bratrich et al., 2004; Gleick, 2003). Today, the signs that global warming affects the water storage capacity of mountain glaciers (Haeberli et al., 1999), the seasonal precipitation patterns (Schmidli et al., 2002) and the frequency of extreme events (Frei and Schar, 2001) demand a re-evaluation of flood protection measures. In addition, the environmental impacts of hydropower use have received intense public attention. As a consequence, the upgrading and renewal of flood protection dykes in the lowlands is now often combined with river

rehabilitation projects, which should allow a more natural morphology and provide habitats for riparian ecosystems (Naiman et al., 1992). Because river rehabilitation often involves removing or dislocating dams and dykes, the planning and design of such projects under the boundary conditions of both flood protection and hydropower schemes should be based on a detailed knowledge of river-groundwater interactions. In this work we test and apply a combination of different tracer methods to track river-groundwater interactions in the canalized Rhone River receiving the outflow of several large hydropower reservoirs.

Located in the central Alps of south-western Switzerland, the Rhone River originates from the Rhone glacier at an altitude of 1763 m above sea level (ASL) and drains the catchment of the Canton Wallis into Lake Geneva. The basin area is 5220 km² and consists of 38 % rocks and glaciers, 46 % forest and pasture and 16 % agricultural land. Seasonal discharge in the Rhone River is controlled by upstream glaciers with low flows during the winter and high flows starting in May and ending with the high altitude freeze in October (Loizeau and Dominik, 2000).

The Rhone catchment area in the Wallis is ideally suited for the operation of hydroelectric power plants due to its topographical characteristics. Over the last century, several large projects were realized; among them is the largest hydroelectric power scheme in Switzerland, Grande-Dixence with a reservoir volume of 0.4 km³ and a total annual energy production of 2100 GWh. At present, the major reservoirs in the Wallis can hold about 1.2 km³ of water in total, which represents about 20 % of the total annual river flow. When operation of high head hydropower plants with large reservoirs started in the 1950's, the winter discharge increased drastically, with average values ranging between 50 and 60 m³s⁻¹ before 1950 and 120 m³s⁻¹ in the 1980's. On average, about 55 % of the total discharge in winter is due to the tailwaters of hydropower plants. In summer, 78 % of the average discharge of 300 m³s⁻¹ comes from natural sources with the hydropower plants adding the remaining 22 % (Loizeau and Dominik, 2000).

Water from high alpine catchments from altitudes of more than 4000 m ASL down to about 1700 m ASL is collected in centralized reservoirs. The tributaries and aquifers

discharging to the main river in the lowland are mainly fed by precipitation below the hydropower reservoirs. This creates two separated hydrological cycles.

During the winter months, most of the reservoir water stored in summer is released by the hydropower plants. This significantly increases the winter discharge of the Rhone River. The storage of the discharge from high - altitude catchments leads to a reduced summer runoff of the Rhone and to a decrease in the number and intensity of flood events in the tributaries of the Rhone River.

After a dramatic flood in 1860, the Rhone River was regulated with dykes for flood protection along the whole valley floor. During the first (1863-1894) and the second (1930-1960) phases of regulation of the Rhone, the main river reaches were canalized to increase discharge and sediment transport capacity. More recent catastrophic floods, such as in 1993 and 2000, revealed the risk of future levee failures and hence triggered the planning of a third correction phase. The 3RC focuses on integrated planning, considering not only economic, social and political aspects, but also explicitly including ecological demands (Kanton Wallis, 2000). In contrast to the past efforts, the new project aims to enlarge the narrow river corridor where possible, giving the river more space. Due to the infrastructural pressure in the floodplain, however, these widenings will also be surrounded by levee structures for flood protection.

For the “Third Rhone River Regulation” it is important to analyze and quantify the exchange between the Rhone and the adjacent groundwater. Due to flood protection measures, partial clogging of the river bed and a network of drainage channels in the floodplain, the groundwater level is much lower than the average Rhone level (Egli, 1996). The planned river enlargement could therefore lead to a significant increase of the groundwater level potentially endangering buildings, infrastructure, as well as the quality of drinking water in pumping stations located near the river.

This paper reports the results of an interdisciplinary study to qualitatively trace the water masses of the artificial high-altitude hydrological cycle from the reservoir to the river and further into the groundwater. The alpine environment as well as the geological situation in the Rhone valley is well suited for applying a combination of

stable isotope analysis with geochemical measurements (sulphate) and transient tracer techniques ($T/{}^3\text{He}$) to address the following questions:

1. Can the seasonality of $\delta^{18}\text{O}$ and sulphate concentration in the Rhone River be used to separate the hydrological cycles above and below 1700 m ASL?
2. Can we identify lateral groundwater sources and quantify river-groundwater exchange in the alluvial aquifer?

The approach should support further risk assessments of changing river-groundwater interactions during rehabilitation projects in heavily regulated Alpine river systems with hydropower schemes.

3.3 Methods and Study Site

The investigation is based on sampling of precipitation, spring water, surface water and groundwater from 2001 to 2003. These campaigns combined isotopic tracers ($\delta^{18}\text{O}$, δD , $T/{}^3\text{He}$) with standard geochemical parameters (e.g. SO_4^{2-} , Cl^- , specific conductance).

Data for the Local Meteoric Water Line (LMWL) were collected monthly between February 2002 and 2003. In collaboration with the Meteorological Survey of Switzerland (SMA), composite samples representing monthly averages were collected, using standard rain gauges according to specifications of the World Meteorological Organization (WMO). The rain gauges were located at different altitudes: 471 m (Martigny), 640 m (Visp), 737 m (Fey), 1260 m (Hérémece), 1617 m (Grächen), 1825 m (Evolène) – all on the southern mountain range of the Rhone valley. The rain samples, stored in polyethylene (PE) bottles and cooled to 4°C were analyzed for $\delta^{18}\text{O}$ and δD . Isotopic compositions at higher altitudes were calculated from extrapolation of the LMWL to the respective altitude.

Surface water was collected in July 2001 and December 2001, surface water and groundwater in April 2002, August 2002, April 2003 and May 2003. Groundwater was

pumped from 2" and 4" bores with a submersible groundwater pump (Grundfos MP1). A pumping time equivalent to the displacement of three borehole volumes resulted in a constant value for specific conductance. Data for Rhone River discharge were kindly provided by the Swiss Federal Office for Water and Geology (FOWG), inflow data of hydropower tailwaters were kindly supplied by the management of the Grande-Dixence and Mauvoisin hydropower plants. Flow velocity in the tributaries and drainage channels was measured using a hydrometric vane. Flow was calculated by multiplying average water velocities in different depths with the cross sectional area of the water body in the river. This area was determined by measuring the distance from shore and depth at various points across the flow stream to construct the flow profile. Inaccuracy of flow measurements can reach up to 10 % mainly due to errors in the determination of the cross sectional area of the water body and to the integration of the velocity profile (P. Perrochet, personal communication).

Samples were analyzed at the EAWAG Kastanienbaum for $^{18}\text{O}/^{16}\text{O}$ and D/H ratios by a Micromass Isoprime Isotope Ratio Mass Spectrometer (IRMS) in continuous flow mode. The $\delta^{18}\text{O}$ and δD isotope compositions of the water samples are conventionally expressed as a per mil deviation from Vienna Standard Mean Ocean Water (VSMOW). The overall analytical errors are 0.3 ‰ and 2 ‰ for $\delta^{18}\text{O}$ and δD respectively. Prior to analysis, the samples were equilibrated with a $\text{CO}_2\text{-He}$ and $\text{H}_2\text{-He}$ mixture, respectively, at 40°C for at least 12 hours. Anions (Cl^- , SO_4^{2-}) were analyzed by means of a Metrohm ion chromatograph, model 761. The detection limit was 5.0 mg/L for sulphate and 0.5 mg/L for chloride.

For the determination of water ages younger than 50 years, the $\text{T}/^3\text{He}$ dating method offers a direct measure for the time since groundwater had its last gas exchange with the atmosphere and provides quantitative groundwater residence times (Beyerle et al., 1999). The mass spectrometric measurements of $\text{T}/^3\text{He}$ were performed at ETH Zurich according to analytical protocols described by Beyerle (2000). All analyzed water samples were corrected for excess air being determined by the analysis of all atmospheric noble gases (Aeschbach-Hertig et al., 1999).

To investigate the water exchange between the river and the groundwater, the research focuses on the Rhone River between Sion and Martigny as well as on a

region about five kilometres downstream of Sion (Figure 7). The mountains north of this river reach consist of sedimentary rocks of the Helvetic Nappes, mainly formed by limestone (GEOVAL, 1986). South of the river the Penninic Nappes with limestone and schistose marls prevail. The Triassic "Zone Houillère" at the basis of the Penninic Nappes contains anhydrite, gypsum, and dolomite. It crops out south-west of the village of Aproz, feeding mineral sources and springs with sulphate-rich water (Cadisch, 1953; GEOVAL, 1986; Labhart, 2001). Hence, sulphate-rich groundwater is expected to provide an excellent geochemical tracer for water influx from the southern mountain range.

The floodplain of the valley floor is filled with alluvial sand and gravel housing the main unconfined aquifer. Laterally, it extends over the whole valley floor up to the rising edges of the rocky valley sides. The base of the aquifer lies at approximately 30 m to 35 m by apparition of fluvio-lacustrine deposits. Different pumping test in this area showed a hydraulic conductivity between $1.4 \cdot 10^{-2} \text{ ms}^{-1}$ and $1.5 \cdot 10^{-4} \text{ ms}^{-1}$ (GEOVAL, 1986) yielding porosities up to 30 % (Hölting, 1996). Together with the hydraulic gradient of around 1 ‰ in the investigated aquifer (GEOVAL, 1986), average flow velocities up to 1.5 km yr^{-1} are possible. In this region, gravel excavation has created several small artificial ponds (Figure 7). P1 covers around $30,000 \text{ m}^2$, with a maximum depth of approximately 30 m and has an estimated volume of around $440,000 \text{ m}^3$. P2 is about twice this size and has maximum depth of around 40 m. The ponds have no visible surface inflow or outflow. Both ponds are still in use for gravel production and cut therefore also in the deeper aquifer strata. In addition, observation wells GW1, GW2, GW3, GW4 and GW5, which all reach down to a maximum depth of 10 m were sampled (Table 2).

3.4 Results

3.4.1 Seasonality of Isotopic Signature in Precipitation

A LMWL for the area of investigation was established and the seasonality of isotopic composition of water was studied in the precipitation, the reservoirs and the

discharge of the Rhone River (Dansgaard, 1964; Schotterer et al., 2000). Based on the monitoring of the isotopic signature of precipitation at different altitudes, a $\delta^{18}\text{O}$ / altitude relationship was calculated. Plotting the isotopic signature versus the sampling altitude (Figure 8) enables determination of the geographical altitude of origin of the water sample (Siegenthaler, 1980).

The mathematical regression of the LMWL data for the upper Rhone valley, defined by the least-squares fit of precipitation data ($\delta\text{D} = 7.58 \delta^{18}\text{O} + 5.2$), matches very closely the Local Meteoric Water Line for Northern Switzerland: $\delta\text{D} = 7.55 \delta^{18}\text{O} + 4.8$ (Pearson et al., 1991). In addition to this altitude effect, the $\delta^{18}\text{O}$ and δD values of precipitation are also controlled by temperature, humidity and water vapor. Because of the higher temperature difference in winter between the source of air-vapour and the area of precipitation, more water vapour can be removed from the air masses on their trajectory, making the high alpine precipitation isotopically depleted in D and ^{18}O in winter (Kendall and Coplen, 2001; Schotterer et al., 2000). This means that in general, the δ values are higher in summer and lower in winter.

Averaging surface water samples from different seasons might lead to erroneous altitude estimates because doing so neglects the seasonal variations in the stable isotope compositions. The average seasonal variation in Switzerland reaches up to 4 ‰ - 6 ‰ (Kendall and Coplen, 2001). In our case, we observed a variation in $\delta^{18}\text{O}$ of precipitation up to 6 ‰ between summer and winter (Figure 8).

	Sulphate [mM]		$\delta^{18}\text{O}$ [‰]		Distance to river [m]	Depth [m]
	May 03	Aug 02	May 03	Aug 02		
GW1	8.39	3.34	-13.36	-12.85	150	9.7
GW2	2.13	0.88	-14.38	-14.29	30	6.5
GW3	0.86	--	-13.87	--	35	7.2
GW4	1.13	--	-13.57	--	125	6.1
GW5	0.73	0.56	-12.36	-12.40	1000	6.2

Table 2: Tracer data for GW1 to GW5

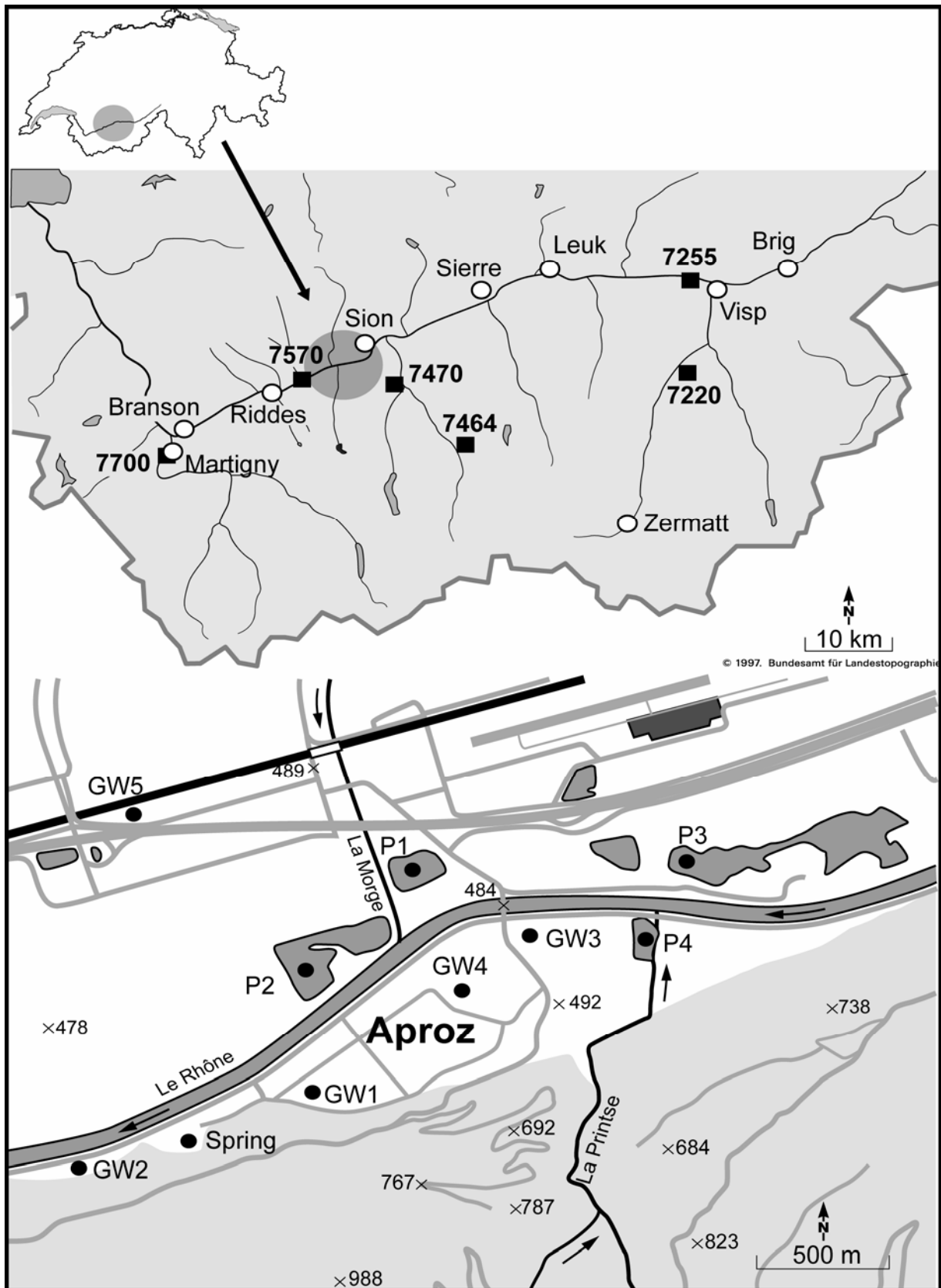


Figure 7: Area of investigation between the towns of Sion and Martigny in the Canton Wallis (Switzerland). The rain gauges were located at different altitudes: 471 m (Martigny, SMA No. 7700), 640 m (Visp, SMA No. 7255), 737 m (Fey, SMA No. 7570), 1260 m (Hérémence, SMA No.7470), 1617 m (Grächen, SMA No.7220), 1825 m (Evolène, SMA No. 7454). P1, P2, P3 and P4 are artificial ponds created by gravel excavation. GW1, GW2, GW3 and GW4 are groundwater observation wells.

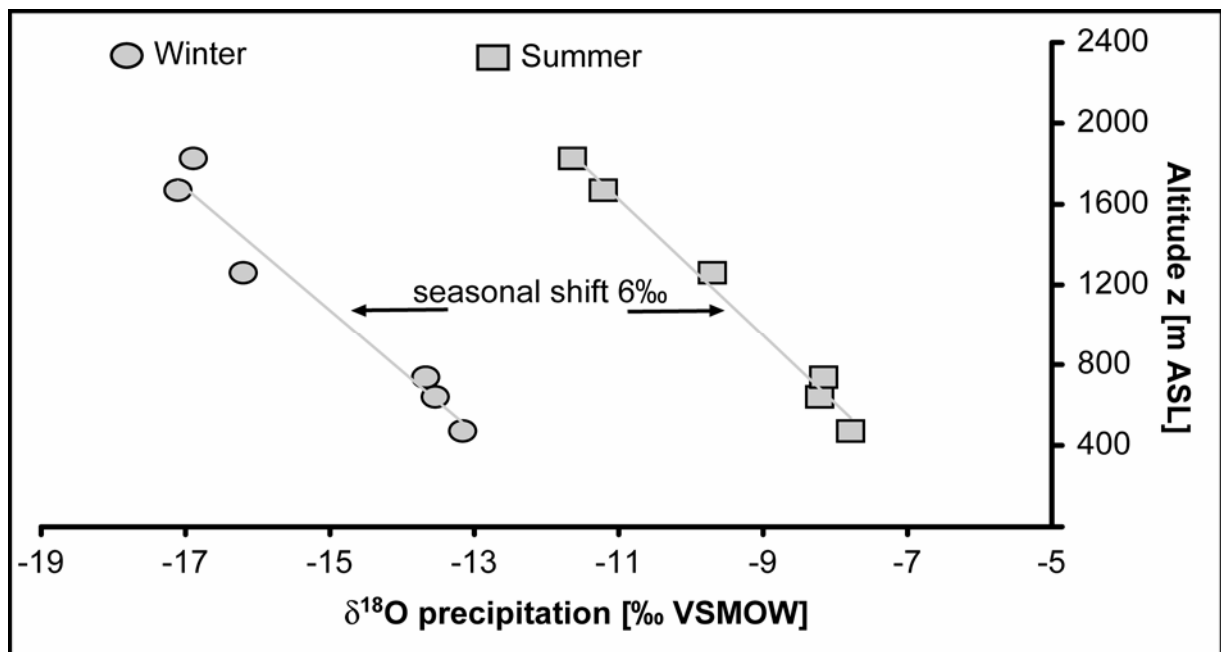


Figure 8: Relation between altitude and $\delta^{18}\text{O}$ in precipitation in the hydrological summer from May to October ($z = -297.95 * \delta^{18}\text{O} - 3406.1$, $r^2 = 0.9502$) and in the hydrological winter from November to April ($z = -285.33 * \delta^{18}\text{O} - 1648.2$, $r^2 = 0.669$). The seasonal shift is up to 6 ‰.

3.4.2 Seasonality in River Water

The stable isotope information in precipitation should also be seen in the receiving river. To assess the seasonal changes of the isotopic composition, the Rhone River and its tributaries were sampled during 48 hours in July 2001 and again in December 2001. The data in Figure 9 compare the river signature in sulphate and $\delta^{18}\text{O}$ in July and December at the hydrometric stations of Sion and Branson.

There is a distance of about 25 km between the two hydrometric stations, with the hydropower plants Grande-Dixence and Mauvoisin discharging within this area. The $\delta^{18}\text{O}$ winter values in the river (-13.3 ‰ to -14.2 ‰) are larger than in summer (-15.2 ‰ to -14.4 ‰), with variations in $\delta^{18}\text{O}$ up to 0.8 ‰. The most depleted $\delta^{18}\text{O}$ -value is slightly more negative than the average $\delta^{18}\text{O}$ values measured in August 2002 in the two large reservoirs in the high alpine region (Grande-Dixence and Mauvoisin: $\delta^{18}\text{O} = -14.9$ ‰). This means that the seasonality in the river water (more negative values in summer than in winter) is reversed in comparison to the seasonality in precipitation (more negative in winter than in summer). Plotting the

summer and winter sulphate concentration against the sampling time in Figure 10 shows that the discharge of the hydropower plants, characterized by an overall very low mineralization (Table 3), dilutes the sulphate concentration in winter, but has only a marginal effect during melt water discharge in summer. This provides the possibility to assess the river-groundwater interactions in more detail.

Most of the groundwater wells and gravel ponds sampled during our campaigns follow the LMWL quite closely. Only P3 shows clear signs of evaporative loss and was therefore excluded from further analysis (Figure 11). In the following, we first analyze the possible groundwater contribution based on the time-series in the Rhone River, and then we document the $\delta^{18}\text{O}$ and sulphate data in the network of groundwater wells (Figure 7).

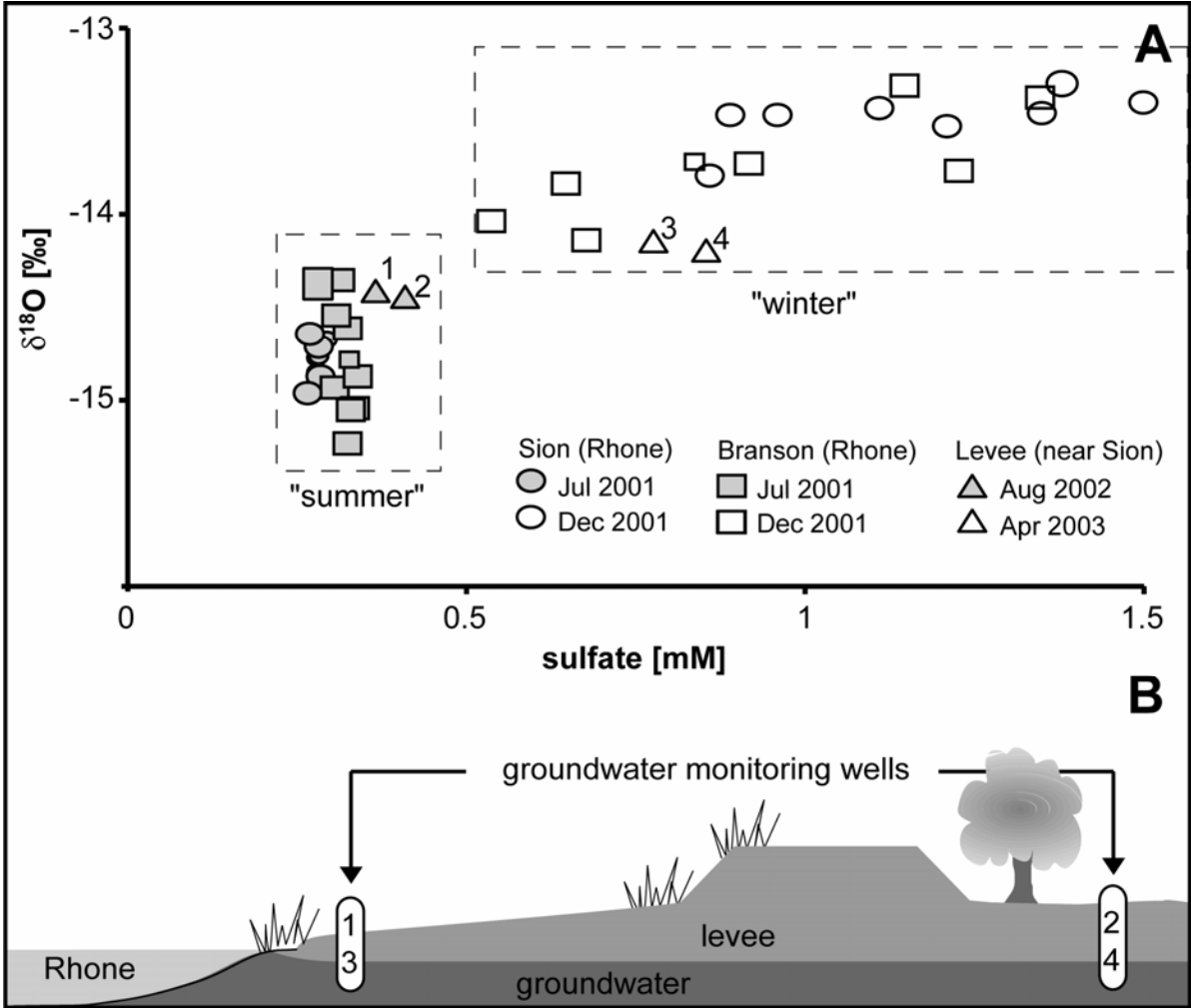


Figure 9: (A) Seasonal geochemical variation of the Rhone River near Sion and Branson during a 48 h sampling campaign in July and December 2001. July and December values cover distinct fields. (B) Scheme of the dyke structure.

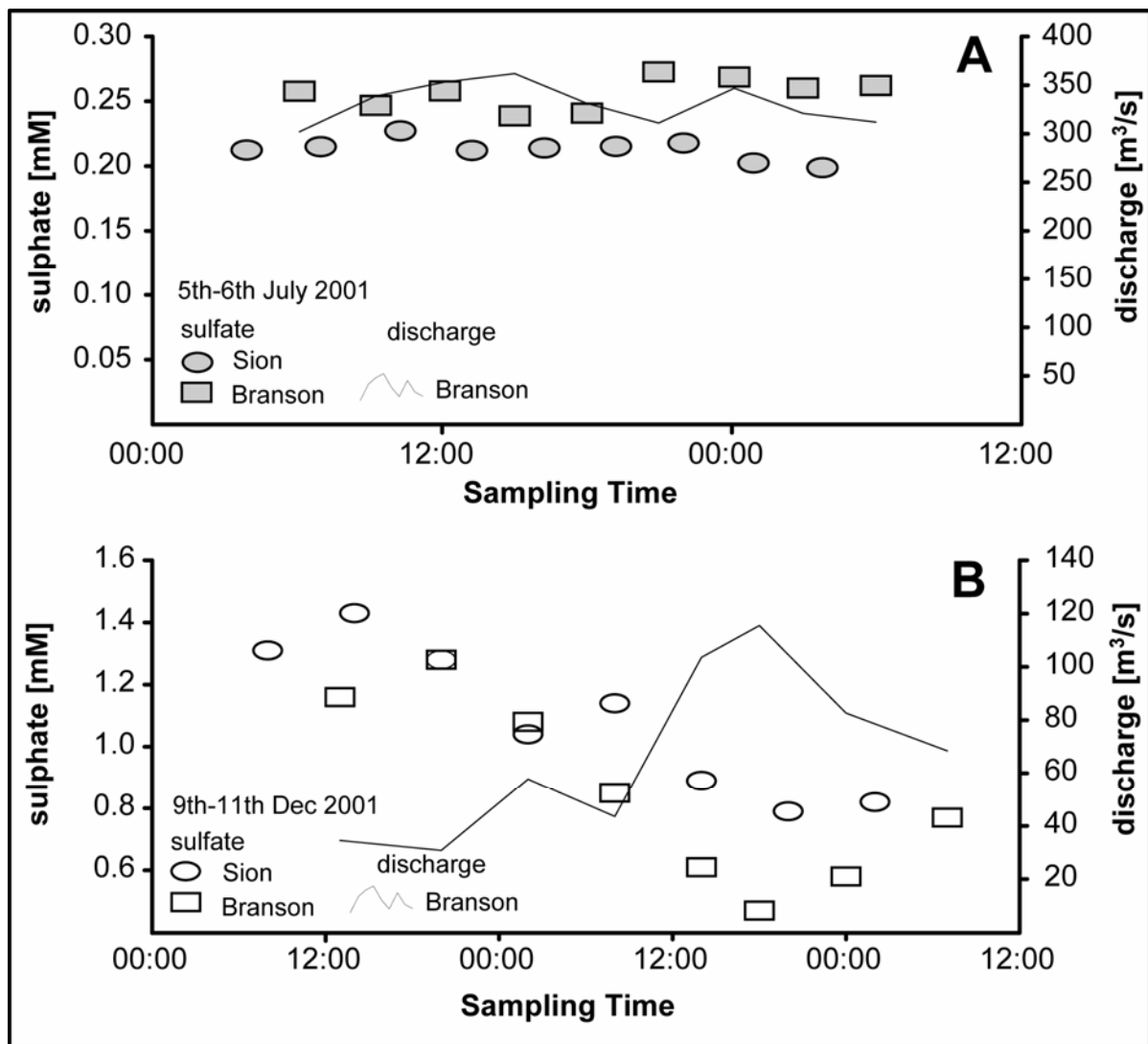


Figure 10: Evolution of sulphate concentration over time in the Rhone in summer (A) and in winter (B). In comparison to the low mineralized discharge of the hydropower plants. Dilution effects can be observed especially in the winter readings, showing a decrease in sulphate concentration with increasing Rhone discharge due to the influence of the tailwater of the hydropower plants.

3.4.3 River-Groundwater Interactions

The river water in comparison to the groundwater is lower concentrated in sulphate. For that reason, the seasonality of the sulphate signal can be used to obtain qualitative and quantitative information about the diffuse exfiltration of aquifer water in the river and the discharge of the channels draining the alluvial floodplain. The sulphate concentration in the Rhone in winter is in general higher upstream (Sion) than downstream (Branson), producing a strong difference in sulphate concentration

between 0.5 mM and 1.5 mM (Figure 9). In summer, the sulphate concentration is significantly lower at a nearly constant value around 0.3 mM and with slightly higher sulphate concentration downstream than upstream (Figure 9).

The clear seasonality in sulphate concentrations is caused by an augmented sulphate load during winter by the drainage of sulphate rich ground water from the floodplain. The strong ion gradient can be interpreted as dilution of river water by sulphate-poor outflow from hydropower plants (Figure 10). Groundwater drainage can be estimated by comparing the discharge and sulphate flux at the upstream (Sion) and downstream (Branson) stations (Annexe 1) using two approaches based on flow and flux: 1) A flow balance between the two stations including the direct inflows of tributaries, drainage channels as well as hydropower plants shows an increase of $\sim 2.5 \text{ m}^3\text{s}^{-1}$ of water in the Rhone River that must be due to diffuse exfiltration from the aquifer. Applying a 10 % error to the flow measurements (see section Materials and Methods) reveals a possible uncertainty in the same order of magnitude as the calculated diffuse exfiltration accounting for $0 - 0.2 \text{ m}^3(\text{km s}^{-1})$. This is not a significant number but opens a possible interpretation range between “exfiltration” and “no- exfiltration“. 2) The flux was determined as the product of discharge and sulphate concentration. The balance shows a variation between the two stations of $64 \text{ to } 85 \text{ moles s}^{-1}$ during summer and of $41 \text{ to } 52 \text{ moles s}^{-1}$ during winter (Annexe 1). The increase in winter sulphate flux is due to the tributaries (1.5 moles s^{-1}), drainage channels (1.9 moles s^{-1}), and hydropower plants (2.0 moles s^{-1}). These directly measured inflow fluxes accumulate to 5.4 moles s^{-1} , accounting for 49 % of the total increase of 11 moles s^{-1} in sulphate flux between Sion and Branson.

	Jul. 2001 $\delta^{18}\text{O}$ [‰]	Aug. 2002 $\delta^{18}\text{O}$ [‰]	Nov. 2001		Dec. 2001 $\delta^{18}\text{O}$ [‰]
			$\delta^{18}\text{O}$ [‰]	SO_4^{2-} [mM]	
Grande Dixence 236 m ASL	-15.1	-15.0	-14.3	0.084	-14.3
Mauvoisin 1975 m ASL	-15.4	-14.8	-14.0	0.072	-13.8
average	-15.3	-14.9	-14.2	0.078	-14.1

Table 3: $\delta^{18}\text{O}$ signature in the reservoirs Grande-Dixence and Mauvoisin. Sampling in July 01 and December 01 was done in the valley outflow of the power-plants whereas in August 2002 and November 2001 the sampling was done directly in the reservoirs. Sulphate concentrations were only measured in November 2001.

Considering tributaries, drainage channels and the tailwaters of hydropower plants as the only direct inflow fluxes, the remaining increase in winter sulphate flux of 5.6 moles s^{-1} (51 %) must be due to diffuse exfiltration from sulphate rich aquifer water to the river. In terms of error-propagation, the 10 % uncertainty has to be considered also in the flux balance. Calculating the unknown sulphate concentration in the groundwater using the estimated diffusive groundwater exfiltration of $2.5 \text{ m}^3\text{s}^{-1}$ and the diffusive sulphate flux of 5.6 moles s^{-1} reveals a concentration value of 2.2 mM. This value corresponds well to the sulphate concentration found in the drainage channel “Grand Canal” which is mainly used to drain groundwater from the valley.

The seasonality of geochemistry can also be detected in the groundwater samples from wells within the dam structure (Figure 9B). The samples taken in April 2003 exhibit the winter signature of the river whereas the levee samples taken in August 2002 follow the summer signature. While the stable isotope signature of the groundwater is similar in winter and in summer, the well further away from the Rhone River (samples 2 and 4) shows higher sulphate concentrations than the well right next to the river (samples 1 and 3).

In Figure 12, the sulphate concentration is plotted against $\delta^{18}\text{O}$. The waters can be interpreted as mixtures of three distinct geochemical end-members or water components. The first component is represented by spring water, originating from the “Zone Houillère”. This highly mineralized water is characterized by a very high sulphate content ($\approx 12.5 \text{ mM}$) and an isotopic signature of $\delta^{18}\text{O} = -13.7 \text{ ‰}$. The water is exploited for production of mineral water and commercialized under the brand name “Aproz”. It is known for its high mineralization due to high sulphate content. GW1 is directly influenced by water of the same origin as the spring. This well is located in the southern floodplain just at the outcrop of the Zone Houillère. The high sulphate concentration in May decreases in August, indicating a dilution effect with infiltrating Rhone water during the high flow season.

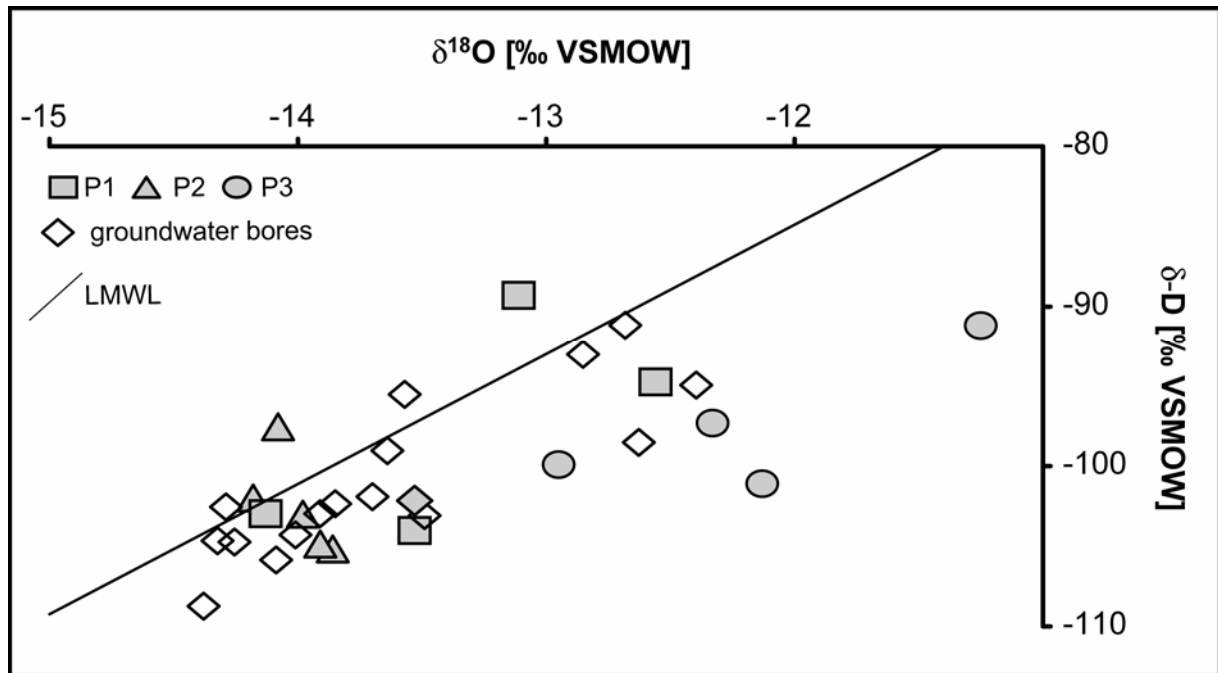


Figure 11: Local Meteoric Water Line (LMWL) for the upper Rhone valley compared to sampling results in groundwater wells and gravel ponds. The well samples and P1 and P2 scatter slightly below the LMWL. The data from P3 are characterized by a smaller slope giving strong indication for evaporation.

The second end-member is represented by the groundwater in wells GW2, GW3 and GW4, which are influenced by the Rhone River and characterised by low sulphate concentrations and $\delta^{18}\text{O}$ signatures varying between -13.5‰ and -14.4‰ . These wells seem to be only minor influenced by sulphate-rich mountain water, as the isotopic compositions of these groundwaters coincide with the River Rhone and are characterised by low sulphate concentrations (Figure 12). Especially the August reading of GW1 and GW2 show strong influence of Rhone water. The third end-member is represented by GW5 and is characterized by low sulphate concentrations and ^{18}O -enriched $\delta^{18}\text{O}$ values that are characteristic for mountain water originating from the northern slope of the Wallis valley.

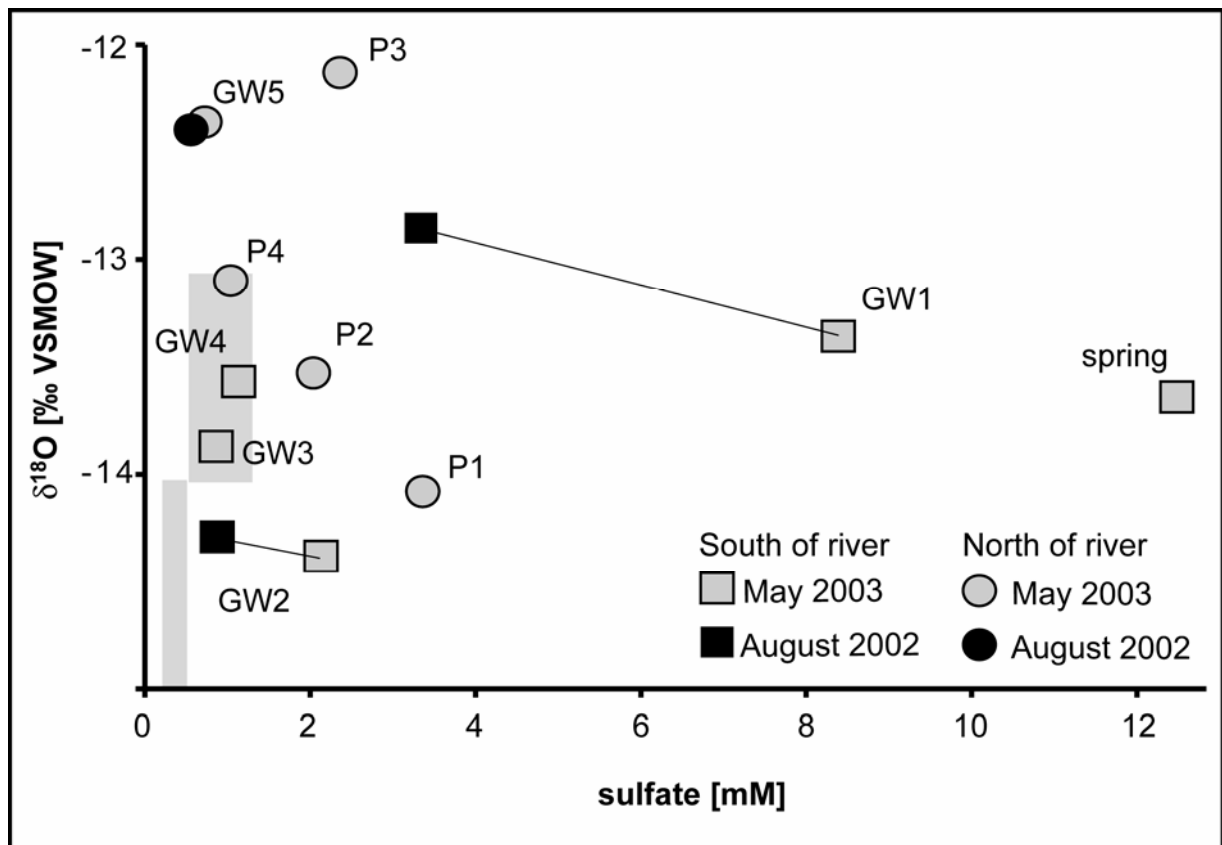


Figure 12: $\delta^{18}\text{O}$ and sulphate concentration from selected groundwater samples (GW) and in gravel ponds (P). The grey area represents the range of values of the Rhone River in summer and in winter (compare Figure 9). The waters can be interpreted as mixtures of three distinct geochemical end-members: 1) spring, 2) Rhone and 3) GW5 (see text).

3.5 Discussion

3.5.1 Seasonality of Tracer Signals

The catchment areas of the hydropower storage schemes reach down to altitudes of about 1700 m ASL. This “border” separates their high altitude water from the undisturbed drainage basins. The discharge of glaciated basins shows distinctive annual variation, since water is stored as snow in winter, released by melting in early summer (Klok et al., 2001) and precipitation is dominated by rainfall in late summer and autumn. During the snow melt period, the $\delta^{18}\text{O}$ signature of melt water becomes enriched in ^{18}O until the snow-pack is completely melted. Taylor (2002) showed that the isotopic change during a melting event is typically 3 to 5 ‰. This seasonal trend can also be followed in the isotopic signature of Grande Dixence and Mauvoisin

(Table 3). The average isotopic signature in the reservoirs increases in average from -15.3 ‰ in July to -14.1 ‰ in December.

In the valley floor, the $\delta^{18}\text{O}$ of the Rhone River tends to follow the seasonality of the reservoirs (Figure 9, Table 3), but river water is more enriched in $\delta^{18}\text{O}$. Evaporation can be excluded as the cause of enrichment, because Rhone water samples from August 2002 plot nearly perfectly on the LMWL. Rozanski (2001) reports that the oxygen and hydrogen isotopic composition of most of the world rivers were close to the LMWL indicating that evaporative fractionation of $\delta^{18}\text{O}$ of riverine water can usually be neglected. Based on the known hydropower release rates, we can estimate the isotopic signature of the “natural” component (N) in the river, using the observed variation in $\delta^{18}\text{O}$. The isotopically more positive signature of the Rhone water (R) in comparison to the water in the reservoirs (H) reflects the contribution of the “natural” components (groundwater and surface runoff) of the river water. July water from the reservoirs contributes 22 % to the total discharge of the Rhone with $\delta^{18}\text{O}_{\text{H-July}} = -15.3 \text{ ‰}$ (Table 3), whereas the water in the Rhone shows an isotopic signature of $\delta^{18}\text{O}_{\text{R-July}} = -14.8 \text{ ‰}$. The remaining 78 % of the total discharge are of “natural” origin with an unknown isotopic signature (Loizeau and Dominik, 2000). A simple mass balance for $\delta^{18}\text{O}$ reveals the isotopic composition of this “natural” component of the river water $\delta^{18}\text{O}_{\text{N-July}}$

$$\delta^{18}\text{O}_{\text{N-July}} = \frac{\delta^{18}\text{O}_{\text{R-July}} - (0.22 \cdot \delta^{18}\text{O}_{\text{H-July}})}{0.78} = -14.7 \text{ ‰} \quad (\text{Eq 4})$$

In winter, a similar calculation (55 % of discharge in the Rhone River from the hydropower plants, 45 % of “natural” origin) yields a stable isotope composition for the natural component of $\delta^{18}\text{O}_{\text{N-Dec}} = -13.2 \text{ ‰}$ (Table 3).

3.5.2 $\delta^{18}\text{O}$ as a Tracer for the Altitude of Water Origin

The average altitude of origin of the discharge water can be estimated from the $\delta^{18}\text{O}$ -altitude relationship (Figure 8 and Table 4). Due to the extrapolation above the

calibrated altitude range, it is not possible to obtain reliable altitude calculations for the water stored in the large reservoirs. The quantitative relation between precipitation and accumulated reservoir water is quite complex. Enrichment of the snow pack by evaporation and snow-atmosphere exchange produces a mean isotope content of the melt water, which is normally higher than that of the original precipitation (Rodhe, 1998). As a consequence, the average $\delta^{18}\text{O}$ in the hydropower reservoirs Grande Dixence and Mauvoisin (Table 3) is more positive than expected for the average altitude of their direct and indirect catchments, which is around 3000 m ASL.

Two pathways from precipitation to groundwater discharge should be considered: One part of the precipitation falling below the lower limit of the reservoir catchments drains directly to the stream by tributaries. A large fraction of the water, however, is retained in soils and aquifers and slowly percolates towards the valley ground. Thus, while snowmelt is clearly responsible for a drastic increase in the volumetric discharge in spring, less than half of that melt water runs off directly to the river in the valley and the remaining infiltrates and forces previously stored groundwater to discharge (Martinec, 1982). This piston effect is responsible for the seasonal change of $\delta^{18}\text{O}$ of the natural component of the Rhone water. This means that the more positive $\delta^{18}\text{O}$ values of summer precipitation appear as the natural component in the river in winter (Schotterer et al., 2000), whereas the more negative isotopic composition of the winter precipitation arrives with the snowmelt in the summer months.

	Equation (^{18}O)	$\delta^{18}\text{O}$ -range [‰]
Hydrological Year 2001-2002	$z = -311.67 x - 2906.5$	--
Hydrological Winter November to April	$z = -297.95 x - 3406.1$	-15.24 to -14.36 mean \approx -14.8
Hydrological Summer May to October	$z = -285.33 x - 1648.2$	-14.15 to -13.25 mean \approx -13.7

Table 4: Equations for calculation of altitudes of water origin in the Rhone River catchment during the two hydrological seasons. z = altitude [m ASL], $x = \delta^{18}\text{O}$ [‰]. See text for explanation. Measured $\delta^{18}\text{O}$ data from Figure 8.

The seasonally varying recharge altitudes of the “natural component” of the water in the Rhone River can be determined using the equation for the hydrological year. This leads to a calculated recharge altitude for the natural summer discharge ($\delta^{18}\text{O}_{\text{N-July}} = -14.7 \text{ ‰}$) in the Rhone of 1675 m ASL and for the natural winter discharge ($\delta^{18}\text{O}_{\text{N-Dec}} = -13.2 \text{ ‰}$) of 1208 m ASL. The estimated altitude range corresponds very well with the concept of two separated hydrological water sources, one above and one below the main hydropower reservoirs. The difference between winter and summer is related to the fact that the higher snowline in summer increases the altitude from where surface runoff is possible.

3.5.3 Identification of Lateral Groundwater Sources in the Alluvial Floodplain

To test the hypothesis of an important groundwater contribution in the natural runoff of the Rhone, five groundwater wells in the area southwest of Sion were sampled in April 2002, August 2002, April and May 2003. The chemical composition of the groundwater wells is summarized in Figure 12.

GW1 is located in the valley floor south of Rhone and is strongly influenced by lateral inflow from sulphate-rich water drained and mineralized by the “Zone Houillère”. Only during high Rhone water levels in August, the sulphate contents in this well were significantly diluted by low mineralized Rhone water. GW2 is located outside of the levee structure of the Rhone on the southern border of the river and at the edge of the mountain slope. Geographically it is comparable to GW1, but the chemical signature differs significantly. In April, during the low water season, this well is affected by water with a high sulphate concentration – but to a much lower extent than GW1. In August, during high water levels of the Rhone, GW1 is significantly affected by admixing of riverine water. Groundwater wells GW3 and GW4 are also strongly affected by Rhone water during the low water season in winter. These are plotted in the grey area in Figure 12 and show little geochemical evidence for other sources than the Rhone.

The observed evolution of the groundwater chemistry is conceptually easy to understand in terms of mixing. GW1 is located directly in the middle of the high

mineralized water originating from the “Zone Houillère”. The location of GW2, GW3 and GW4 is geometrically sheltered from the direct influence of the sulphate rich hang water and therefore more influenced by the Rhone River. This is shown by a very constant sulphate and $\delta^{18}\text{O}$ composition. Regardless of the high or low water season, GW5 seems neither affected by the Rhone River nor by the sulphate plume of the water originating from the “Zone Houillère” and hence seems to represent a different geochemical component defining the groundwater on the northern side of the Rhone valley.

The comparison of the different wells reveals a rather heterogeneous aquifer that can be geochemically separated into zones with infiltration of river water over short distances and input from the lateral slopes. Close to the river, the groundwater in the valley floor is diluted with low mineralized riverine water during high discharge in summer.

With a depth of around 30 and 40 m, respectively, the ponds integrate over the whole depth of the aquifer, whereas the shallow wells (<10 m depth) receive the water of the uppermost level of the aquifer. The deeper part of the aquifer is less affected by the input of river water and hence river driven dilution effects are of minor importance in the ponds. P1 and P2 are located between the Rhone and the northern mountain slope. On the sulphate/ $\delta^{18}\text{O}$ graph, the values from the ponds can be interpreted as a binary mixture of riverine water and sulphate-rich “spring” water from the southern mountain slope (Figure 7). The pronounced high sulphate concentrations especially indicate significant water input from the south and give direct evidence that groundwater has to flow under the river in order to find its way into the ponds. Temperature and conductivity profiles as well as groundwater age ($\text{T-}^3\text{He}$ method, Beyerle et al., 2002) were obtained in P1 in April 2003 and May 2003. Concentration-temperature-depth (CTD) -profiles of physical properties of the water column show the onset of stratification in temperature as well as in specific conductance. In April, the temperature in the deep water body at 30 m was 8.4°C. Within the following 30 days, the deep water body warmed up about 3 °C to reach finally 11.5°C. Such dramatic increase of deep water temperature of a stratified water column is very unusual and cannot be caused by solar radiation as a simple calculation with Bears law, taken from Cole (1995) shows:

$$\beta = 0.27\eta + 0.6 \rightarrow H(z) = (1-\beta) \cdot H_a e^{-\eta z} \quad (\text{Eq 5})$$

in which β denotes the fraction absorbed at the water surface ($\beta = 0.25$ for pure water and 0.45 for lower eutrophic water columns), η stands for extinction coefficient [m^{-1}], z is variable for the depth of the water column [m], H_S represents the solar radiation [$\text{kWh} (\text{m}^2\text{a})^{-1}$] and H_a refers to the radiation [Wm^{-2}].

In 5 m (depth of the metalimnion of the water column in the gravel pond), the initial estimated solar radiation H_S of $1000 \text{ kWh} (\text{m}^2\text{a})^{-1}$ at the surface is reduced by extinction to $\sim 220 \text{ kWh} (\text{m}^2\text{a})^{-1}$ at 5 m depth. Dividing this remaining warming energy by the heat capacity of water ($4.1 \text{ kJ} (\text{kgK})^{-1}$) and applying that on the remaining 25 m of the epilimnion of the water column leads to a maximum possible theoretical increase in temperature of $\sim 0.6 \text{ }^\circ\text{C}$ within a 30 day period. A simple sensitivity analysis reveals that even higher heat fluxes in the order of $1500 \text{ kWh} (\text{m}^2\text{a})^{-1}$ would only insignificantly increase water temperature to 0.9°C within one month. Also it has to be noted that the stability of the water column would strongly increase due to heating of the surface water causing a further reduction of warming of the deep water below the thermocline. The rapid temperature increase in the stratified deep water therefore points to a high groundwater exchange with the surrounding aquifer.

3.5.4 What is the Longitudinal Travel Velocity of the Groundwater

The change in $\text{T-}^3\text{He}$ in the deep water of P1 provides a second, independent argument of the rapid exchange of the deep water. In April, after the maximum extend of winter mixing, the pond water has already remarkably high water ages (1.3 years).

Sampling Well	Distance from P1 [km]	Water age [y]	GW-flow velocity [km yr ⁻¹]
P1	0	~ 3	2.3
North-East Riddes	~ 4.5	~ 5	
North East Branson	~ 15.7	~ 15	1.1

Table 5: Water ages determined by $\text{T-}^3\text{He}$ dating allow determination of the average flow velocity within the valley aquifer

The starting stratification in the lake prevents He from degassing out of the water body. Inflow of groundwater to the pond, which already has a significant residence time underground, increases the water age in the lake by about three years in a very short time. The only explanation is a complete exchange of water in the lake with groundwater flowing through.

The isotopic analyses confirm that the gravel ponds are part of the flowing groundwater. Figure 11 shows that the sampling values of P1 and P2 scatter around the LMWL in the same manner. Only P3 shows a lower slope indicating stagnating water affected by evaporation. P3 is no longer used for gravel excavation. The groundwater exchange is slowed down by clogging of the lake bottom by organic and/or inorganic sediments (Yehdegheo et al., 1997). In contrast, P1 and P2 are still in use for gravel production that slows down clogging by regularly excavation allowing “flowing” conditions in the ponds. In a longitudinal sense, T-³He dating allows determining the average flow velocity within the valley aquifer (Table 5). Measurements done between Sion and Branson in shallow groundwater bores as well as in the ponds already discussed yield an estimated average flow velocity within the aquifer between 1.1 and 2.3 km yr⁻¹ which agrees well with the hydraulic estimates made in the methods section.

3.6 Conclusions

Summarizing all the data, the introductory questions can be answered as follows:

1. Can the seasonality of $\delta^{18}\text{O}$ and sulphate concentration in the river Rhone be used to separate the hydrological cycles above and below 1700 m ASL?

A local meteoric water line for the area of investigation was established as well as the seasonality of isotopic composition in precipitation, in the reservoirs and in the discharge of the Rhone River. The results show, that $\delta^{18}\text{O}$ values in precipitation are higher in summer and more negative in winter. In our case, we observed a variation in $\delta^{18}\text{O}$ of precipitation up to 6 ‰ between the different seasons. In the receiving river, however, the water is more enriched in $\delta^{18}\text{O}$ and its seasonality is reversed in

comparison to the precipitation data. The seasonal shift of $\delta^{18}\text{O}$ in river water shows here a variation of up to 1.5 ‰ with more positive $\delta^{18}\text{O}$ values in winter than in summer.

The average altitude of origin of the natural component of the discharge water can be estimated from the $\delta^{18}\text{O}$ -altitude relationship to altitudes between 1675 m ASL (summer) and 1208 m ASL (winter). This altitude range corresponds very well with the concept of two separated hydrological water sources, one above and one below the main hydropower reservoirs.

2. Can we identify lateral groundwater sources and quantify river-groundwater exchange in the alluvial aquifer?

Sulphate-rich groundwater is an excellent geochemical tracer for water influx from the southern mountain range and can be used for identification of lateral groundwater sources in the area of investigation. Low sulphate concentrations in sampling station GW3 and GW4 indicate, that the groundwater here is mainly affected by river water. They are characterized by an averaged signature of the Rhone. The deep groundwater is chemically affected by inputs from the slopes of the southern mountain ranges and is characterized by high sulphate concentrations. Sampling of P1 as well as GW2 shows clear signs of a southern groundwater component which flows under the riverbed. GW5 represents the northern side of the shallow valley aquifer, characterized by significantly more positive delta values and lower sulphate concentration, characteristic for the northern slopes. The aquifer seems to be mainly recharged upstream of the test site. This is indicated by the low groundwater ages in the area of investigation. Looking at the continuously increasing water ages towards Branson, a rather large groundwater velocity within the aquifer of 1.7 km yr^{-1} can be calculated as an upper limit.

Sulphate flux in the river is a valuable tracer to quantify the river-groundwater interaction. Diffuse groundwater drainage can be estimated by comparing the SO_4^{2-} flux at the upstream (Sion) and downstream station (Branson). A simple mass balance reveals slight exfiltration ranging between 0 and $5 \text{ m}^3\text{s}^{-1}$ and resulting in a

total increase in sulphate flux in the river up to 51 %. This number is, however, within the range of uncertainty due to a measurement accuracy of ± 10 %. This opens a possible interpretation range between “exfiltration” and “no-exfiltration”. River water infiltrating in the aquifer mainly takes place during the summer months.

3.7 Acknowledgement

We thank the following individuals for their help with sampling campaigns and access to existing data:

Mr. Richard (Aproz SA), René Décorvet (BEG), Pascal Ornstein (CREALP) and Michael Brögli, Stephan Klump, Daniel McGinnis, Michael Schurter (EAWAG). Furthermore, Jacques Darioli and Bernard Hagin (EOS) as well as Mr. Evequoz (Evequoz SA).

Bruno Schädler, Ronald Kozel, Daniel Streit (FOWG), Olivier Ménétrety (Commune Nendaz), Burtel Bezzola, Richard Dössegger (SMA), Tony Arborino, Dominique Bérod and Alexandre Vogel (Canton Valais).

This work was financially supported by the Rhone-Thur project (www.rhone-thur.eawag.ch)

4

Temperature Fluctuations as Natural Tracer for River- Groundwater Interaction under Hydropeaking Conditions

Fette, M., Beer, J., Cirpka, O. A., Hoehn, E., Siber, R. and Wehrli, B.
Journal of Hydrology (submitted)

“Il y eut d’autres conséquences non moins graves: il fallut élever les digues des affluents, des filtrations se produisirent dans le Rhône, moins importantes, à vrai dire, qu’on ne l’a prétendu, car il se forme une certaine imperméabilisation du lit.”
(Mariétan, 1953)

4.1 Abstract

The upper Rhone River between Sion and Branson in Switzerland is highly canalized. The monotonous morphology and the large differences in hydraulic head between the river and the adjacent aquifer are strong predictors for clogging of the river bed. The hydraulic regime of the river is dominated by the operation of water reservoirs, leading to hydropeaking, i.e., diurnal and weekly fluctuations of discharge and temperature. We use temperature as a natural tracer to study bank filtration at four well transects located in river reaches with different hydropeaking intensity. Travel times of temperature fluctuations are determined by cross-correlation between time series measured in the river and in nearby wells. Low-pass filtering before cross correlating the data set allows quantifying base infiltration. High-pass filtering before cross-correlating the same data set allows the determination of short term infiltration caused by hydropeaking. The travel times of temperature signals range from 21 h to 254 h for long term time series and 7 h to 20 h under hydropeaking conditions. From these values, we estimate the hydraulic conductivity between the river and the monitoring wells, which is up to ~50 times smaller than values derived from pumping tests in the groundwater of the overbank. The results reveal that, along the investigated reach, the river is permanently clogged. Single flooding events indicate that the lower, permanently wetted part of the river bank is more severely clogged than higher parts, which are flooded only a few hours per day in the summer. The analytical framework presented here can be applied to quantify river bed clogging in streams with strong temperature variability.

4.2 Key Words

bank filtration, clogging, temperature, seepage velocity, cross-correlation

4.3 Introduction

River-groundwater interactions are of fundamental importance in the design of irrigation and drainage systems or wells near streams. The factors that affect hydrological exchange between channels and groundwater include aquifer geometry and hydraulic properties. Furthermore, channel slope and width as well as temporal

fluctuations in water table heights are important factors (Harvey et al., 1996). Numerous methods exist for quantitative analysis of surface water-groundwater interactions. Stuyfzand (1989) quantified the infiltration rate into groundwater by bank filtration from the River Rhine in the Netherlands by stable-isotope methods. The same approach was used to investigate the hydraulic connection between the Columbia River and the Blue Lake aquifer in Portland, OR (McCarthy et al., 1992). Seasonal variations in the composition of stable isotopes were used to determine travel times from the river water to the monitoring wells at a site at the river Danube in Germany (Stichler et al., 1986). Wett (2002) measured groundwater levels, temperature and electric conductivity in the river and in adjacent groundwater wells at the river Ens in Austria in order to quantify bank filtration. Sheets (2002) cross-correlated time series of electric conductivity in the Great Miami River in Ohio to determine the average travel time from the infiltrating river to the monitoring wells. Stream aquifer interactions are influenced significantly by riverbed clogging. Laboratory experiments elucidated the clogging process in coarse gravel river beds (Cunningham et al., 1987; Schaelchli, 1992). Schaelchli (1992) found that the clogging intensity in riverbeds depends mainly on the shear stress at the river bottom, the concentration of the suspended load, the hydraulic gradient between river and groundwater, and the grain size distribution of the river bed. A field survey showed that the determined thickness of the clogged layer did not exceed 50 cm (Brunke, 1999). Blaschke (2003) investigated the cyclic behavior of clogging in a heavily modified river reach of the Danube in Austria and found considerable variability in space and time of clogging cycles and declogging episodes.

4.3.1 Hydropower and Channelling of Rivers

For the last two centuries, most river systems in Central Europe and elsewhere were regulated for flood protection. About 50 years ago, large hydropower schemes were developed in the Alps, Scandinavia, the Pacific Northwest and in other mountainous regions, causing strong modifications of the hydrological regimes (Bratrich et al., 2004; Gleick, 2003).

The operation of a reservoir created by a dam has significant effects on the tailwaters in the valley and on the relations between river and adjacent groundwater. Alpine reservoirs are mainly filled in summer during the snow and glacier melting period, whereas the stored water is used for hydropower production during the winter months. In a seasonal perspective, this has an equilibrating effect on the tailwater in the valley. In comparison to natural conditions, the river discharge increases in winter and decreases in summer. As an additional effect, the amplitude and frequency of large flood events decrease due to retention in the reservoirs.

In a diurnal and weekly perspective, the flow regime of the river is characterized by the occurrence of rapidly oscillating floods caused by hydropower operation. These so-called hydropeaks are not powerful enough to compensate the lack of natural flood events in order to remove the clogging of the riverbed (Baumann and Meile, 2004).

With the aim of deflecting these hydropeaks, structural measures like the construction of levees used to be the preferred measure. These changes in channel morphology reduced water flow resistance by smoothing the river bed and decreasing the hydraulic radius (Shankman and Smith, 2004). Settling and straining of suspended and bedload sediments on the riverbed may cause a substantial clogging with a reduction of the conductivity of the river bed material (Blaschke et al., 2003; Schaelchli, 1992). The flat river bed with uniform embankments and the steady flow conditions of canalised rivers inhibit destabilization of the river bed and promote permanently clogged conditions (Schaelchli, 2002). As a result, the difference in hydraulic head between river water and groundwater increases whereas the exchange between river water and groundwater decreases.

Integrated into the framework of an extended rehabilitation project at the river Rhone, Switzerland, this paper reports a method to trace river-groundwater interaction under hydropeaking conditions. The seasonal temperature regime in the river Rhone is superposed by regular diurnal and weekly temperature variations. These conditions are well suited for the application of temperature as natural tracer. In this study, we address the following questions:

1. Is it possible to quantify river-groundwater interactions based on temperature records in a river reach with a strong hydropeaking regime?
2. Can these insights be used to analyze clogging in the river bed?

4.4 Methods

4.4.1 Study Area

The headwaters of the River Rhone (Figure 13A) originates from the Rhone Glacier (1763 m ASL) and flow through the Rhone Valley into Lake Geneva (374 m ASL). Along these 167.5 km, the Rhone drains a catchment of 5220 km² consisting mainly of forest and pastures (46 %), rocks and glaciers (38 %), and agricultural land (16 %). Naturally, the system shows a nivo-glacial flow regime (Loizeau and Dominik, 2000).

The natural hydrological regime of the river has been massively altered by the construction of hydropower plants in the valley. The seasonal storage of water in the high alpine reservoirs reduced the amplitude and frequency of intermediate flood events mainly in the lateral valleys. Before construction of the dams, discharge volumes exceeding 500 m³ s⁻¹ were observed on 23 days per year, whereas today such high discharges occur only at an average of five days per year (Wueest, 2002). Hydropower operation also increased the winter discharge in the River Rhone from 50-60 m³s⁻¹ in 1950 to 120 m³s⁻¹ in the 1980's (Loizeau and Dominik, 2000). On average, about 55 % of the total discharge in winter originates from the hydropower plants. In summer, 78 % of the average discharge of 300 m³s⁻¹ comes from natural sources with the hydropower plants adding the remaining 22 % (Loizeau and Dominik, 2000). The operation of roughly 50 dams in the Rhone watershed reduced the annual suspended solid load carried into Lake Geneva by almost 50 % to approximately 1.5 million tons (Wueest, 2002).

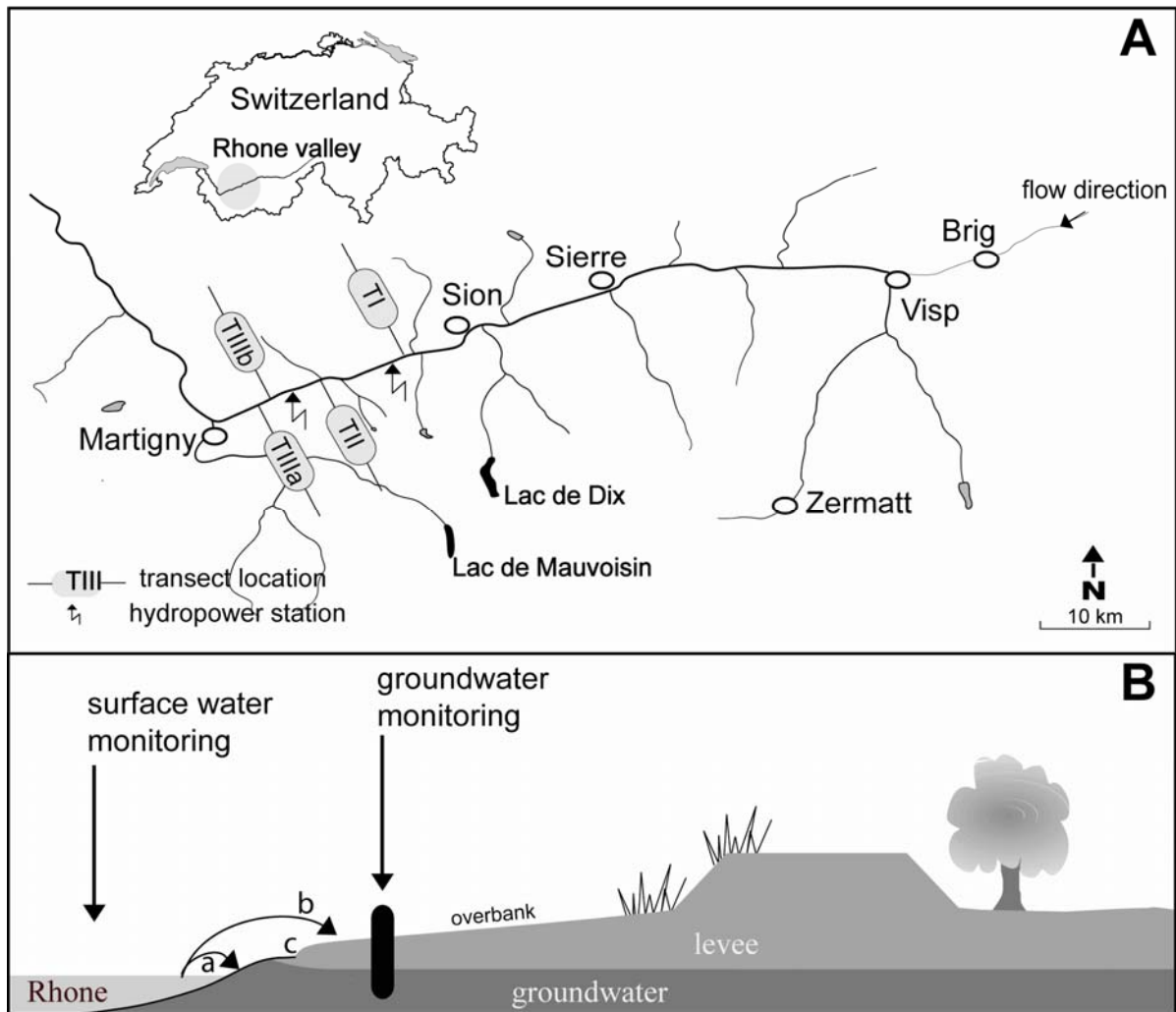


Figure 13: (A) Study sites. Two hydropower plants release water downstream of transects TI. (B) Schematic situation of transects TI to TIII.

Today, the River Rhone is highly canalised and reaches with a near-natural flow regime are rare. Along 36 km (22 %), the mean natural annual discharge volume has been reduced by more than 20 %, and over a distance of 109 km (65 %) hydropeaking is prevailing (Margot et al., 1992). Areas with intact connectivity between the Rhone River and the groundwater are virtually non-existent, mainly due to extensive use of the Rhone for hydropower generation (Peter et al., 2005).

In the area of investigation, transect TI represents a river reach under no direct hydropeaking influence (Figure 13A). TII is located ~ 4 km downstream of the tailwaters of the Grande-Dixence hydropower plant and characterized by strong hydropeaking regime. TIII is additionally altered by the tailwaters of the Mauvoisin Hydropower plant and hence most affected by hydropeaking (Figure 13B).

Geology and Hydrogeology:

The mountains north of the river reach consist of sedimentary rocks of the Helvetic Nappes, mainly formed by limestones, and often characterized by carstic formations. South of the river, the Penninic Nappes with schistose, quartzic, dolomitic and gypsic series prevail (GEOVAL, 1986). The bed-rock of the valley in the area of investigation has its base at around 800 m below surface (Besson et al., 1991).

Besides the River Rhone itself, there are several artificial and natural water courses in the flood plain of the valley: two main channels parallel to the river and multiple little drainage channels of minor depth drain the valley ground (Figure 14).

Groundwater flow is in general parallel to the Rhone. In the study region, there is also a flow component from the river to the channels.

The floodplain in the valley is composed of alluvial sediments, acting as the main aquifer which consists mainly of coarse sand (hydraulic conductivity $K \approx 10^{-3} \text{ m s}^{-1}$) or sandy-silty gravel ($K \approx 10^{-4}-10^{-5} \text{ m s}^{-1}$) (Lambelet, 1999). Pumping tests showed a hydraulic conductivity between $1.4 \cdot 10^{-2} \text{ m s}^{-1}$ and $1.5 \cdot 10^{-4} \text{ m s}^{-1}$ (GEOVAL, 1986). The base of the aquifer lies approximately 30 m to 35 m below surface.

The hydraulic gradient is about 1 ‰ in the investigated aquifer (GEOVAL, 1986), average groundwater flow velocities are up to 1.5 km yr^{-1} (Fette et al., 2005). The aquifer is underlain by lacustrine deposits, acting as aquitard.

The structure of the man-made levee is rather heterogeneous. The upper layer of the levee and the overbank were constructed with permeable material originating from the bed of the River Rhone (Kanton Wallis, 2000). It consists mainly of sandy gravel, intersected by lenses of fine sand and silt. During river floods, sand is deposited, covering the whole overbank. These sand deposits have an average thickness of 60 cm. The levee is underlain by impermeable silty material originating from the alluvial floodplain. This layer, located about three meters underneath the actual levee, is part of the flood protection system constructed during the first correction of the River Rhone (Egli, 1996).

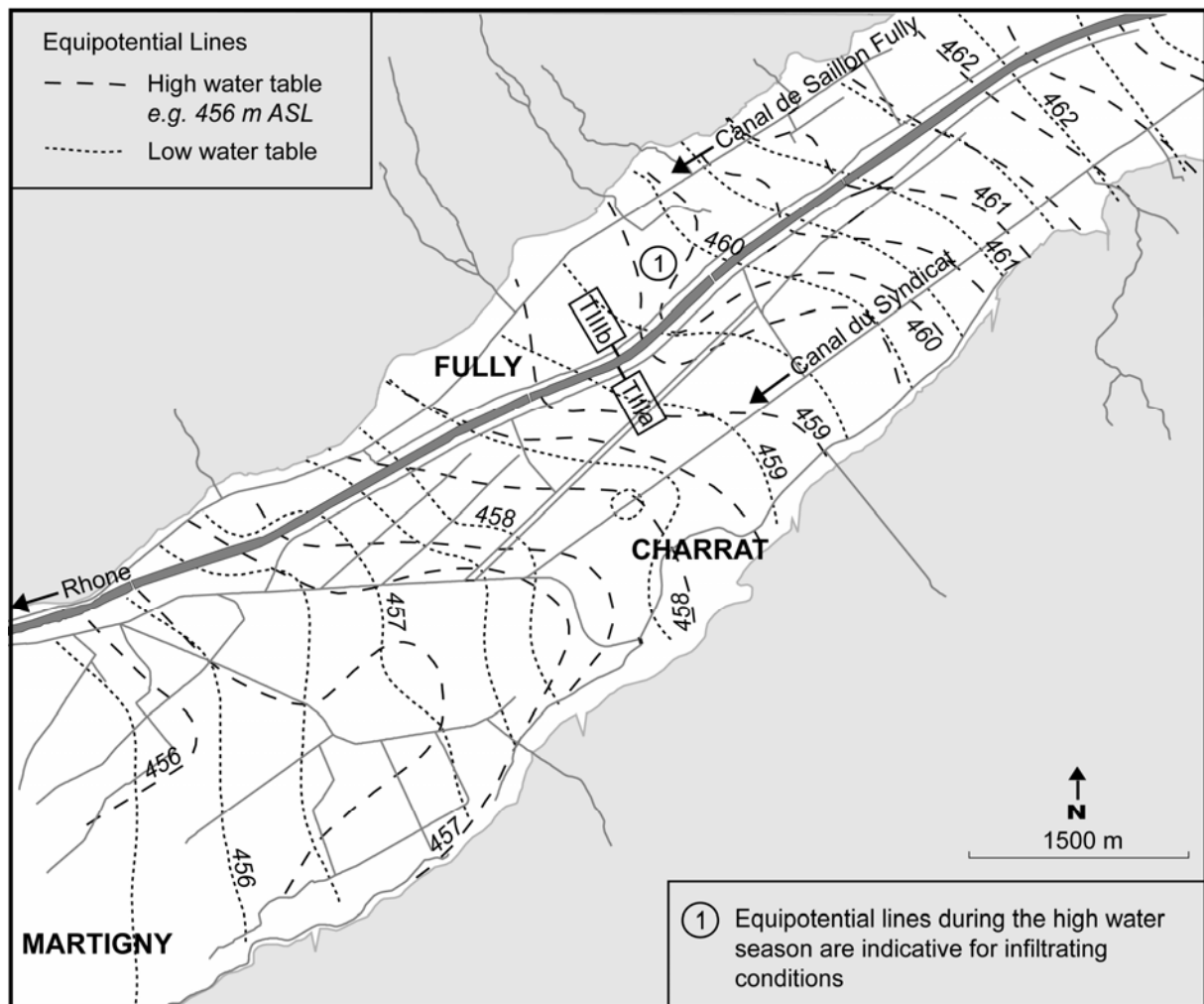


Figure 14: Map of groundwater equipotentials in the Rhone valley aquifer in the region of transect TIII. The equipotential lines show averaged water levels between 1995 and 2001 for summer and winter with high and low water levels, respectively (CREALP, 2001).

4.4.2 Acquisition and Evaluation of Data

In order to determine the effects of hydropeaking on river-groundwater interaction, we measured the water level and temperature in the river and wells at different distances from the river over a period of four years using standard piezo-resistive pressure gauges and PT-100 thermometers, respectively (Figure 13B, Table 6). The available data set in Transect TI covered a period from June 1999 to September 2003 with a temporal resolution of one hour. Transects TII and TIII covered a period from October 1998 to September 2004 with a temporal resolution of two hours.

Transect		Location	Distance from river	Depth
			[m]	[m]
T1	R	in the river	--	
	G	in the overbank	2.5	5
TII	R	in the river	--	
	G	in the overbank	2.5	2
TIIIa	R	in the river	--	--
	G	in the overbank	2.5	7
TIIIb	R	in the river	--	--
	G	in the overbank	2.0	11

Table 6: Geometric set-up of the different wells in transects T1 to TIII. R: river, G: groundwater

Due to low water levels in the river during winter time, some loggers in the Rhone River regularly measured air temperature instead of water temperature. This effect can be observed in TII and TIIIb and is visible in extreme river temperature fluctuations (Annexe 2 and 3). For that reason, only the data set during the high water period from May to August, called seasonal series, of each transect could be used for calculations.

4.4.3 Interpretation of Data

Temperature and water level signals provide different information. The water level indicates the hydraulic connection between wells. The groundwater table rises almost immediately with the stream stage elevation. The correspondence of the subsurface water level with the surface water level is based on pressure propagation, which is influenced by the ratio of transmissivity (product of specific storage and aquifer thickness, storage coefficient) and storativity in the aquifer. The pressure propagation is too fast in order to infer hydraulic conductivity from head measurements with the given temporal resolution. By contrast, the temperature signal reflects heat transfer in the groundwater on time scales that can be resolved by the measurements.

Estimation of Hydraulic Conductivity from Temperature Data

The infiltrating water reflects the seasonal and diurnal temperature fluctuations of the river. The amplitude and time shift of temperature maxima or minima with respect to

the river are used to characterize the groundwater recharge process (Hoehn, 2002; Silliman and Booth, 1993).

Prior to time series analysis, the temperature data are filtered. A low-pass filter eliminates the high-frequency components up to the cut-off frequency. This filter method stresses the seasonal information of the temperature signal. The high-pass filter, in contrast, passes only high frequency components and points out the short-term information of the temperature signal caused by hydropeaking. The lag between the two times series is determined for different time-shifts by calculating the cross-correlation r_{T_1, T_2} of two temperature signals T_1 and T_2 by:

$$r_{T_1, T_2} = \frac{\sum_{i=1}^n (T_{1,i} - \bar{T}_1)(T_{2,i} - \bar{T}_2)}{\sqrt{\left(\sum_{i=1}^n (T_{1,i} - \bar{T}_1)^2\right)\left(\sum_{i=1}^n (T_{2,i} - \bar{T}_2)^2\right)}} \quad (\text{Eq 6})$$

in which n denotes the number of available data. The correlation coefficient obtained from the cross-correlation quantifies to which extent the variations observed in one time-series can be explained by a linear relation to the time-shifted variations in the other series.

We interpret the time shift of maximum correlation as travel time τ_T of temperature propagation. Assuming that (1) heat transfer is dominated by convection, (2) the temperatures in the aqueous and solid phase are identical (local thermal equilibrium), and (3) the flow field is divergence free, the heat equation in the aquifer reads as:

$$\left(1 + \frac{\rho_s c_s (1-n)}{\rho_w c_w n}\right) \frac{\partial T}{\partial t} + \frac{\mathbf{q}}{n} \cdot \nabla T = 0 \quad \Rightarrow \quad \frac{\partial T}{\partial t} + \mathbf{v}_T \cdot \nabla T = 0 \quad (\text{Eq 7})$$

in which indices w and s refer to the water and soil phase, respectively; t denotes time [s]; T stands for temperature [K]; ρ is the mass density [kg m^{-3}], c the specific heat capacity [$\text{J K}^{-1} \text{kg}^{-1}$], n is porosity [-], and \mathbf{q} is the Darcy flow vector [m s^{-1}]. The term $\mathbf{q}/n = \mathbf{v}$ is known as pore velocity. It represents the velocity at which a conservative tracer is transported through the aquifer. The temperature velocity \mathbf{v}_T [m s^{-1}] quantifies the propagation of temperature fluctuations, which is slower than

that of a tracer because of heat exchanges with the aquifer matrix. The ratio of seepage velocity to temperature velocity is the thermal retardation factor R :

$$R = \frac{|v|}{|v_T|} = 1 + \frac{\rho_s c_s (1-n)}{\rho_w c_w n} = 1 + \beta \frac{(1-n)}{n} \quad (\text{Eq 8})$$

in which β is the dimensionless heat distribution coefficient. With porosities n ranging from 0.1 to 0.2 and heat capacities for soil $\rho_s c_s = 1.9 \cdot 10^6 \text{ J m}^{-3} \text{ K}^{-1}$ (sand), $\rho_s c_s = 2.3 \cdot 10^6 \text{ J m}^{-3} \text{ K}^{-1}$ (wet clay) and water $\rho_w c_w = 4.185 \cdot 10^6 \text{ J m}^{-3} \text{ K}^{-1}$, R ranges between 3 and 5 (De Marsily, 1986). The travel time τ_T [s] of a temperature fluctuation is given by integration of the inverse velocity along the trajectory of the water parcel:

$$\tau_T(x) = \int_0^x \frac{1}{|v_T(s)|} ds = \int_0^x \frac{Rn}{|q(s)|} ds \quad (\text{Eq 9})$$

The specific discharge q follows Darcy's law:

$$q = -K \nabla h \quad (\text{Eq 10})$$

with the hydraulic conductivity tensor K [ms^{-1}], and the hydraulic head h [m]. Thus, assuming uniform and isotropic conditions, the hydraulic conductivity K can be evaluated from the travel time τ_T and head difference Δh along the distance L by:

$$K = \frac{RnL}{\tau_T \Delta h} \quad (\text{Eq 11})$$

The hydraulic conductivity depends via the kinematic viscosity on the temperature. For the temperature range of $3^\circ\text{C} - 9^\circ\text{C}$, observed in the investigated aquifer, the fluctuations of viscosity due to temperature fluctuations is within a factor of 1.2.

Accuracy and Limits of the Method

In general, using temperature as a tracer is suitable for quantitative analysis of groundwater flow. The observed travel time is integrated over the trajectory of water parcels. Thus, hydraulic conductivities derived from travel times are path-averaged quantities, too. The conversion from travel times to hydraulic conductivities requires knowledge of the porosity n . All following calculations are based on porosity values ranging between $n = 0.1$ and $n = 0.2$.

The analysis is based on the assumptions that (1) heat transfer is dominated by convection and (2) groundwater and solid matrix are in thermal equilibrium. Rapid temperature fluctuations could cause strong temperature gradients leading to significant conductive/dispersive heat transfer. A spectral analysis reveals that the propagation speed of temperature fluctuations contains a conductive/dispersive contribution that increases with frequency. Also, for high-frequency fluctuations the assumption of thermal equilibrium may not be appropriate. To locally equilibrate temperatures in the aqueous and solid phases requires a relaxation time. If the temperature fluctuates on smaller time scales than the characteristic time of local heat transfer, the solid phase will not have the same temperature, and the aqueous-phase temperature will propagate faster than assumed in our calculations. The upper limit of wave propagation for the latter situation is the unretarded seepage velocity q/n , rather than $q/(Rn)$.

4.5 Results

4.5.1 Time Series of Water Level and Temperature

The time series of the river Rhone display pronounced seasonal, diurnal and weekly fluctuations of the water level and temperature.

Seasonal Series

On a seasonal timescale, the water levels in the Rhone River and the adjacent groundwater increase with snowmelt in May and decrease with starting winter freeze in October (Figure 15A and B). These changes correspond with seasonally increasing water temperatures in late February and decreasing temperatures in beginning October (Figure 15C). The resulting temperature signal in the adjacent groundwater well follows with significant time shift (Figure 15D).

Weekly and Daily Series

Weekly and daily variations in water level and temperature are characterized by hydropeaking (Figure 16). Power production and hence hydropeaking starts generally on week-days around 6 AM and stops late in the evening. The weekends are characterized by “natural” conditions. Long-term water level data reveal that the amplitude of hydropeaking is in general more pronounced in winter than in summer. Temperature shows an indifferent picture.

The water originating from the high-alpine reservoirs has a fairly uniform temperature of 4 - 6.5°C over the entire year. In winter, when the discharge in the river is low, the return water typically warms the river by 0.5 K (Figure 16A). During summer, water retention in the reservoirs reduces flow in the river, which leads to an increase in water temperature. These processes result in average water temperatures of 5.5 °C in winter and 9.1 °C in summer at the monitoring station of Porte du Scex upstream of Lake Geneva (BWG, 2000). This corresponds to a temperature increase of 1.2 K in winter and a summer decrease of 0.7 K compared to data of Uetrecht (1906) recorded before construction of the hydropower plants in the Wallis. The seasonal trend is superposed by diurnal and weekly temperature fluctuations resulting in an average water temperature in January 2000 of 2.6°C between Monday and Friday, but only 1.9°C during the weekend. On a daily time scale, the returned turbine water abruptly lowers the temperature of the river (Figure 16B) by up to several Kelvin (Meier et al., 2004; Wueest, 2002). Water temperature in the Rhone River in comparison to the adjacent groundwater shows positive and negative gradients. Table 7 gives an overview about the average water temperatures between May and August 2000 to 2003. On a seasonal average, the water temperatures in TI and TII

are warmer in the Rhone than in the groundwater. Temperature observations in TIIla and TIIlb show the opposite: groundwater is in general colder than the surface water.

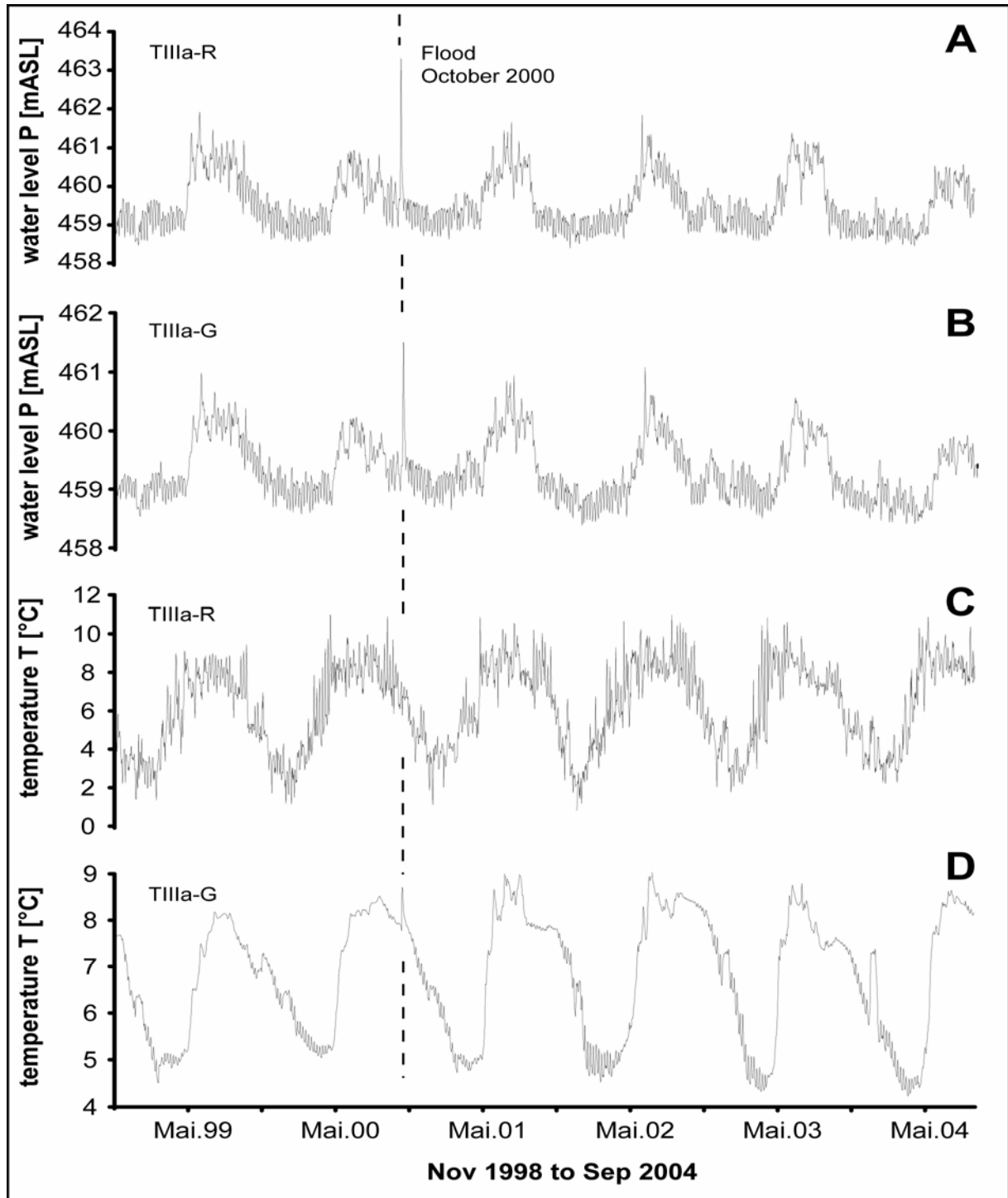


Figure 15: Time series of daily averaged levels and temperatures in TIIla-R and TIIla-G between October 1998 and September 2004. (A) Water level in TIIla-R increases with beginning snowmelt in May and decreases with starting winter freeze in October. Note the October 2000 flood (15.10.2004). (B) Water level in TIIla-G follows slightly attenuated the Rhone River signal. (C) Temperature fluctuation in TIIla-R is slightly shifted to the seasonal water level fluctuation. (D) Attenuated temperature fluctuation in TIIla-G follows the signal of the Rhone River with significant time shift.

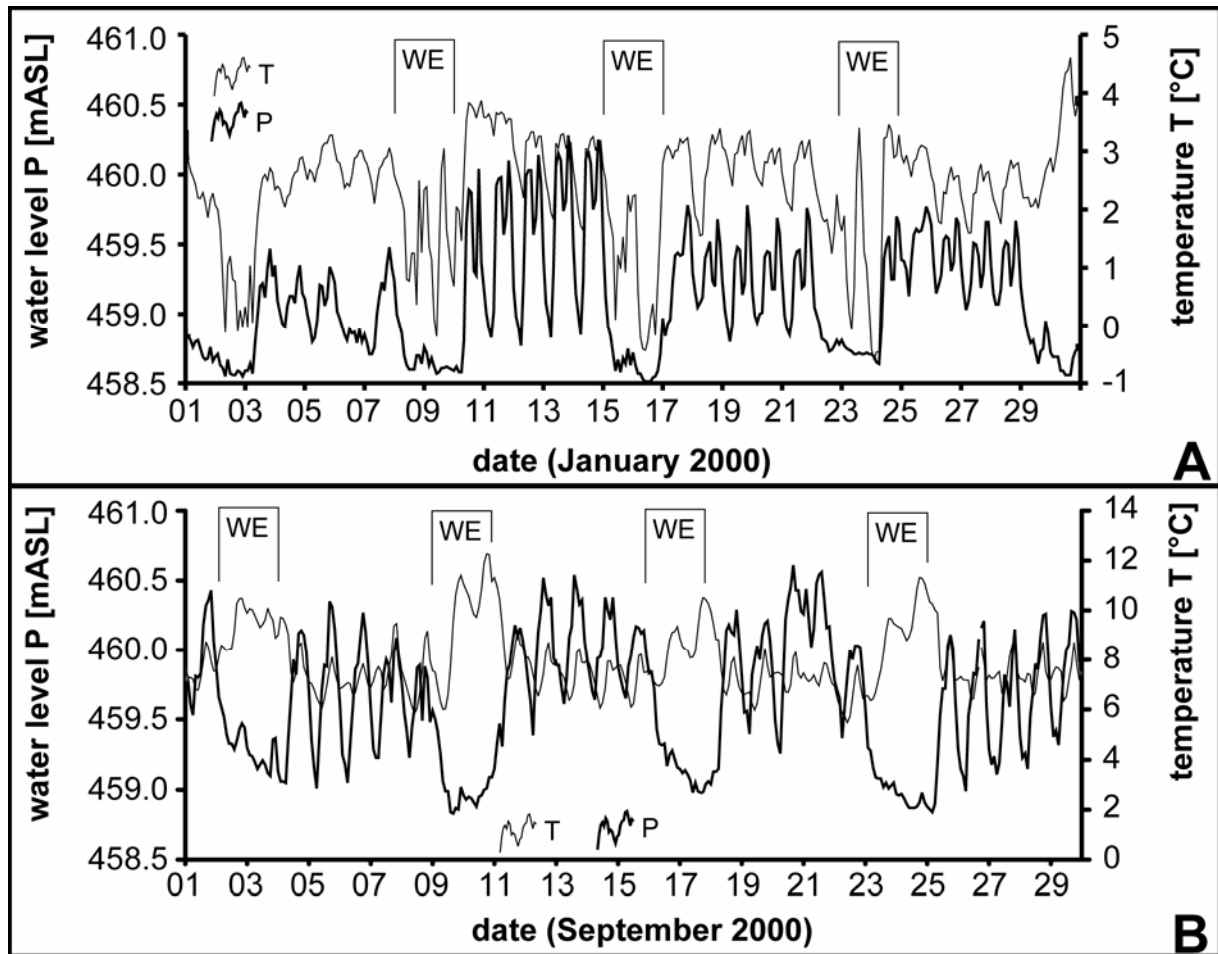


Figure 16: Hydropeaking regime at station TIII-R downstream of large hydropower facilities for a typical winter (January 2000) and late summer (September 2000) situation. (A) Return-water from reservoirs increases the temperature in the cold river water. Temperatures below 0°C in the Rhone are most probably artefacts due to water levels dropping below the logger (B) Hydropeaking during summer week-days decreases the river temperature compared to week-ends.

The highest difference in temperature between the river and the groundwater can be observed in 2003 in TII (Figure 17) and in TIIIb (Figure 18). Rhone water in TII was on average 0.8°C colder than groundwater whereas in TIIIb the river water was on average 1.9°C warmer than groundwater. These facts are important for the interpretation of the diurnal temperature fluctuations.

As can be seen in the comparison of the water tables of the river and the adjacent groundwater, pressure gradients towards the aquifer dominate (Figure 19). Gradients towards the river occur only sporadically during the winter months at night time (Figure 19C). Infiltrating conditions dominate especially during the summer months (Figure 19D). The hydraulic gradient of the three other transects shows similar patterns.

Year	TI-R	TI-G	TII-R	TII-G	TIIla-R	TIIla-G	TIIlb-R	TIIlb-G
2000	8.3	8.6	8.1	8.3	8.4	7.9	8.6	8.2
2001	8.4	8.5	8.2	8.6	8.5	8.0	8.6	8.0
2002	8.5	8.6	8.2	8.7	8.5	7.9	8.8	8.1
2003	8.2	8.3	7.9	8.7	8.2	7.8	9.9	8.0

Table 7: Average water temperature in the Rhone River and the adjacent groundwater between May and August of the indicated year.

Flood Events

Various flood events fell into the monitoring period, the most pronounced of which took place in October 2000 (Figure 15 and Figure 20A). A maximum discharge of up to $\sim 980 \text{ m}^3\text{s}^{-1}$ in the Rhone River at the OFEG gauging station near Martigny was caused by intense precipitation within a few days period.

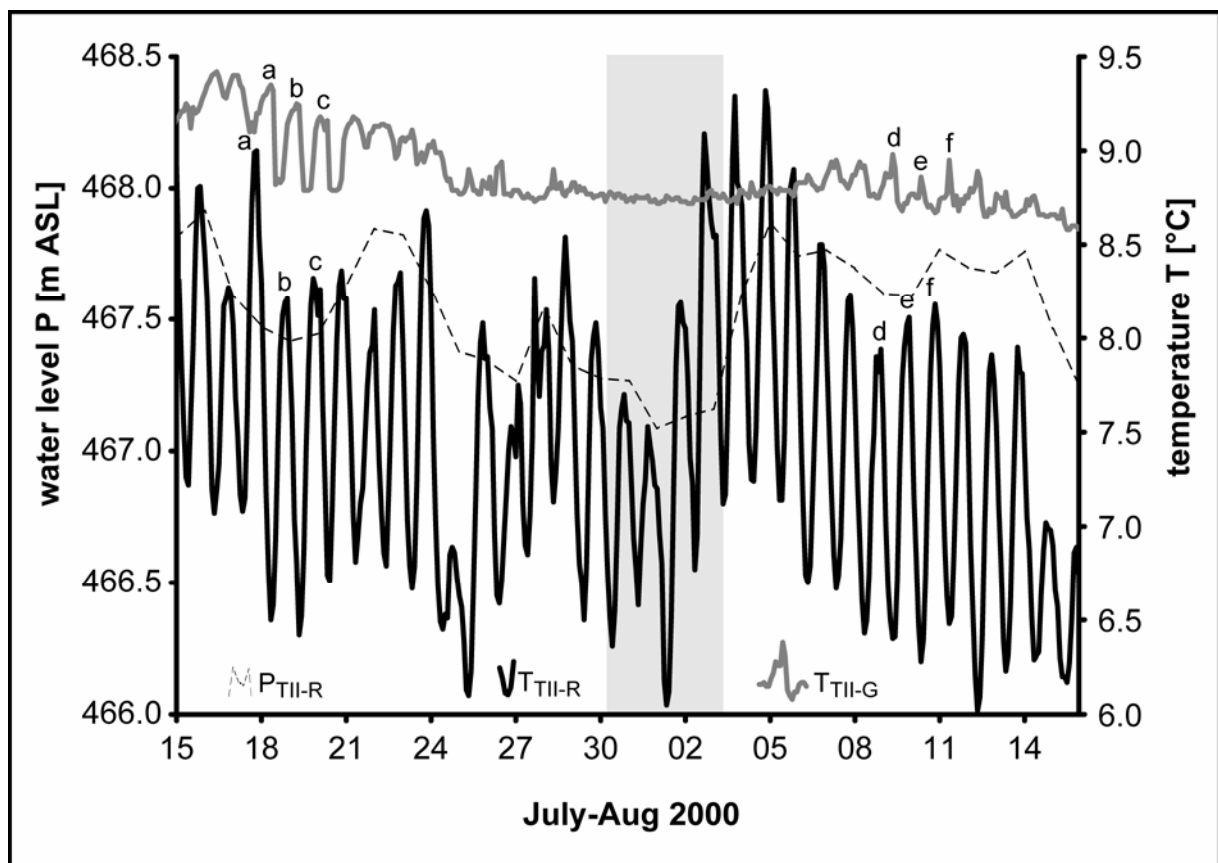


Figure 17: Water level (for clarity plotted as daily average) and temperature (two-hourly resolution) in TII between 15th July and 15th August 2000. With a water level in TII-R above ~ 467.3 m ASL, the temperature fluctuation in TII-R is directly transferred into the groundwater TII-G. Temperature peaks in TII-G follow with a time lag between 8 h and 12 h to the initiating peaks in TII-R (a=12h, b=10h, c=8h, d=10h, e=10h, f=12h). Below a water level in of 467.3 m ASL in TII-R (grey box), no direct response to the temperature fluctuations can be detected in TII-G. See text for further explanation.

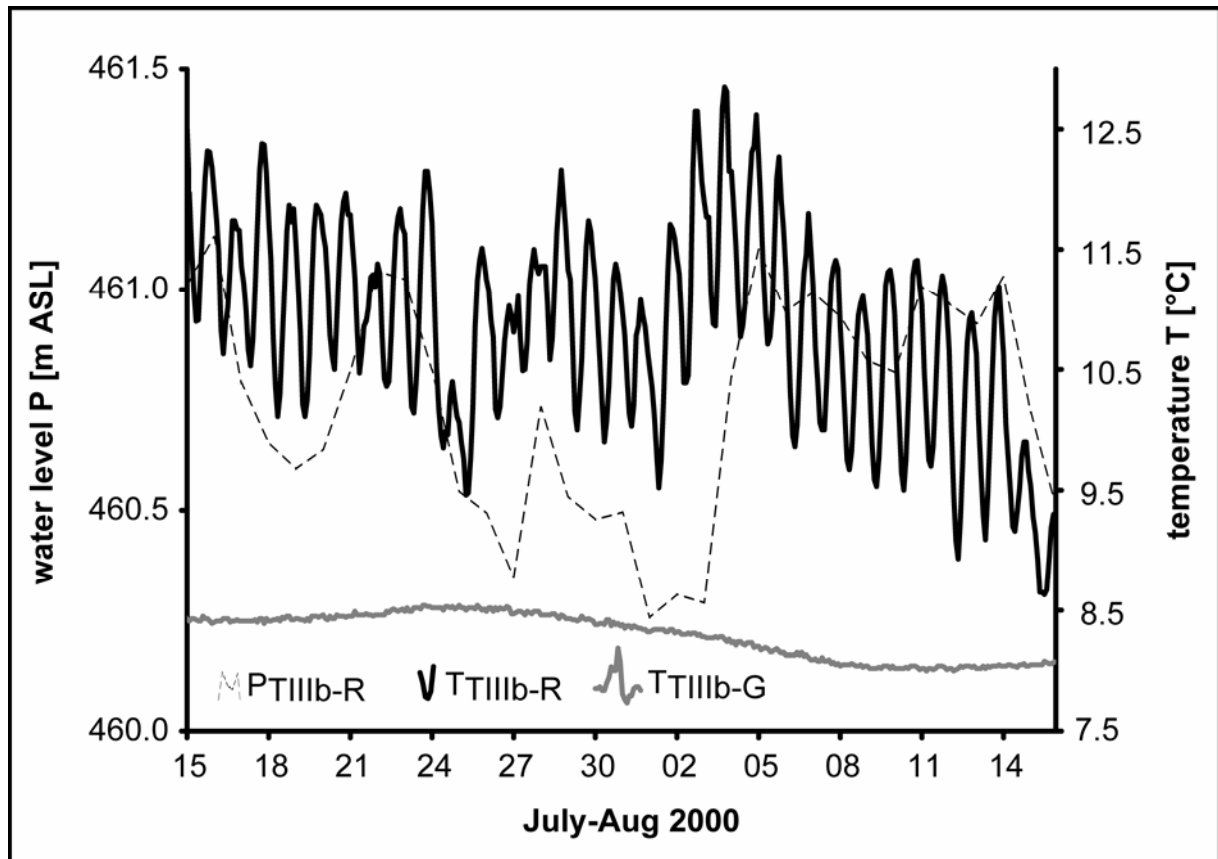


Figure 18: Water level (for clarity plotted as daily average) and temperature (two-hourly resolution) in TIIIb between 15th July and 15th August 2000. Even with a water level in TIIIb-R above the level of increased infiltration of 460.4 m ASL, no temperature fluctuation in TIIIb-G can be observed.

This event resulted in decreasing groundwater temperature in well TIIIa-G when the river passed the level of 460.5 m ASL ($\sim 280 \text{ m}^3\text{s}^{-1}$) (Figure 20A, see also Figure 13B arrow a). In the following it will be shown, that this water level corresponds to a transition zone between the highly clogged, permanently flooded part of the river bed and a more permeable part in the upper river bed only affected during hours of hydropower production or special hydrological events.

The overbank was flooded when the water level exceeded the value of 461.8 m ASL (arrow b in Figure 13B). When the water level in the Rhone reached its maximum of 464.5 m ASL, the temperatures in TIIIa-R and TIIIa-G became approximately equal. Afterwards, the temperature in TIIIa-G suddenly increased by approximately 1.5 K up to $\sim 9^\circ\text{C}$ before decreasing to $\sim 8^\circ\text{C}$. This temperature jump in the groundwater may be due to heating of the infiltrating water by the warm soil matrix, which had a temperature similar to the average air-temperature of 10°C in October 2000 in the region.

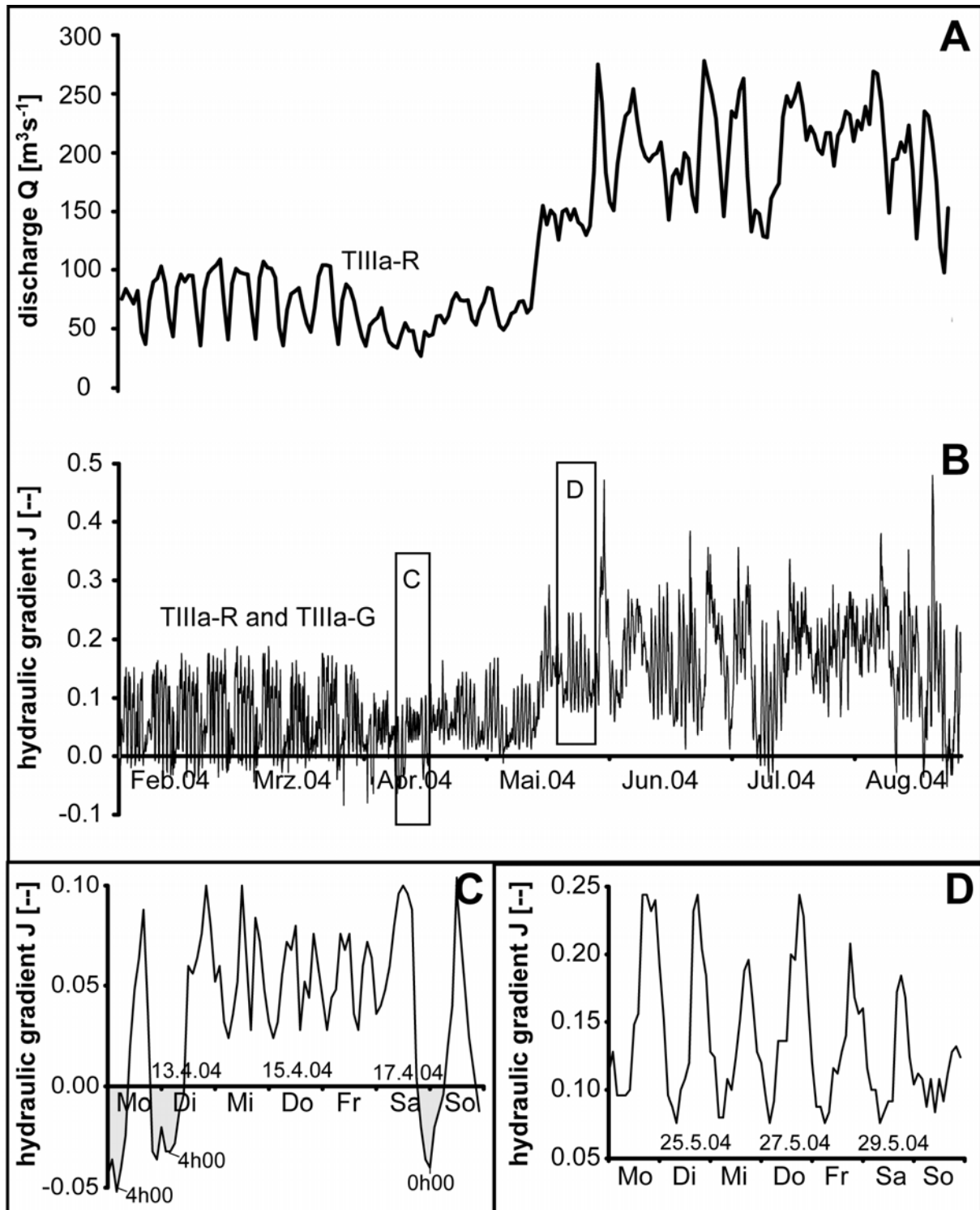


Figure 19: (A) Discharge rate of the river Rhone (OFEFG Branson) between February 2004 and August 2004. (B) Hydraulic gradient between TIIIa-R and TIIIa-G. An increasing gradient with snow melt can be observed. (C) Hydraulic gradient for the period of time between 12th and the 18th of April 2004. Before the flood season, negative hydraulic gradients can only be seen during off-hydropower periods (grey area). (D) After the snow melt period (24th to 30th of May 2004) no groundwater exfiltration to the river is hydraulically possible.

4.5.2 Hydraulic Conductivity Estimated from Temperature Data

The observed seasonal, weekly and daily temperature fluctuations in the river are propagated by bank filtration into the adjacent groundwater. The temperature variations observed in the monitoring wells are delayed in time and damped in the extent of the fluctuation (Figure 15B and D).

Seasonal Series

The velocity v_T of temperature propagation in the aquifer was determined using the temperature response of the initiating Rhone temperature signal in the adjacent groundwater. Figure 21 shows the filtered and cross correlated temperature signals between wells TI-R/TI-G (weakly influenced by hydropeaking) and TIIIa-R/ TIIIa-G (highly affected by hydropeaking), respectively. To investigate the long term fluctuations in the temperature signal, the low-pass filtered data set was cross correlated. A clear peak after 21 h (Figure 21A) and 254 h (Figure 21B) shows the travel time of the temperature signal between the river and the adjacent groundwater well.

Weekly and Daily Series

High-pass filtering before cross correlating the same data set reveals a clear diurnal and weekly hydropeaking signal overlaying the seasonal pattern and giving indication for further continuous infiltration during hydropeaking hours (Figure 21, C and D). This signal can be interpreted as temperature response of the aquifer caused uniquely by hydropeaking. The travel times of the temperature signals of only 7 h to 20 h for the first positive peak and reveal higher permeabilities in upper parts of the river bed, which are flooded only temporarily (Table 8C). In order to estimate the seepage velocity v , the temperature velocity v_T must be corrected by the retardation factor calculated according to equation (Eq 8).

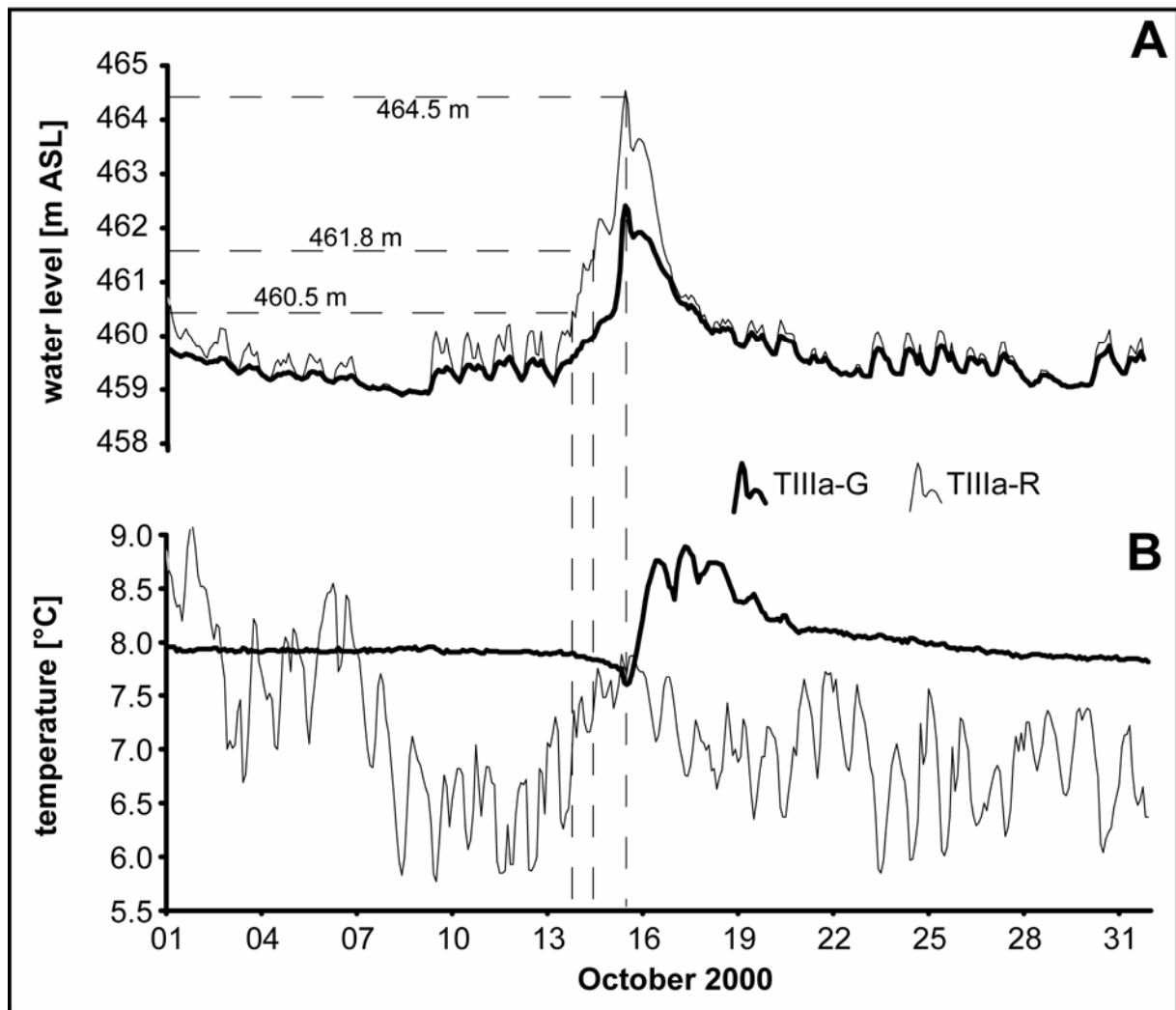


Figure 20: October 2000 flood in Tilla. (A) A Rhone water level of 460.5 m ASL ($\sim 280 \text{ m}^3\text{s}^{-1}$) was recorded the 14th of October 2000 at 00:00h. The flood reached a water level of 461.8 m ASL in the Rhone approximately ten hours later which marks the starting point of the flooding of the overbank in Tilla (arrow b in Figure 13B). The maximum level of 464.5 m ASL was reached the 15th of October 2000 by 12:00h. (B) The temperature in Tilla-G decreased significantly at a Rhone water level of 460.5 m ASL, before strongly increasing when the Rhone reached 464.5 m ASL. At this point the river and the groundwater had the same temperature.

With estimated values for effective porosity $0.1 \leq n \leq 0.2$, and the dimensionless heat distribution coefficient $0.45 \leq \beta \leq 0.54$, we arrive at values of the retardation coefficient in the range of $3.2 \leq R \leq 5.1$. This range was used in the evaluation of seepage velocities listed in Table 8. Applying Darcy's law (Eq 10 and Eq 11) leads further to the determination of hydraulic conductivity K .

4.6 Discussion

4.6.1 Comparison with Literature Data

Egli (1996) performed pumping tests in the area of investigation along two well transects about one kilometer downstream of TIIIb. The values of hydraulic conductivity K , derived from pumping tests, ranged between $2.5 \cdot 10^{-4}$ and $5.9 \cdot 10^{-3} \text{ m s}^{-1}$. Further investigations (BEG, 2001) indicate hydraulic conductivities for our investigated transects between $6 \cdot 10^{-3} \text{ m s}^{-1}$ at TII and $4 \cdot 10^{-4} \text{ m s}^{-1}$ at TIII (Table 8A).

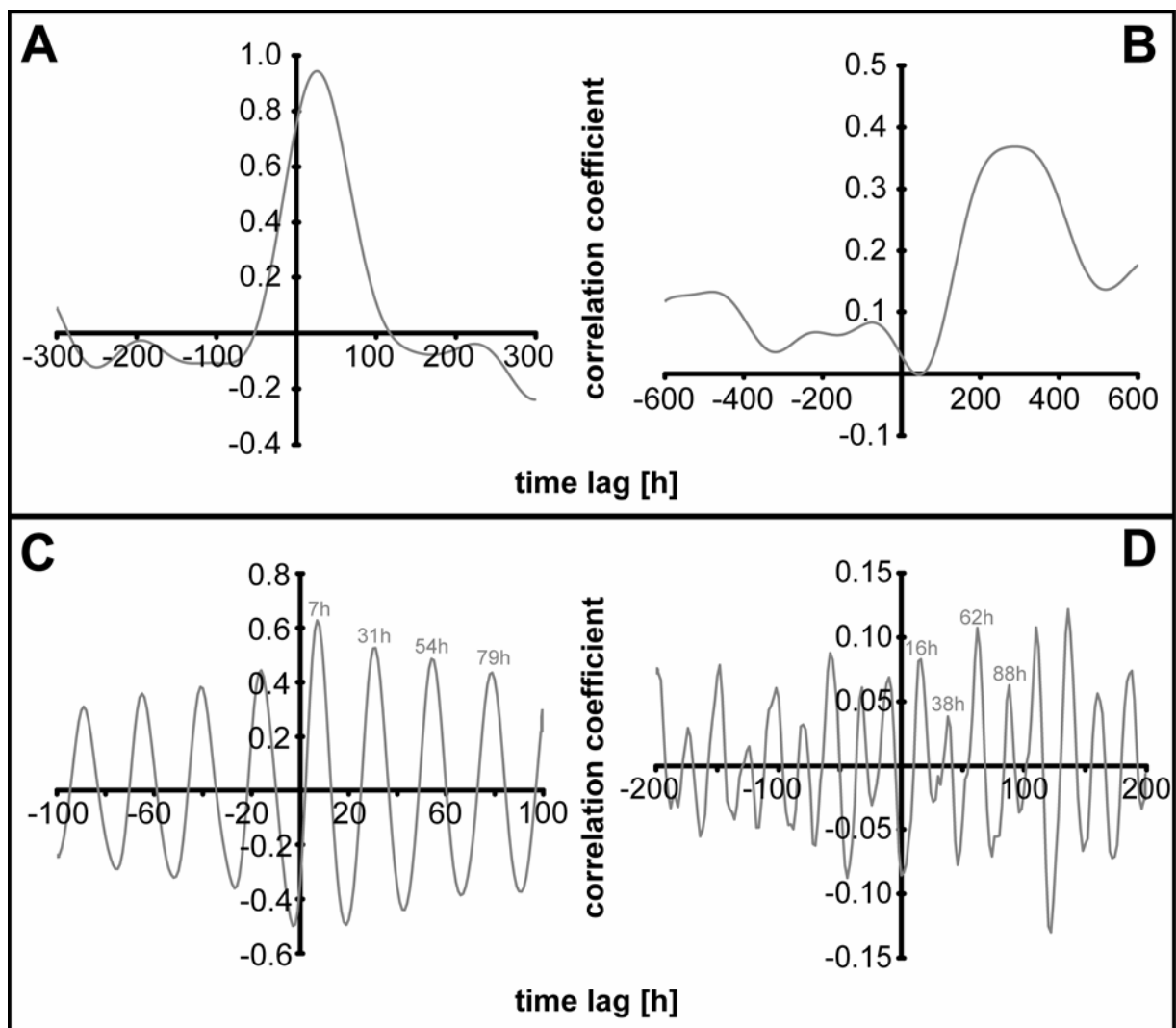


Figure 21: Filtered and cross-correlated summer temperature data (May and August 2000) for TI-R/TI-G and TIIIa-R/TIIIb-G, respectively (A) TI: Low pass filtering (cut-off = 200 h) before cross-correlation (lag = 300 h). (B) TIIIa: Low pass filtering (cut-off = 200 h) before cross-correlation (lag = 600h). (C) TI: High pass filtering (cut-off = 48 h) before cross-correlation (lag = 100 h). (D) TIIIa: High pass filtering (cut-off = 48 h) before cross-correlation (lag = 200 h).

Because these hydraulic conductivities were determined by pumping tests, they yield integral information on the matrix properties of the levee, but can not resolve the situation directly at the river-groundwater interface.

Our method to determine hydraulic conductivities from cross-correlation of temperature signals is not aiming on integral information within the levee body but focuses on the interface between river and groundwater. The low-pass filtered and cross-correlated data (Table 8B) reveal smaller hydraulic conductivities K in comparison to literature data of up to a factor of 5, approximately. A difference in hydraulic conductivity of a factor of only 5 is stand alone not convincing and significant, because of the log-normal distribution of the hydraulic conductivity.

Seasonal and diurnal Perspective		TI	TII	TIIIa	TIIIb
A AVERAGE (reported)	Hydraulic Conductivity K [$\cdot 10^{-4}$ m/s]	--	0.61–0.63	4.2-4.7	4.2-4.7
B SEASONAL (computed on the base of the first positive peak of the low-pass filtered correlation)	Maximum correlation coefficient r [-]	0.94	0.20	0.37	0.39
	Temperature travel time τ_T [h]	21	54	254	208
	Temperature velocity v_T [m/d]	2.9	1.1	0.2	0.2
	Seepage velocity v [m/d]	9.0-14.4	3.5-5.6	0.7–1.2	0.7-1.2
	Specific infiltration rate q [m/d]	1.44-1.81	0.56-0.70	0.12-0.15	0.15-0.18
	Mean hydraulic gradient J [‰]	0.38	0.40	0.15	0.19
	Hydraulic Conductivity K [$\cdot 10^{-6}$ m/s]	44-55	16-20	9.2-12	9.0-11
C DIURNAL (computed on the base of the first positive peak of the high-pass filtered correlation)	Maximum correlation coefficient r [-]	0.6	0.2	0.08	0.11
	Temperature travel time τ_T [h]	7	20	16	20
	Temperature velocity v_T [m/d]	8.6	3.0	2.4	3.75
	Seepage velocity v [m/d]	27.1-43.3	9.5-15.2	11.9-18.9	7.6-12.1
	Specific infiltration rate q [m/d]	2.5-3.1	1.02-1.28	0.63-0.79	0.97-1.21
	Mean hydraulic gradient J [‰]	0.38	0.40	0.15	0.19
	Hydraulic Conductivity K [$\cdot 10^{-4}$ m/s]	1.3-1.6	0.4-0.5	1.5-1.8	0.9-1.2

Table 8: (A) Literature data for hydraulic conductivity (BEG, 2001). Parameters derived from the cross-correlation in the riverbank area between the measuring point in the Rhone R and the adjacent groundwater well G (recorded between May and August 2000). (B) Results for the seasonal perspective are derived from temperature data after low-pass filtering and cross-correlation. (C) Results for the diurnal perspective are derived from temperature data after high-pass filtering and cross-correlation. Section C shows the computed matrix properties based on the time lag of the first positive peak of the correlation.

Together with other physical factors promoting clogging, like intense positive hydraulic gradient between the river water level and the groundwater, deposition of fine material in the Rhone River bed due to insufficient bed shear stress as well as high turbidities in the river water we consider the results significant.

Furthermore, a clear correlation with hydropeaking intensity is obvious. T1, which is only weakly affected by hydropeaking shows the highest hydraulic conductivities. In contrast, the transects TIIIa and TIIIb, which are most heavily affected by hydropeaking, show lowest hydraulic conductivities within the investigated river reaches.

The high-pass filtered data, describing infiltration at high water levels under hydropeaking conditions agree well with the literature data and show similar results for all of the investigated transects (Table 8C). The amplitudes of the correlation coefficients r , however, are quite weak.

4.6.2 Clogging

The specific infiltration rates (q) for the seasonal investigations (Table 8B) determined by cross-correlation of temperature signals vary between $0.1 \text{ m d}^{-1} < q < 1.8 \text{ m d}^{-1}$. They range near the lower end of the known infiltration rates of Swiss rivers compiled by Hoehn (2002), who reported rates $q = 0.05 \text{ m d}^{-1}$ for River Töss and $q = 3 \text{ m d}^{-1}$ for River Rhine. Specific infiltration rates under hydropeaking conditions, characterizing the intermittently flooded part of the river bed vary between $0.6 \text{ m d}^{-1} < q < 3.1 \text{ m d}^{-1}$ (Table 8C). In the case of TIIIa and TIIIb these values are based on very low correlation coefficients. The choice of the correct peak for the calculation of seepage velocity, hydraulic conductivity and specific infiltration is of major importance. Due to mixing of the Rhone River water with the adjacent groundwater, always the first positive peak if the high-pass filtered cross-correlation is relevant for the characterisation of the infiltration under hydropeaking conditions (Figure 21C and D and Table 8C).

The flow of each river contains a variable amount of suspended fine particles. In response to interaction between the turbulence of the channel flow, the settling properties of the suspended particles and the seepage rate, a certain amount of the fine particles intrude into the river bed. As a result of different processes, these fine particles are deposited on the river bed or are incorporated into its top layer so that the pore space is reduced, i.e., the river bed is progressively clogged (Schaelchli, 1992). The characteristics of such clogged river beds are: (a) a dense positioning and a compact texture (low porosity), (b) comparatively high resistance against increasing discharges, and (c) reduced hydraulic conductivity (Schaelchli, 1992).

Under natural conditions this clogged layer can break up during high-flood events, so that the deposited fine particles are resuspended and flushed downstream. This declogging mechanism is governed by the dimensionless flow shear stress Θ . For increasing values up to $\Theta < 0.056$, the clogging process is accelerated; for $\Theta > 0.060$, the clogged layer starts to break up (Schaelchli, 1992; Schaelchli, 1993).

Baumann (2004) calculated the dimensionless flow shear stress Θ for different locations and discharge conditions up to $110 \text{ m}^3\text{s}^{-1}$ in the river Rhone. Only in one profile downstream of the water release of the Grande Dixence reservoir (comparable to transect TII in this study) values up to $\Theta = 0.059$ were found under hydropeaking conditions indicating slightly destabilized conditions of the riverbed (Baumann and Meile, 2004). Our results confirm that significant de-clogging in the river bank does not take place.

4.6.3 Temporal and Spatial Variations in Clogging

Analysing the water level and temperature hydrographs during a major flood event (Figure 20) shows that diurnal and seasonal variations in hydraulic conductivity must be caused by two distinct zones within the river bank: a lower zone being permanently saturated and characterized by low hydraulic conductivities as well as a better permeable upper zone, respectively. This zone is flooded during hydropower production.

The water level and temperature records of the flood event in October 2000 in transects TI, TII and TIII allows to locate this boundary zone about 1 to 1.5 m below the top of river bank (Figure 13B - point c, Fehler! Verweisquelle konnte nicht gefunden werden.). For TII, TIIIa and TIIIb, this zone corresponds to the average summer water level in the river at these transects. Figure 17 shows the effect of two different layers of different permeabilities in TII during July and August 2003. The diurnal variations in temperature are transferred into the groundwater until the water level in TII-R is above ~467.3 m ASL (Fehler! Verweisquelle konnte nicht gefunden werden.). Temperature peaks in TII-G follow with a time lag between 8 h and 12 h (Figure 17) to the initiating peaks in TII-R (a = 12 h, b = 10 h, c = 8 h, d = 10 h, e = 10 h, f = 12 h) and follow hence the diurnal pattern (Table 8C).

The time-lags observed in Figure 17 are slightly higher in comparison to the diurnal time-lag of 10 h computed in Table 8C. Below this limit (Figure 17, grey box), the diurnal temperature variations in the groundwater disappear caused by lower hydraulic conductivity in the lower part of the river bed. Infiltration follows the seasonal pattern (Table 8B). Between the 3rd and the 6th of August, the temperature in the Rhone River approaches the temperature in the groundwater body. We assume for that reason, that no diurnal variation in the temperature signal of TII-G can be observed.

We guess, however, that the diurnal approach is only applicable under conditions like the one shown in Figure 17 where a considerable temperature gradient between the river and the groundwater leads to a significant cross-correlation coefficient (Table 8C). The significance level in auto-correlation analysis is in general set to $r^2 = e^{-1} = 0.37$ (Perrochet, P., personal communication). For the seasonal approach, this limit of correlation is only exceeded for transects TI and TIIIb, for the diurnal approach only in TI. Furthermore, during summer 2003, the temperature gradient between TIIIb-R and TIIIb-G (Figure 18, Table 7) was two times larger than the temperature observed in TII (Figure 17), but no significant transfer of the temperature signal to the groundwater could be observed. Severe clogging of the river bed caused by permanent and intense hydropeaking could be the reason for this non-establishment of layers of different permeability.

Flood Event in October 2000	TI	TII	TIIIa	TIIIb
Elevation of top of riverbank [m ASL]	n.a.	468.5	461.8	462.0
Elevation level of infiltration [m ASL]	472.4	467.3	460.5	460.4
Average water level between 05/02 and 08/02 [m ASL]	473.0	466.9	460.2	460.2

Table 9: Elevation levels of enhanced infiltration: The start of enhanced infiltration occurs during a flood event at the water level when the temperature in the wells suddenly starts to drop. The average water levels were calculated from averaging the difference between the maximum and the minimum daily water level.

4.6.4 Quantification of the Seepage Rate

The Research Centre on Alpine Environment, CREALP, established an averaged equipotential map over the period between 1991 and 2001 for the high water and the low water season. These maps were overlaid by means of a GIS with the geographical and structural data of the riverbed of the River Rhone to determine the permanently saturated river-groundwater interface during the low water season in winter and the high water season in summer.

Between the villages of Aproz and Branson the ~20 km long river reach was found to have a directly saturated connection between river and groundwater table of $6.3 \cdot 10^6 \text{ m}^2$ during the low water period in winter and $7 \cdot 10^6 \text{ m}^2$ during the flood season in summer. Multiplying the calculated surface for the summer months with the average specific infiltration rates found in Table 8B results in absolute infiltration rates between $Q \sim 2.7 \text{ m}^3(\text{km s})^{-1}$ for TI and $Q \sim 0.6 \text{ m}^3(\text{km s})^{-1}$ for TIII. In 2004 the average discharge in the Rhone River at TI (BWG gauging station Sion) was $\sim 12.4 \cdot 10^6 \text{ m}^3\text{d}^{-1}$ and $Q \sim 14.2 \cdot 10^6 \text{ m}^3\text{d}^{-1}$ at TIII at the gauging station in Branson (BWG, 2004). Assuring continuous hydraulic conditions the river Rhone is characterized by seepage rates of ~37 % in TI (unaffected of hydropeaking) and ~7 % in TIII (highly affected by hydropeaking), respectively.

4.6.5 Consequences for River Rehabilitation

Tracing the river-groundwater interaction reveals details of the reduced permeability of the river bank. A high degree of clogging in the lower part of the river bank strongly impedes surface water-groundwater exchange. Rehabilitation scenarios are therefore facing conflicting objectives. The more dynamic river morphology and hydraulics achieved by widenings typically also mitigate the siltation of the river bank. River-groundwater interactions are re-established resulting in benefits for the epigean fauna, (Brunke and Gonser, 1997; Walther, 2002) spawning conditions for fish (Jungwirth, 1998) as well as the replenishment of the adjacent aquifer for flood control (Hunt, 1990). In the River Rhone as a formerly braided system, widenings deserve special consideration as a rehabilitation measure.

Improving vertical connectivity (Ward, 1989), however, can not be achieved without serious trade-offs. During the summer months, the groundwater table in the Rhone Valley lies typically up to 0.5 m below the average water level in the river. If rehabilitation measures increase the permeability, the water level in the river-near aquifer could rise and potentially damage the valley's agriculture, infrastructure (Greco, 2001) and public drinking water supply (Regli et al., 2004; Regli et al., 2003). This danger is specifically important when levees are dislocated and the lower parts of the river bank are disrupted (Fehler! Verweisquelle konnte nicht gefunden werden.). In this case, the hydraulic conductivity in this currently highly clogged lower part of the river- groundwater interface will increase temporarily and the considerable hydraulic gradients between river and groundwater will lead to much larger seepage rates. This intensified infiltration of river water could lead to water quality problems for drinking water supplies located near the river.

4.7 Conclusion

Stream-groundwater interactions are influenced significantly by riverbed-clogging processes especially in canalised river reaches (Bardossy and Molnar, 2004; Gutknecht et al., 1998; Schaelchli, 1993). The results of our study suggest that the river reach between Sion and Branson is clogged, especially in the lower, permanently flooded part of the river bank. We estimate that, depending on the

transect, the hydraulic conductivity in the river bed is between a factor of ~3 and ~50 smaller than in the aquifer. This results in slow seepage velocities of river water infiltration despite of pronounced hydraulic gradients between the river water surface and the adjacent groundwater. The clogging of the river bed is most pronounced in reaches of the river that are highly affected by hydropeaking.

Subject of the current research is the existence of layers with higher permeability causing daily varying infiltration of Rhone water into the aquifer. Based on investigations of single flood events as well as high-pass filtering and cross-correlation of temperature records, we hypothesize, that this short term infiltration takes place in the upper part of the river bed and is characterized by hydraulic conductivities comparable to those measured by pumping tests in the groundwater of the overbank. Further studies should provide more insight into this vertical zonation of hydraulic conductivities.

Temperature as a tracer is a reliable and inexpensive tool for quantifying river-groundwater interaction on a seasonal base. We have shown here, that clogging in heavily modified river reaches can be quantitatively assessed by cross-correlation of seasonal temperature fluctuations in the river and groundwater wells in the river bank. The diurnal and weekly fluctuations due to the hydropeaking regime provided further insights into matrix properties of the discontinuously flooded part of the river bed.

4.8 Acknowledgement

The study was funded as a contribution to the Rhone-Thur project (www.rhone-thur.eawag.ch), which is supported by the Swiss Federal Office for Water and Geology, the Swiss Agency for the Environment, Forests and Landscape, the Swiss Federal Institute for Environmental Science and Technology (EAWAG) and the Swiss Federal Institute for Forest, Snow and Landscape Research (WSL). The natural science module of this project was directed by Armin Peter. We thank him for his enthusiastic leadership and the following individuals for their help with sampling campaigns, access to existing data and scientific input: Toni Arborino, Dominique Bérod, Alexandre Vogel and René Décorvet.

5

Seasonal Variability in the Chemical and Isotopic Composition of Alluvial Groundwaters in the Rhone Valley

“N’étant pas navigable à cause de son cours trop rapide et trop irrégulier, le Rhone n’est aucune utilité comme voie de communication. Au contraire il est un obstacle: pour le traverser il faut de nombreux ponts.” (Mariétan, 1953)

5.1 Introduction

Several authors investigated the interaction between a river and the adjacent groundwater body using geochemical tracers. Stuyfzand (1989) quantified the infiltration rate into groundwater by bank filtration from the river Rhine in the Netherlands by stable-isotope methods. The same approach was used to investigate the hydraulic connection between the Columbia River and the Blue Lake aquifer in Portland, OR (McCarthy et al., 1992). Using physical methods, Wett (2002) measured groundwater levels, temperature and electric conductivity in the river and in adjacent groundwater wells at the river Ens in Austria in order to quantify bank filtration. Sheets (2002) cross-correlated time series of electric conductivity in the Great Miami River, Ohio to determine the average travel time from the infiltrating river to the monitoring wells.

The previous chapters extend the existing knowledge to river systems affected by hydropeaking using a combination of the tracers ^{18}O and sulphate (Chapter 3) and temperature (Chapter 4). These methods allowed only the quantification of river groundwater-interaction on a seasonal scale, but were not specific enough to detect varying infiltration rates under diurnal and weekly hydropeaking conditions.

This chapter documents additional results in the limitations of geochemical tracers at short time scales and on the insights obtained at larger temporal and spatial scales. A sampling campaign over an annual cycle in selected wells of transects TIII addressed the issues of temporal and spatial variability of tracer signals. Fortnightly sampling of river water and groundwater allowed a more precise characterisation of the infiltration and exfiltration behaviour of the Rhone River on a seasonal base. The following questions that indirectly arose from the previous chapters were investigated more in detail:

1. Response of isotopic and geochemical tracers to daily fluctuations
using stable isotopes as tracer substances in chapter 3 showed good results in the investigation of river groundwater interaction on a seasonal time scale. This chapter addresses the question whether they can also be used for the investigation of river groundwater exchange under hydropeaking conditions.

2. Location of groundwater recharge

In chapters 3 and 4 it was shown that infiltration of river water into the aquifer in the investigated areas is rather limited on seasonal as well as on diurnal time scales. This chapter addresses the question whether groundwater infiltration could occur further upstreams.

3. Data from shallow wells

The existing shallow groundwater wells in the overbanks of transects TIIIa and TIIIb were not documented in chapter 4. These shallow sampling wells were sampled and analyzed in parallel to the deep wells for stable isotopes and major ions. They give additional insights in the river-groundwater interaction and support the findings made in the previous chapters. For completion, these results are presented in the following paragraphs.

5.2 Study Site and Methods

The area of investigation is identical to transect TIII in chapter 4 but expanded laterally to the valley slopes located north and south of the river. Vertically the study site was augmented by adding sampling results from shallow wells (Figure 22). The classification of the monitoring wells was modified from official and semi-official nomenclatures. Table 10 gives an overview.

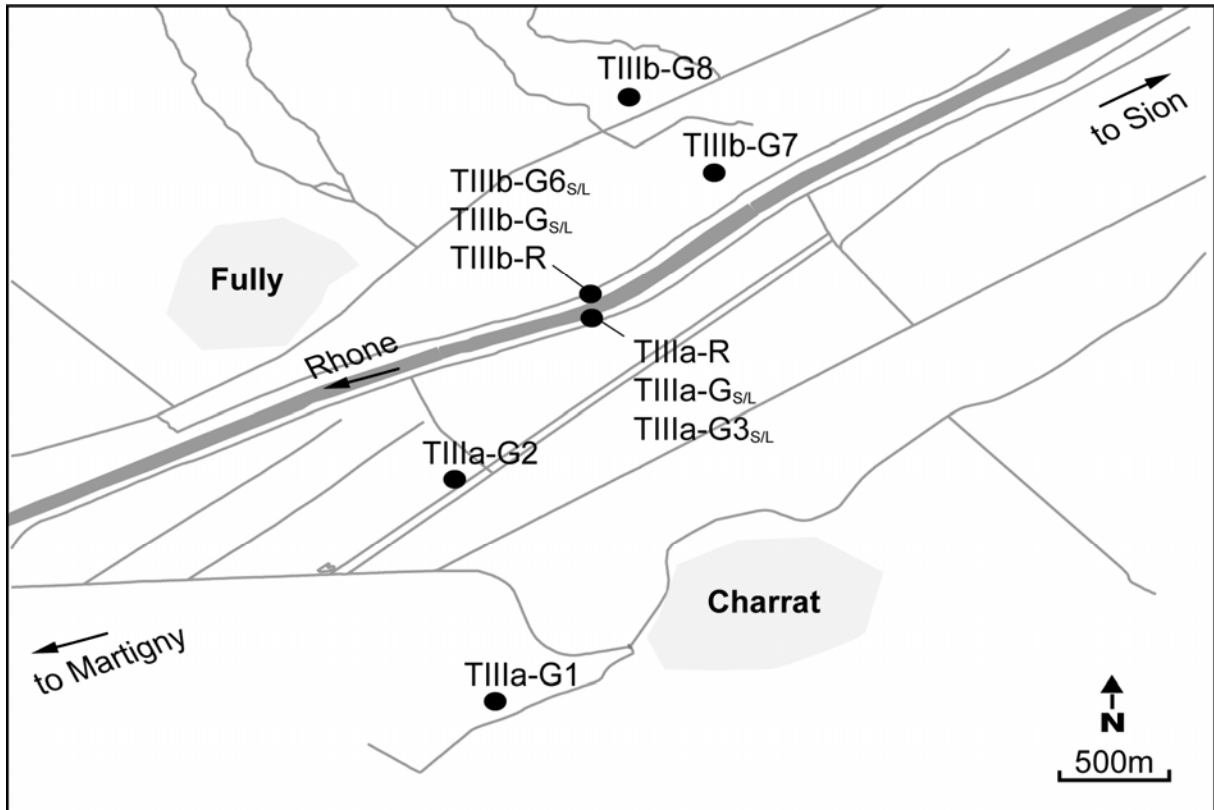


Figure 22: Study site between Martigny and Sion. Wells TIIIa-R, TIIIa-G_L, TIIIb-R and TIIIb-G_L are identical to the wells defined in chapter 4 (Figure 13A and B). The additional wells TIIIa-G₁, TIIIa-G₂, TIIIa-G₃, TIIIb-G₆, TIIIb-G₇ and TIIIb-G₈ enlarge the transect to the valley slopes north and south of the river. Subscripts S and L are indicative for “short” and “long” wells.

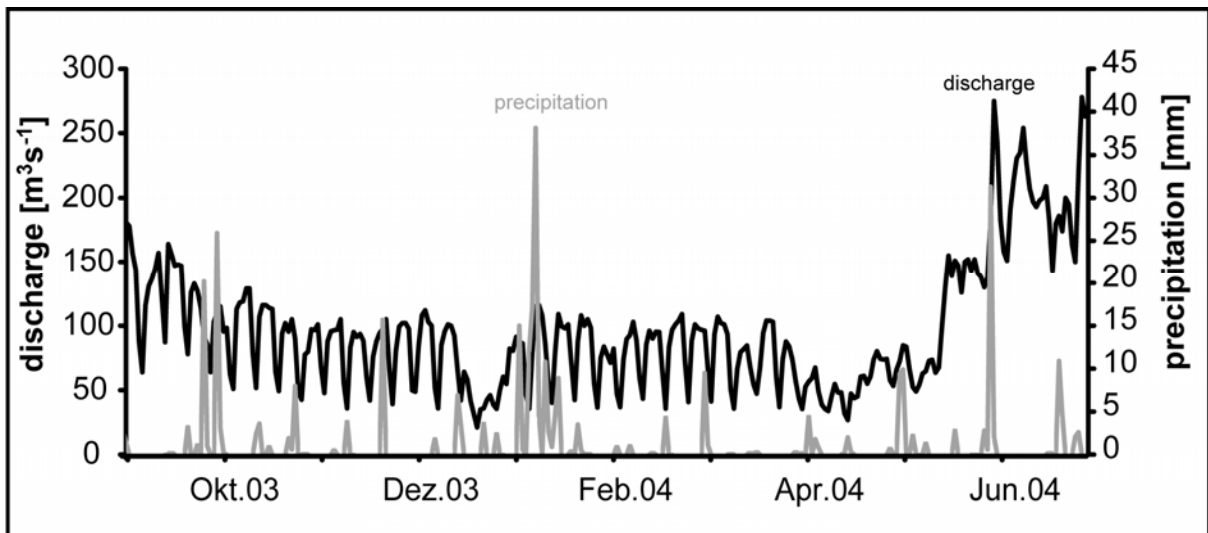


Figure 23: Discharge hydrograph of surface water the Rhone at transect TIIIa-R and precipitation at the monitoring station in Sion.

this work	nomenclature	
	field name	source
P1	Lac des Ecussons	field name
P2	Lac des Epines	
P3	Lac de la Bourgeoisie	
P4	Lake next to river Printse	
GW1	05-F06	Hydro Rhone Project see (GEOVAL, 1986))
GW2	05-K02	
GW3	05-B1	
GW4	05-D02	
GW5	05-F75	
TIIIa-G1	06-Y25	
TIIIa-G2	06-X09	
TIIIb-G7	06-T56	
TIIIb-G8	06-T67	
TI-R	PM3-Rho	GEOVAL SA, Sion
TI-G	PM3-S1L	
TII-R	PT9-Rho	BEG SA, Vétroz
TII-G	PT9-S11 L	
TIIIa-G3 _S	PT8-S1C	
TIIIa-G3 _L	PT8-S1L	
TIIIa-G _S	PT8-S5C	
TIIIa-G _L	PT8-S5L	
TIIIa-R	PT8-Rho	
TIIIb-R	PT5-Rho	
TIIIb-G _S	PT5-S6C	
TIIIb-G _L	PT5-S6L	
TIIIb-G6 _S	PT5-S10C	
TIIIb-G6 _L	PT5-S10L	

Table 10: Conversion table of nomenclatures

The results in this chapter are mainly based on a continuous sampling campaign between September 2003 and July 2004. On a fortnightly base, selected groundwater wells and the river in the TIII (Figure 22) area were sampled and analyzed for stable isotopes, cations and anions.

The analyzed period was mainly characterized by two hydrological seasons and a few rain events within those periods: 1) The low water period from September to April was characterized by a maximum discharge between ~ 50 and $150 \text{ m}^3\text{s}^{-1}$. Intense precipitation on January, 13th 2004 were responsible for significant water level increase in the groundwater wells TIIIa-G1, TIIIa-G2, TIIIb-G7 and TIIIb-G8 (Figure

24), while the discharge in the river itself increased only marginally. 2) With the beginning snowmelt during May 2004, the Rhone discharge increased to about $270 \text{ m}^3\text{s}^{-1}$. The observed groundwater wells did not show significant increase in water level in this spring period.

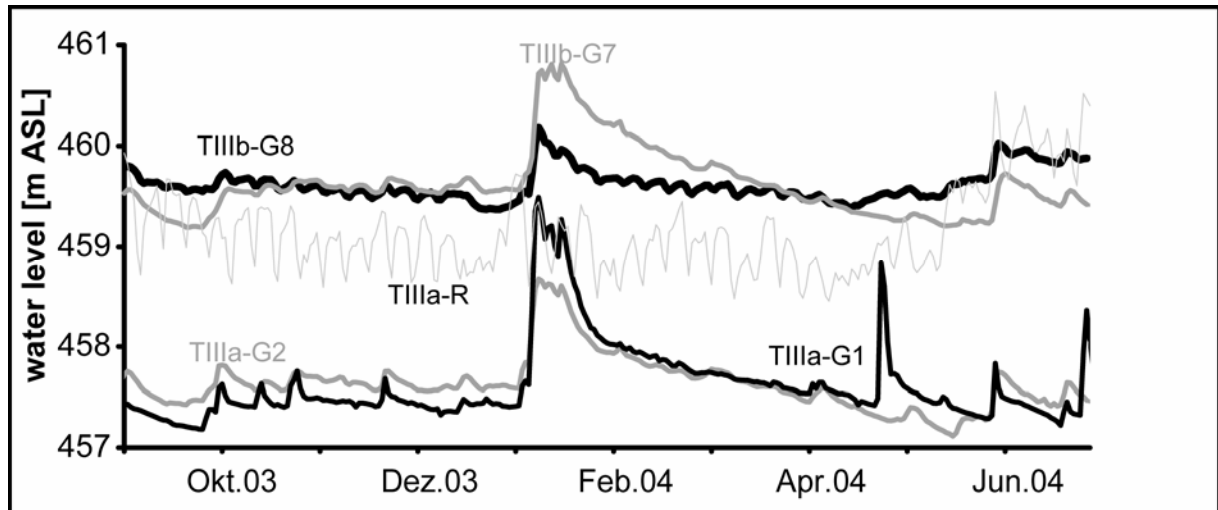


Figure 24: Hydrograph in the Rhone TIIIa-R and in the groundwater wells TIIIa-G1, TIIIa-G2, TIIIb-G7 and TIIIb-G8, recorded in the period of time between September 2003 and June 2004.

5.3 Results and Discussion

5.3.1 Tracers at short time scales

Reservoirs release water to the Rhone River by the turbines of hydropower plants located in the valley. This results in clear fluctuations of discharge and hence water level in the river. Figure 25 shows times series of $\delta^{18}\text{O}$ and water level measurements in the Rhone River near Branson. Water level fluctuation is characterized by clear “double hydropeaks” up to 75 cm on weekdays but only marginal fluctuations on Saturday and Sunday.

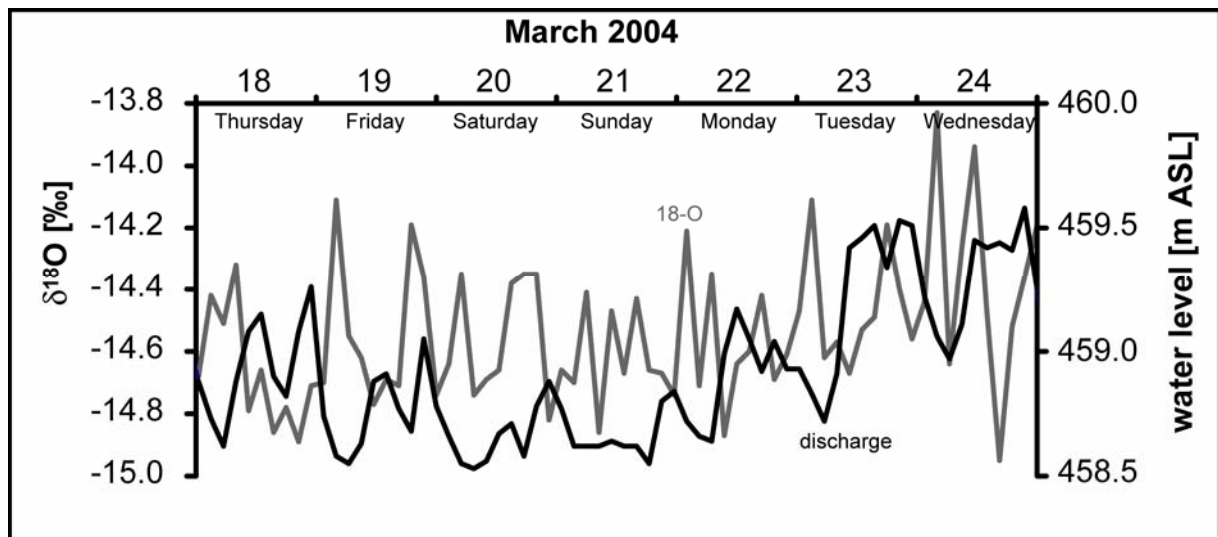


Figure 25: Time series of discharge and $\delta^{18}\text{O}$ in the Rhone River near Branson. Using three automatic sampling devices connected in series, samples were taken between the 18th and the 25th of March 2004 with a temporal resolution of 1.5 h.

Therefore, one would expect the same regular fluctuations in stable isotope composition of the Rhone water caused by isotopically depleted reservoir water. As shown in Figure 25 no correlation between water level and isotopic composition can be observed. Applying an average precision of 0.26 ‰ (chapter 2.5.2) results in a $\delta^{18}\text{O}$ signal with no significant trend, respectively no regular fluctuations. One reason for this noisy $\delta^{18}\text{O}$ signal in the river might be the similarity of the isotopic signal in the river ($\delta^{18}\text{O}_{\text{average}} = -14.5 \text{ ‰}$) with the $\delta^{18}\text{O}$ content in the reservoir water in winter ($\delta^{18}\text{O}_{\text{average}} = -14.1 \text{ ‰}$) as shown in Table 3.

This interpretation was drawn from a sampling campaign that lasted for only one week in winter. It might be possible, that the investigation of $\delta^{18}\text{O}$ records over a long period of time using filtering and cross correlation techniques would identify existing correlations. However, due to the costly and time consuming analytical procedure of stable isotope analytics, the method applied in chapter 4 can not be used.

5.3.2 Lateral Recharge

The river water in comparison to the groundwater is depleted in sulphate. For that reason, the seasonality of sulphate concentration in the river can be used to obtain qualitative and quantitative information about the exfiltration of aquifer water in the

river and the discharge of the channels draining the alluvial floodplain. Fette et al. (2005) showed that 51 % of the increase in winter sulphate flux must be due to diffuse exfiltration from the aquifer to the river. Fette et al. (submitted) revealed, however, that at the investigated transects, exfiltration of groundwater in summer is virtually not existent. Hence, sulphate rich groundwater must enter the river further upstream.

Indication for this location is given by Schuerch (2000b). He studied the aquifer of the Pfywald area, which is situated upstream, east of the town of Sion. This unconfined Rhone alluvial aquifer, composed of superficial glacial outwash deposits, is an important source of groundwater. The average groundwater flow velocity in the Rhone aquifer is about 110 m d^{-1} and hence significantly higher than in the Aproz area (Figure 7), calculated to around 5 m d^{-1} (Fette et al., 2005). During the high discharge period in June and August, the Rhone River strongly recharges the Pfywald aquifer with weakly mineralized water. For August 1996, Schuerch (2000a) and (2000b) found, that 75 % of the aquifer recharge was Rhone River water and 25 % SO_4 -rich groundwater. On the other hand, during the low discharge periods (November to April), the aquifer of the Rhone alluvium was exclusively recharged by SO_4 -rich water from the slopes of the Rhone valley, because the Rhone River bed in this area was almost dry in winter (Schuerch, 2000a, Schuerch, 2000b)

5.3.3 Spatial Variability in Aquifer Geochemistry

Because of its dense groundwater well setting within the levee, transects TIIIa and TIIIb allow a broader analysis on the interaction between the river, the adjacent aquifer and groundwater recharge from the slopes (Figure 22). A geochemical approach, using ^{18}O and sulphate as a tracer (Fette et al., 2005) as well as a geophysical approach, correlating temperature records (Fette, submitted) revealed only limited interaction between the river and the groundwater.

Further results of a continuous sampling campaign between September 2003 and July 2004 reconfirm the observations and provide further insights. Normalizing $\delta^{18}\text{O}$ and sulphate to alkalinity reveals a mixing line between the endmembers TIIIa-G1

and TIIIb-G7 (groundwater originating from the valley slopes) and TIIIa-R/ TIIIb-R (river water) (Figure 26A). The geochemical properties of the groundwater in well TIIIa-G2 (Figure 22, Figure 26A), distant around 500 m from the river, falls clearly on this mixing line.. G8 shows a very distinct signature which must be due to additional effects (Figure 26A). Distinct summer/winter variations are observed in the River but are dampened considerably in the groundwater wells (except TIIIa-G2).

The comparison of these mixing lines with river near groundwater in TIIIa-G_{L/S} and TIIIb -G_{L/S} shows an almost identical summer geochemical signature in TIIIa-G_L/TIIIb-G_L with the summer pattern in the river (Figure 26B). The short wells TIIIa-G_S and TIIIb-G_S of the levee, however, are located somewhere between the river and “slope groundwater” endmembers and reflect therefore a different geochemical signature.

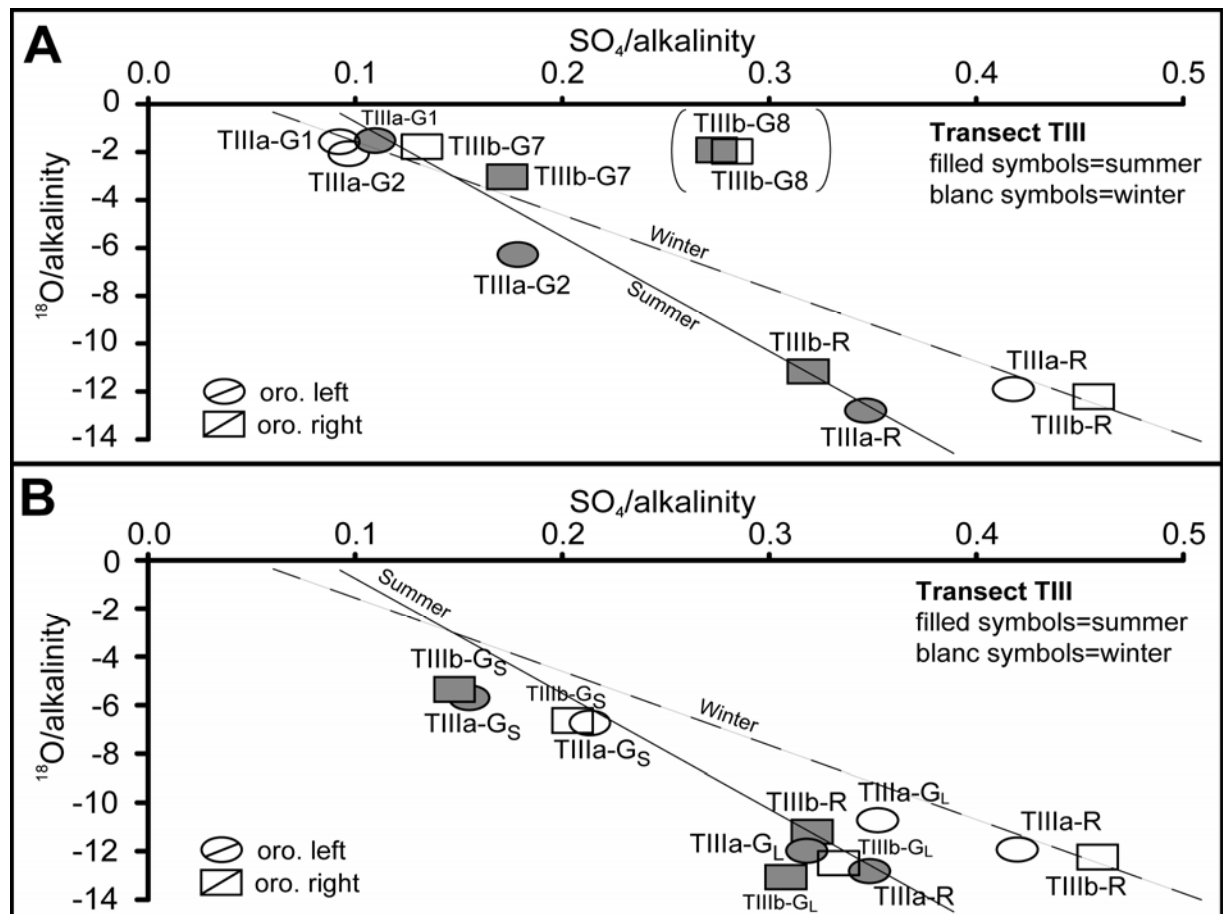


Figure 26: (A) Groundwater wells far from the Rhone River. The geochemical signatures are different in all wells in comparison to the river. Winter trendline (solid) and summer trendline (dashed) calculated by means of linear regression show the mixing behaviour. TIIIb-G8 has been considered an outlier. (B) Groundwater wells close to the river within the levee. Long wells are similar to the geochemical signature in the river-short wells are not and are located on a mixing line between River and Groundwater. Trendlines from (A) are copied to (B) for comparison.

The geochemical properties of the groundwater wells in the levee-body (Figure 13A and B, Figure 22) reveal an increased connectivity especially in the long wells. alluvial aquifer. This leads to the conclusion, that the long wells (Table 6) are better connected to the Rhone River than the short wells (Fehler! Verweisquelle konnte nicht gefunden werden.). For that reason, the results in chapter 4 are based on monitoring of the long wells.

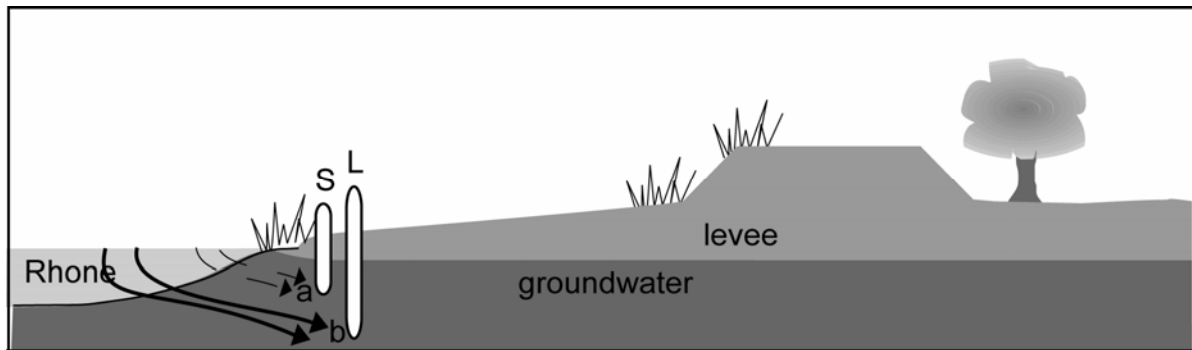


Figure 27: Connectivity between the Rhone River and the groundwater is increased in the lower groundwater (b) represented by measurements in the long well L. Groundwater measured in the short well (S) is less influenced by surface water infiltration (b).

5.3.4 Temporal Variations in Aquifer Geochemistry

For observation of single events during the low and the high water season, the TIII-wells were sampled between September 2003 and June 2004 on a two-weekly base. The water level hydrographs during this period of time in different wells are shown in Figure 24.

Precipitation Event in January:

Run-off from an Alpine basin depends strongly on snow-melt, which in such environments can occur very rapidly and induce very sharp changes in the amount and isotopic composition of discharge (Gat and Gonfiantini, 1981). Water level variations in TIIIa-G1, TIIIa-G2, TIIIb-G7 and TIIIb-G8 (Figure 24) indicate that the precipitation event was mainly focused on the mountain slopes.

It did not cause significant variations in the river discharge hydrograph (**Fehler! Verweisquelle konnte nicht gefunden werden.**) or the water level in the river (Figure 24) but was source of a simultaneous increase of the concentrations in

alkalinity, sulphate and $\delta^{18}\text{O}$ ratio in the Rhone River (Figure 28). These short-term geochemical variations in the Rhone River due to the rain event in January were not observed in the adjacent groundwater wells TIIIa-G_S nor TIIIa-G_L (Figure 29).

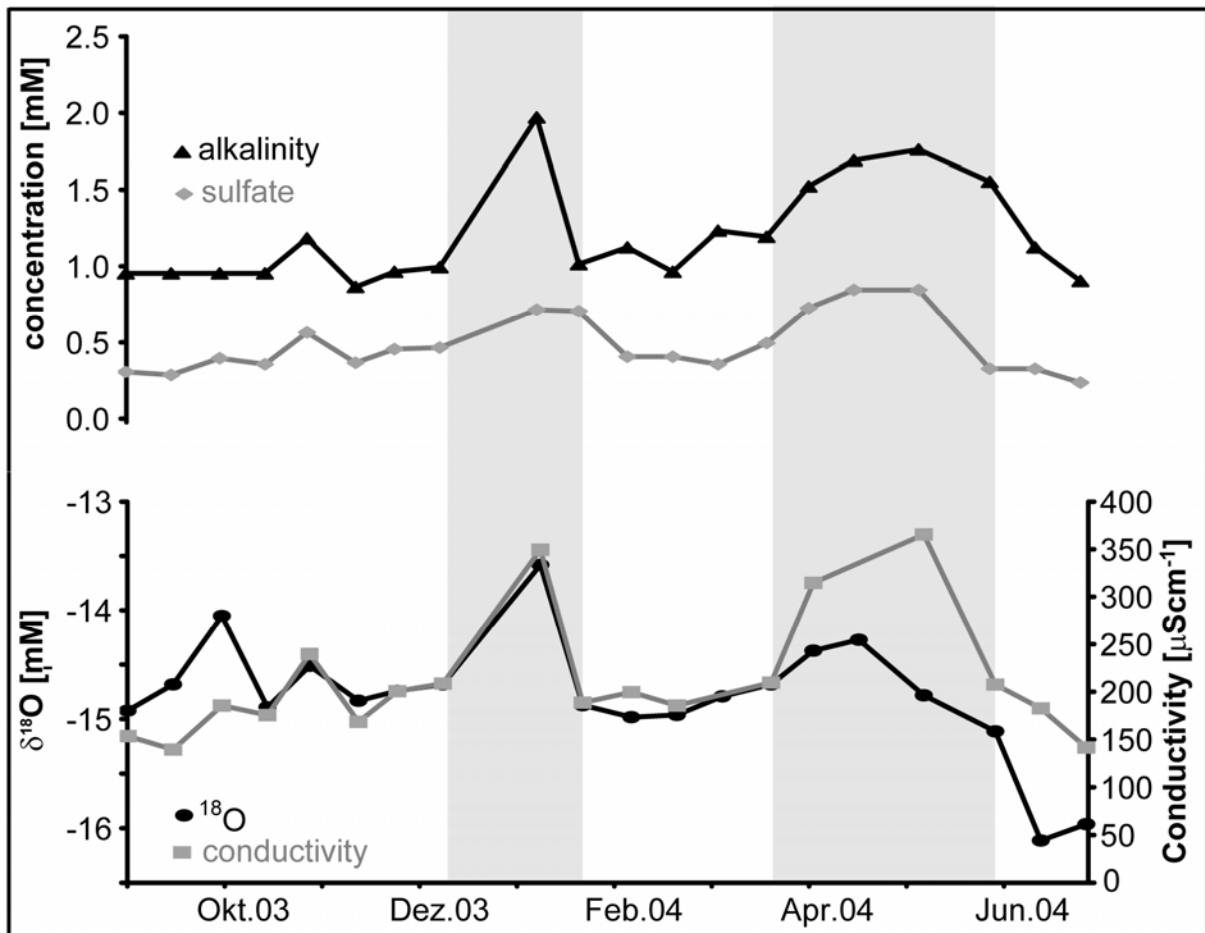


Figure 28: Hydrograph of different chemical parameters in the Rhone River at TIIIa-R

This extends the findings made in chapter 4 to the low water season, indicating limited interaction between the surface water and the groundwater. Furthermore, it supports other evidence (Schuerch, 2000a, Schuerch, 2000b) of a zone with increased river-groundwater interaction that could be localized in the Pfywald area (see chapter 5.3.1). There the precipitation event led most probably to an exfiltration of groundwater to the river causing higher mineralization, and hence higher concentrations of the monitored parameters in the river.

Snowmelt Period starting in April/ May

The snow-melt period is announced in the Rhone River geochemistry (TIIIa-R) in early April by increasing concentrations in sulphate, alkalinity and $\delta^{18}\text{O}$ ratio (Figure

28). This increase is most probably caused by 1) an increase of water discharge in the tributaries and 2) percolating melt water pushing higher mineralized and isotopically less depleted ground water in the Rhone River. A couple of weeks later, with the beginning high discharge water season in mid-May, a sudden decrease in sulphate and alkalinity concentrations as well as $\delta^{18}\text{O}$ were observed in the adjacent groundwater. Figure 29 shows, in the long and in the short well nearest to the Rhone River, an increase in concentration of alkalinity and sulphate during the whole low discharge period. With increasing discharge in the Rhone River mid-May the concentrations in all plotted parameters decrease, also $\delta^{18}\text{O}$ ratio drops towards more negative values and indicates infiltration of Rhone River water to the more depleted aquifer. Interestingly, while sulphate and $\delta^{18}\text{O}$ show quite similar data in the short and the long well, alkalinity exhibits elevated concentrations in the short well. This might be due to two different layers in the aquifer: a deeper layer that is mainly influenced by the Rhone River and a shallow layer mainly influenced by mountain water percolating from the mountain slopes.

5.3.5 Conclusion

Summarizing all the collected and interpreted data leads to the following answers of the introductory questions:

- the response of isotopic tracers to daily fluctuations of discharge in the Rhone River due to hydropeaking is not sensitive enough to use it for the investigation of river-groundwater interaction.
- As a result from the interpretation of mixing between river water and groundwater originating from the mountain slopes it could be shown that the deep groundwater wells TIIIa-G_L and TIIIb-G_L are better connected to the Rhone River than the short wells. For that reason, the results in chapter 4 are based on monitoring of the long wells.
- the results in this chapter based on geochemical tracers and interpreted on a seasonal time scale support the findings made in chapter 3 and 4. Neither exfiltration nor infiltration can be observed during the low water period, whereas limited infiltration of river water in the adjacent aquifer can be observed during the

high water season beginning in May. Furthermore, specific literature indicates groundwater recharge in the Pfywald area.

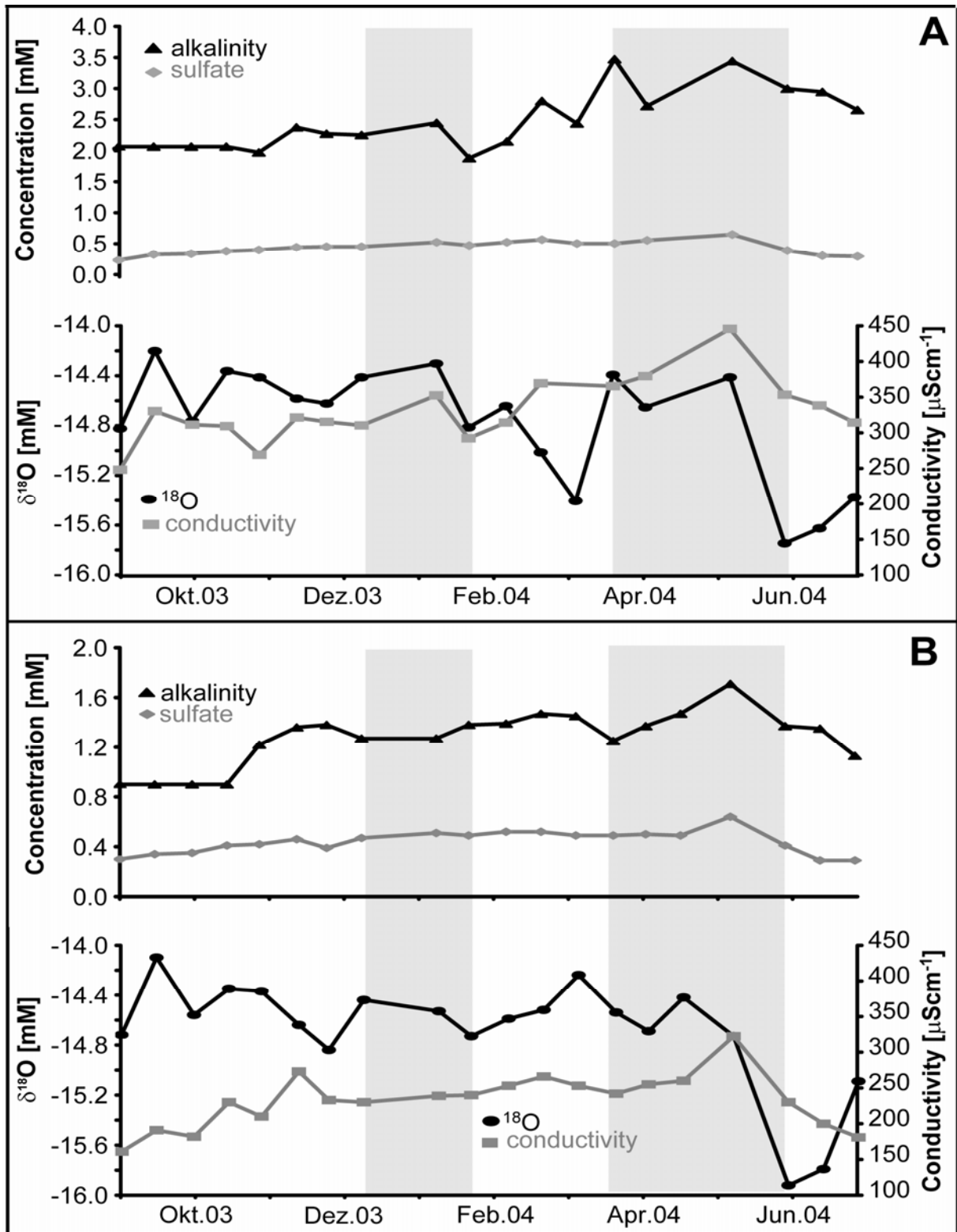


Figure 29: (A) hydrograph in Tilla-G_s und (B) hydrograph in Tilla-G_L

6

Ecological Consequences of Hydropeaking

Fette, M., Weber, C., Peter, A. and Wehrli, B.

Submitted to and adapted from: Journal for Nature Conservation

Adapted from: EAWAGnews 55

“Jusqu’ici je me suis surtout attaché à exposer le côté pratique de la lutte contre l’eau en Valais. Je ne voudrais pas omettre de dire aussi la grande beauté de notre fleuve (...) symbole d’une force inflexible, toujours jeune et triomphante, qui descend vers le soleil, il suscite dans notre esprit des pensées vivifiantes.” (Mariétan, 1953)

Hydropower is an important source of electricity, and the recently deregulated energy market in Europe now promotes long-range trade within the continental grid (Flodmark et al., 2004). Until 2020 the electric power consumption in Europe might rise by 40 % (European Greenpower Marketing, 2004). With an increasing share of renewable energy sources such as wind power, peak production by hydropower schemes will be in high demand to stabilise variable production rates.

In 2000, Switzerland exported 7.1 TWh of a total annual production of 38 TWh. Among the electricity exporters, the country ranks third in the European electricity market (Portmann, 2003). Switzerland's hydroelectric power plants provide 58 % of the domestic energy production. About 60 % of this hydropower is generated in the Alps (Truffer et al., 2001; Wueest, 2002). Approximately 130 large hydrodams retain a quarter of the annual discharge within the main alpine watersheds of the rivers Rhone, Ticino, Rhine, Reuss and Aare (Wueest, 2002).

In the Canton Wallis (the upper Rhone valley), high capacity reservoirs were built in the last 50 years, storing a significant water volume during times of snowmelt and rainfall. The two main hydropower stations of the Grande Dixence hydropower scheme, for example, turbinated 611 millions m³ of water in 2003 resulting in a total annual energy production of 2877 GWh (Grande Dixence, 2004). These power plants can bring more than 1000 MW of power online within one to two minutes.

6.1 A Difficult Situation for Ecology

Production of hydropower accounts for a wide range of environmental disturbances of alpine river systems (Truffer et al., 2003). Storage hydroelectric power schemes disrupt the river continuum (Vannote et al., 1980) acting as barriers for the longitudinal migration and drift of organisms (Stanford et al., 1996) and trapping sediment particles (Friedl and Wueest, 2002; Vorosmarty et al., 1997). Storage plants produce energy on demand, therefore they are brought online exclusively during periods of peak consumption. The resulting daily hydropeaking, characterized by intense and erratic fluctuations in water discharge impacts the biota downstream by disrupting the hydrological patterns and triggering catastrophic invertebrate drift

(Cortes et al., 2002). Further ecological consequences like a reduced persistence of vital habitat features (Whiting, 2002) or a reduction of fish biomass (Baran et al., 1995) are well documented in the literature.

Moreover, reservoir outlets are commonly located close to the bottom of dams, leading to a sudden decrease in water temperature when a large amount of cool bottom water is released at hydropeaking (Flodmark et al., 2004; Meier et al., 2004). In fish, having a body temperature varying with the surrounding (poikilotherm), food intake, digestion, absorption, catabolism, anabolism and excretion are all affected by the ambient temperature (Flodmark et al., 2004).

6.1.1 Reduced Benthic Diversity due to Hydropeaking Effects

Hydropeaking regimes are reducing aquatic biodiversity. The number of aquatic invertebrate species in streams that are subject to hydropeaking is lower than in streams with natural flow regimes. Tockner (2004) determined the aquatic macrozoobenthos Ephemeroptera-Plecoptera-Trichoptera (EPT) taxa along the Rhone River in the Wallis. He found 65 EPT-taxa corresponding to 80 % normally found in natural habitats. Highest numbers of taxa were observed in the headwaters while the lower, canalized reaches contributed only insignificantly to the total number of taxa (Tockner et al., 2004).

The same trend is observed, although less pronounced, for riparian ecosystems. Species diversity of terrestrial invertebrates is strongly dependent on the morphology of the stream bank: along artificially straightened river reaches, the number of species is approximately 50 % lower compared to stretches with a natural morphology (Fette et al., 2002). Tockner (2004) found significantly reduced numbers of terrestrial arthropods especially in river reaches strongly affected by canalisation and even smaller numbers in parts characterised by intense hydropeaking. The low density of terrestrial arthropods at the Rhone valley indicates limited trophic cross linking between the river and the adjacent groundwater (Tockner et al., 2004).

This means that the broadening of the river corridor may improve the terrestrial fauna along the riverbank, but in order to create better conditions for natural aquatic communities, the hydropeaking regime has to be mitigated (Fette et al., 2002).

6.1.2 Fish Ecology

The fish fauna in River Rhone is characterized by small species diversity. The assemblage is highly dominated by the brown trout whose population structure clearly differs from that of undisturbed populations (Weber and Peter, in preparation). Brown trout biomass varies considerably along the River Rhone. The highest values are found next to structured banks as those fixed by riprap. In exchange, in reaches with limited cover availability (e.g. canalized reaches or unstructured instream stripes) small biomasses were observed. Present data indicate a significant positive reaction of brown trout biomass to cover variables (Weber and Peter, in preparation), and, therefore, correspond well with results from previous studies (Heggenes, 1988).

Despite this positive reaction on cover availability, the biomass found in River Rhone is quite small. Concerning the banks, one reason certainly is that riprap structures –although they offer cover– represent poor substitutes for the structural richness of a natural river shore. The habitat conditions in riprap banks are relatively monotonous, and current protected sections are limited to the immediate shoreline zone. Shallow areas with precious habitats for young trout and other fish species are largely missing in these reaches. Accordingly, results by (Schiemer and Zalewski, 1992) indicate that in a reach with natural bank morphology higher fish biomasses can be found than along artificially fixed shorelines. In the instream sections of the River Rhone, the reduction in habitat heterogeneity is especially obvious. High current velocities dominate while pool-riffle sequences are largely missing.

Probably, the rehabilitation of the fish community in River Rhone can only be successful when structural improvements are linked with measures addressing the hydrological deficits such as hydropeaking and residual flow.

6.2 Possible Solutions

Rehabilitation is a major issue in river management. However, a high proportion of Rehabilitation projects fail because there is a fundamental lack of understanding of the principal mechanisms that create and maintain biodiversity and biocomplexity along river corridors (Karaus et al., submitted). The actual ecological performance of River Rhone shows massive deficits in a longitudinal and a lateral sense.

6.2.1 Longitudinal

The longitudinal benthic and fish fauna is characterized by a highly unnatural structure. The stability of fish habitat is massively affected due to poor cover availability and changing water levels. A high correlation between fish biomass and monotonous shoreline and instream morphology could be established (Fette et al., submitted).

Would rehabilitation efforts aimed at improving the shoreline and instream structures result in higher biomasses of brown trout and other fish-biological parameters? In the literature, most examples of river rehabilitation deal with measures like restructuring of banks, construction of instream structures or local widenings offering a more diverse habitat situation. Not only structure-dependent species like the brown trout benefit in such rehabilitated river reaches, but also other taxa with more specialized habitat, spawning or trophic requirements. In many cases positive effects on fish communities like higher species diversity (Jungwirth et al., 1995) and the return of natural reproduction (Habersack et al., 2000) were reported. Similarly, structural measures along the shoreline are of great importance for terrestrial organisms: along artificially straightened sections of streams, the number of species is approximately 50 % lower compared to stretches with natural morphology (Fette et al., 2002). The central question in the case of a hydrologically impaired river like the Rhone is whether structural measures alone will be effective. Doubts are legitimate as low biomass values were also found in several riprap stretches, with the best available habitat structure. Some trends are obvious among the many possible explanations

for this observation. The individual trout biomasses in reaches strongly affected by hydropeaking are generally smaller than in residual flow stretches or hydrologically unaltered sections of the River Rhone (Fette et al., *submitted*).

Among the several impacts of hydropeaking on fish reported in the literature (Baran et al., 1995; Whiting, 2002), the discussion of habitat persistence (Bain et al., 1988; Freeman et al., 2001) is of special importance for the case of River Rhone, especially in its lower part. With rapid fluctuations of the water level up to one meter, riprap structures are not permanently covered by water. Because the cover is not constantly available, the structure-dependent brown trout are facing a serious reduction of the habitat quality.

The reaction of other aquatic organisms on hydropeaking is similar. Benthic organisms, for example, are massively disturbed by the scouring effects due to the higher flow velocities (Cereghino and Lavandier, 1998). The aquatic invertebrate fauna living in the shoreline zone of hydropeaking-affected rivers is highly impaired compared with stretches of natural discharge regime (Fette et al., 2002). Forming the nutritional basis for many species, such effects on the invertebrate community can also have indirect feedbacks on the fish assemblage.

6.2.2 Lateral

The lateral dimension describes habitats in the transition zone between the river channel and its floodplain. Especially habitats in the interstitial zone of the river bed are among the first habitats that disappear as a consequence of river regulation and flow control (Karaus et al., *submitted*). For that reason, intact habitats in the heterogeneous transition zone between river and groundwater are virtually non-existent any more in the lower reaches of the Rhone River.

A high degree of clogging strongly impedes surface water-groundwater exchange. The transient changes in water level are not limited to the river itself, but also measurable in the near-river aquifer. This hydrological disturbance is likely to inhibit the ecological recovery when the lateral connectivity is improved by rehabilitation measures such as river widenings.

6.2.3 Possible Solutions

Rehabilitation scenarios are facing conflicting boundary conditions. The fish ecological situation can be significantly improved by effective rehabilitation of the longitudinal habitat structure. This success generally achieved by widenings is also positive in lateral terms by removing the clogging of the river bank.

River-groundwater interactions are re-established resulting in benefits for the epigean fauna (Brunke and Gonser, 1997; Walther, 2002), spawning conditions for fish (Jungwirth, 1998) as well as the replenishment of the adjacent aquifer for flood control (Hunt, 1990). In the river Rhone as a formerly braided system widenings are a rehabilitation measure that deserves special consideration.

Improving vertical connectivity, however, can not be achieved without serious trade-offs. During the summer month, the groundwater table in the Rhone Valley lies typically 0.5 meters below the average water level in the Rhone River. If rehabilitation measures increase the permeability, the water level in the river-near aquifer could rise and potentially damage the valley's agriculture, infrastructure (Greco, 2001) and public drinking water supply (Regli et al., 2004).

The boundary conditions are obvious: the River Rhone is heavily impacted by morphologic structures and intensively used for hydropower production. While the morphologic structures can be restored by creating river widenings, the status quo of the hydropower schemes is generally accepted because of the following reasons:

- the licences for the operation of most of the hydropower plants in Switzerland are valid for 80 years
- hydropower plants play an important role in terms of regulating the European power grid
- hydropower is considered a renewable energy with a favourable CO₂ balance in comparison with widespread fossil electricity production.

Normalization of the hydrologic situation though is essential for the success of the third correction of the Rhone River. It will therefore depend on the effective attenuation of hydropeaks in the river reaches being subject of rehabilitation measures. This can be realized by a combination of different hard technical and soft operational measures:

- River widenings should be planned as large, as long and as networked as appropriate. The reconstructed levee constraining the wider riverbed should be sealed to prevent rising water tables in the urbanised valley ground (Greco, 2001).
- In order to attenuate the hydropeaks in the connected river, the turbinated water should be stored in retention basins or underground reservoirs before being continuously discharged into the river (Moog, 1993). Underground reservoirs, however, are limited to smaller schemes with low tailwater discharge.
- Slower, more consistent powering up and down of the turbines could result in a more moderate hydropeaking rate (Halleraker et al., 2003). Such “soft” methods are effective only in combination with the “hard” approaches outlined above (Baumann, 2001).

Restoring a river while improving flood protection measures and adapting hydropower schemes for a more ecological operation requires an integrated approach and a considerable financial effort. The costs will be acceptable if alpine hydropower is considered a “green energy” (Bratrich et al., 2004) which requires ecological investments and is therefore not available for subsidising other more expensive sources of electricity.

6.3 Conclusion and Outlook

Local river widenings are measures often applied as revitalisation tools. Broadening a river bed leads to the development of natural river banks and creates more diverse aquatic habitats (Peter et al., 2005). In order to secure the valley bottom, however, flood protection dams will always be needed. Even if these new levee structures were not artificially sealed, re-clogging of the river bed would be just a matter of time due to the prevailing hydrological conditions. In the long run, replacing old dams with modern structures should hence not have any varying impacts on the hydrological status quo of the groundwater.

Geochemical tracers were used to qualitatively identify the interaction between river and groundwater. It could be shown that sulphate rich groundwater is an excellent tracer for water influx from the southern mountain range and can be used for identification of lateral groundwater sources in the area of investigation. The characterisation of river-groundwater interaction under hydropeaking conditions requires a high temporal resolution of samples which is the limiting factor for the use of wet-chemical methods. For that reason, temperature as a reliable and inexpensive tracer was used for the quantification of river-groundwater interaction under hydropeaking conditions. The results reveal that the hydraulic conductivity in the river bed is up to ~50 times smaller than in the aquifer. This results in slow seepage velocities of river water infiltration despite of pronounced hydraulic gradients between the river water surface and the adjacent groundwater. The clogging of the river bed is most pronounced in reaches of the river that are highly affected by hydropeaking. In the upper part of the river bed, only wetted during hydropeaking hours, hydraulic conductivity of the soil matrix is significantly higher and comparable to the values reported in literature.

Reduced permeability in the permanently wetted part of the river bed is caused by the high and permanent entry of fine sediments in the canalised river reach. Significant de-clogging in the river bank does not take place. For that reason, intact habitats in the heterogeneous transition zone between river and groundwater are virtually non existent. The absence of the epigeal fauna in the groundwater wells of the canalised reach between Sion and Martigny indicates disruption of the migration pathways between the surface water and groundwater habitat. The impairment of the hydrological exchange and biological connectivity between the river channel, and its groundwater aquifer may not only have consequences for the surface and subsurface fauna, but also for groundwater purity and supply in that region (Walther, 2002).

The investigation of river-groundwater interaction on a seasonal scale using stable isotopes, sulphate and temperature as tracers showed clear and coherent results. To a great extent, this is also true for infiltration and exfiltration under hydropeaking conditions. But there are still some open questions and discrepancies needing further research. The advanced work should focus on the further development of using

temperature as a tracer. Therefore, the expansion of the monitoring programme to a related tracer like electrical conductivity and processing of the data using time series analysis is advised for comparison of the results. In a next step, the application of a model, simulating the different processes in the river-groundwater interface could be helpful.

The presented work was part of a broad study on hydrologic, biologic and socioeconomic impacts of the 3RC. The overall results until today show, that reduction of hydropeaking seems to be the key for successful river- rehabilitation. Two boundary conditions are already quite obvious: the Rhone is already heavily impacted by hydraulic structures and is intensively used for power generation, so it is unrealistic to expect that the lower reaches of the Rhone will revert to an idyllic landscape rich in fauna and flora.

R References

- Aeschbach-Hertig, W., Peeters, F., Beyerle, U. and Kipfer, R., 1999. Interpretation of dissolved atmospheric noble gases in natural waters. *Water Resources Research*, 35(9): 2779-2792.
- Araguas-Araguas, L., Froehlich, K. and Rozanski, K., 2000. Deuterium and oxygen-18 isotope composition of precipitation and atmospheric moisture. *Hydrological Processes*, 14(8): 1341-1355.
- Bain, M.B., Finn, J.T. and Booke, H.E., 1988. Streamflow Regulation and Fish Community Structure. *Ecology*, 69(2): 382-392.
- Baran, P. et al., 1995. Effects of reduced flow on Brown Trout (*Salmo-Trutta L*) populations downstream dams in French Pyrenees. *Regulated Rivers-Research & Management*, 10(2-4): 347-361.
- Bardossy, A. and Molnar, Z., 2004. Statistical and geostatistical investigations into the effects of the Gabeikovo hydropower plant on the groundwater resources of northwest Hungary. *Hydrological Sciences Journal-Journal des Sciences Hydrologiques*, 49(4): 611-623.
- Baumann, P., 2001. Schwall und Sunk in schweizerischen Fliessgewässern. Grundlagenstudie im Auftrag des BUWAL, Abteilung Gewässerschutz und Fischerei, Bern.
- Baumann, P. and Meile, T., 2004. Makrozoobenthos und Hydraulik in ausgewählten Querprofilen der Rhone. *Wasser Energie Luft*, 96(11/12): 320-325.
- BEG, 2001. 3e correction du Rhone (secteur Bas-Rhone). Profils de mesures geotechniques PT5, PT8 et PT9 - Suivi annee 2000, Vétroz.
- Besson, O., Rouiller, J.D., Frei, W. and Masson, H., 1991. Campagne de sismique-reflexion dans la vallée du Rhône (entre Sion et Martigny, Suisse). *Bulletin Murithienne*, 109: 45-63.
- Beyerle, U. et al., 1999. Infiltration of river water to a shallow aquifer investigated with H-3/He-3, noble gases and CFCs. *Journal of Hydrology*, 220(3-4): 169-185.
- Beyerle, U. et al., 2000. A mass spectrometric system for the analysis of noble gases and tritium from water samples. *Environmental Science & Technology*, 34(10): 2042-2050.
- Blaschke, A.P., Steiner, K.H., Schmalfluss, R., Gutknecht, D. and Sengschmitt, D., 2003. Clogging processes in hyporheic interstices of an impounded river, the Danube at Vienna, Austria. *International Review of Hydrobiology*, 88(3-4): 397-413.
- Bradshaw, A.D., 1996. Underlying principles of restoration. *Canadian Journal of Fisheries and Aquatic Sciences*, 53: 3-9.
- Bratrich, C. et al., 2004. Green hydropower: A new assessment procedure for river management. *River Research and Applications*, 20(7): 865-882.

- Brunke, M., 1999. Colmation and depth filtration within streambeds: Retention of particles in hyporheic interstices. *International Review of Hydrobiology*, 84(2): 99-117.
- Brunke, M. and Gonser, T., 1997. The ecological significance of exchange processes between rivers and groundwater. *Freshwater Biology*, 37(1): 1-33.
- BWG, 2000. Temperature data for gauging point Rhône - Porte du Scex (2009) . Electronic source: http://www.bwg.admin.ch/lhg/moni/00/2009T_00.PDF, Access date 11/10/04.
- BWG, 2004. Hydrological data for Gauging Point Branson- Rhone (2024) . Electronic source: http://www.bwg.admin.ch/lhg/123/2024Q_04.pdf, Access date 12/01/2004.
- Cadisich, J., 1953. *Geologie der Schweizer Alpen*. Wepf & Co.
- Cereghino, R. and Lavandier, P., 1998. Influence of hypolimnetic hydropeaking on the distribution and population dynamics of Ephemeroptera in a mountain stream. *Freshwater Biology*, 40(2): 385-399.
- Clark, I. and Fritz, P., 1999. *Environmental Isotopes in Hydrogeology*. Lewis Publishers.
- Cole, T.M. and Buchak, E.M., 1995. "CE-QUAL-W2: A two dimensional, laterally averaged, hydrodynamic and quality model, Version 2.0, "Instruction Report EL-95-, US Army Engineer Waterways Experiment Station, Vicksburg MS.
- Cortes, R.M.V., Ferreira, M.T., Oliveira, S.V. and Oliveira, D., 2002. Macroinvertebrate community structure in a regulated river segment with different flow conditions. *River Research and Applications*, 18(4): 367-382.
- Craig, H., 1961. Isotopic Variations in Meteoric Waters. *Science*, 133(346): 1702-1703.
- CREALP, 2001. Région Sion-Branson. Extraits des cartes de la surface piézométrique moyenne hautes-eaux et basses eaux sur la période d'observation 1995-2001. Data by courtesy of Centre de recherche sur l'environnement alpin CREALP.
- Cunningham, A.B., Anderson, C.J. and Bouwer, H., 1987. Effects of sediment-laden flow on channel bed clogging. *Journal of Irrigation and Drainage Engineering-Asce*, 113(1): 106-118.
- Dansgaard, W., 1964. Stable Isotopes in Precipitation. *Tellus*, 16(4): 436-468.
- De Marsily, G., 1986. *Quantitative Hydrogeology - Groundwater Hydrology for Engineers*. Academic Press, San Diego, XIX, 440 S. pp.
- Drever, J.I., 1997. *The geochemistry of natural waters surface and groundwater environments*. Prentice Hall, Upper Saddle River, N.J., XII, 436 S. pp.
- Egli, D., 1996. *Caractéristiques hydrogéologiques de la digue du Rhône entre Branson et Fully*. Diploma thesis Thesis, Université de Neuchâtel.
- European Greenpower Marketing, 2004. *Hervorragende Aussichten für Wasserkraft*, 3rd European Conference on Green Power Marketing, Lausanne.
- Fette, M., submitted. Temperature Fluctuations as Natural Tracer for River-Groundwater Interaction under Hydropeaking Conditions. *Journal of Hydrology*.
- Fette, M., Kipfer, R., Hoehn, E., Schubert, C. and Wehrli, B., 2005. Assessing river-groundwater exchange in the regulated Rhone river (Switzerland) using stable isotopes and geochemical tracers. *Applied Geochemistry*, 20(4): 701-712.
- Fette, M., Pätzold, A., Tockner, K. and Wehrli, B., 2002. The Third Rhone Correction: rehabilitation despite operation of a power plant. *EAWAG news*, 55e: 21-23.

- Fette, M., Weber, C., Peter, A. and Wehrli, B., submitte. Hydropower production and river rehabilitation. Journal for Nature Conservation.
- Flodmark, L.E.W., Vollestad, L.A. and Forseth, T., 2004. Performance of juvenile brown trout exposed to fluctuating water level and temperature. Journal of Fish Biology, 65(2): 460-470.
- Freeman, M.C., Bowen, Z.H., Bovee, K.D. and Irwin, E.R., 2001. Flow and habitat effects on juvenile fish abundance in natural and altered flow regimes. Ecological Applications, 11(1): 179-190.
- Frei, C. and Schar, C., 2001. Detection probability of trends in rare events: Theory and application to heavy precipitation in the Alpine region. Journal of Climate, 14(7): 1568-1584.
- Friedl, G. and Wueest, A., 2002. Disrupting biogeochemical cycles - Consequences of damming. Aquatic Sciences, 64(1): 55-65.
- Gat, J.R. and Carmi, I., 1970. Evolution of Isotopic Composition of Atmospheric Waters in Mediterranean-Sea Area. Journal of Geophysical Research, 75(15): 3039-3048.
- Gat, J.R. and Gonfiantini, R., 1981. Stable isotope hydrology-Deuterium and Oxygen-18 in the water cycle. Technical Report Series 210, Vienna.
- GEOVAL, 1986. Projet Hydro Rhône. Rapport après trois ans d'observation. GEOVAL No: GEO 3/05.
- Gleick, P.H., 2003. Global freshwater resources: Soft-path solutions for the 21st century. Science, 302(5650): 1524-1528.
- Grande Dixence, 2004. 53e rapport. Exercice 2002-2003.
- Greco, A., 2001. Hochwasserschutz Reuss. Vernässungen entlang des linken Reussdammes in Attinghausen. 97177 AG/kh, CSD Ingenieure und Geologen AG. Im Auftrag des Kantons Uri, Amt für Tiefbau, Altdorf.
- Gutknecht, D., Blaschke, A.P., Sengschmitt, D. and Steiner, K.H., 1998. Kolmationsvorgänge in Flusstauräumen- Konzeptionen und Beobachtungen. Österreichische Ingenieur- und Architekten- Zeitschrift ÖIAZ, 143(1): 21-32.
- Habersack, H., Koch, M. and Nachtnebel, H.P., 2000. Flussaufweitungen in Österreich - Entwicklung, Stand und Ausblick. Österreichische Wasser- und Abfallwirtschaft, 52(7/8): 143-153.
- Haeberli, W., Frauenfelder, R., Hoelzle, M. and Maisch, M., 1999. On rates and acceleration trends of global glacier mass changes. Geografiska Annaler Series a-Physical Geography, 81A(4): 585-591.
- Halleraker, J.H. et al., 2003. Factors influencing stranding of wild juvenile brown trout (*Salmo trutta*) during rapid and frequent flow decreases in an artificial stream. River Research and Applications, 19(5-6): 589-603.
- Harvey, J.W., Wagner, B.J. and Bencala, K.E., 1996. Evaluating the reliability of the stream tracer approach to characterize stream-subsurface water exchange. Water Resources Research, 32(8): 2441-2451.
- Heggenes, J., 1988. Physical habitat selection by brown trout (*Salmo trutta*) in riverine systems. Nordic Journal of Freshwater Research, 64: 74-90.
- Hoehn, E., 2002. Hydrogeological issues of riverbank filtration- a review. In: C. Ray and NATO (Editors), Riverbank Filtration Understanding Contaminant Biogeochemistry and Pathogen Removal. Kluwer, Dordrecht, pp. 17-41.
- Hölting, B., 1996. Hydrogeologie Einführung in die allgemeine und angewandte Hydrogeologie. Enke, Stuttgart, XIII, 441 S. pp.
- Hunt, B., 1990. An approximation for the bank storage effect. Water Resources Research, 26(11): 2769-2775.

- Jungwirth, M., 1998. River continuum and fish migration - going beyond the longitudinal river corridor in understanding ecological integrity. In: M. Jungwirth, S. Schmutz and S. Weiss (Editors), Fish migration and fish bypasses. Fishing News Book. Blackwell Science Ltd, pp. 19-32.
- Jungwirth, M., Muhar, S. and Schmutz, S., 1995. The Effects of Recreated Instream and Ecotone Structures on the Fish Fauna of an Epipotamal River. *Hydrobiologia*, 303(1-3): 195-206.
- Kanton Wallis, 2000. Dritte Rhonekorrektur. Synthesebericht - Juni 2000, Dienststelle für Strassen- und Flussbau Sion.
- Karaus, U., Guillong, H. and Tockner, K., submitted. The contribution of lateral habitats to aquatic- macroinvertebrate diversity along river corridors. *Biological conservation*.
- Kendall, C. and Caldwell, E.A., 1998. Fundamentals of Isotope Geochemistry. In: Elsevier (Editor), Isotope Tracers in Catchment Hydrology. Elsevier.
- Kendall, C. and Coplen, T.B., 2001. Distribution of oxygen-18 and deuterium in river waters across the United States. *Hydrological Processes*, 15(7): 1363-1393.
- Klok, E.J., Jasper, K., Roelofsma, K.P., Gurtz, J. and Badoux, A., 2001. Distributed hydrological modelling of a heavily glaciated Alpine river basin. *Hydrological Sciences Journal-Journal Des Sciences Hydrologiques*, 46(4): 553-570.
- Labhart, T., 2001. *Geologie der Schweiz*. Ott Verlag, Thun.
- Lambelet, C., 1999. Synthese hydrogéologique de la région de Fully (VS). Modélisation 2D de l'écoulement souterrain Rhône- nappe en travers de cette zone. Diploma Thesis Université de Neuchâtel Thesis.
- Loizeau, J.L. and Dominik, J., 2000. Evolution of the Upper Rhone River discharge and suspended sediment load during the last 80 years and some implications for Lake Geneva. *Aquatic Sciences*, 62(1): 54-67.
- Margot, A., Sigg, R., Schädler, B. and Weingartner, R., 1992. Beeinflussung der Fliessgewässer durch Kraftwerke (>300kW) und Seeregulierungen. In: H.A.d. Schweiz (Editor), Tafel 5.3, Bern.
- Mariétan, I., 1953. *La lutte contre l'eau en Valais*. Griffon, Neuchatel, 22 pp.
- Martinec, J., Oeschger, H., Schotterer, U., Siegenthaler, U., 1982. Snowmelt and groundwater storage in an Alpine basin, *Hydrological Aspects of Alpine and High Mountains- Exeter Symposium*. IAHS.
- McCarthy, K.A., McFarland, W.D., Wilkinson, J.M. and White, L.D., 1992. The dynamic relationship between ground-water and the Columbia River - using deuterium and O-18 as tracers. *Journal of Hydrology*, 135(1-4): 1-12.
- Meier, W., Frey, M., Moosmann, L., Steinlin, S. and Wüest, A., 2004. Wassertemperaturen und Wärmehaushalt der Rhone und ihrer Seitenbäche, Report, EAWAG, WSL, Kastanienbaum.
- Meile, T., Schleiss, A. and Boillat, J.L., 2005. Entwicklung des Abflussregimes der Rhone seit dem Beginn des 20. Jahrhunderts. *Wasser, Energie, Luft*, 97(5/6): 133-142.
- Merlivat, L. and Jouzel, J., 1979. Global Climatic Interpretation of the Deuterium-Oxygen-18 Relationship for Precipitation. *Journal of Geophysical Research-Oceans and Atmospheres*, 84(NC8): 5029-5033.
- Micromass, 2003. *Isoprime EA User manual Issue 1*.
- Moog, O., 1993. Quantification of Daily Peak Hydropower Effects on Aquatic Fauna and Management to Minimize Environmental Impacts. *Regulated Rivers- Research & Management*, 8(1-2): 5-14.

- Naiman, R.J. et al., 1992. Fundamental elements of ecologically healthy watersheds in the Pacific Northwest coastal ecoregion. In: R.J. Naiman (Editor), *Watershed management: balancing sustainability and environmental change*. Springer, New York, pp. 127-187.
- Pearson, F.J. et al., 1991. *Applied Isotope Hydrogeology- a case study in northern Switzerland*. Technical Report 88-01.
- Peter, A., Kienast, F. and Woolsey, S., 2005. River rehabilitation in Switzerland: scope, challenges and research. *Large Rivers Vol. 15, No. 1-4. Arch. Hydrobiol. Suppl.* 155/1-4:643-656.
- Portmann, M., 2003. *Das Stromnetz im liberalisierten Strommarkt*, Institut für elektrische Energieübertragung und Hochspannungstechnik (ETH Zürich).
- Regli, C., Guldenfels, L. and Huggenberger, P., 2004. Revitalisierung von Fliessgewässern im Konflikt mit der Grundwassernutzung. *Gas-Wasser-Abwasser*, 4: 261-272.
- Regli, C., Rauber, M. and Huggenberger, P., 2003. Analysis of aquifer heterogeneity within a well capture zone, comparison of model data with field experiments: A case study from the river Wiese, Switzerland. *Aquatic Sciences*, 65(2): 111-128.
- Rodhe, A., 1998. Snowmelt dominated systems. In: C. Kendall and J.J. McDonnell (Editors), *Isotope tracers in catchment hydrology*. Elsevier, Amsterdam, pp. 839 S.
- Rozanski, K., Froehlich, K., Mook, W.G. and Stichler, W., 2001. *Surface Waters*. NAPC Hydrology Section.
- Schaelchli, U., 1992. The clogging of coarse gravel river beds by fine sediment. *Hydrobiologia*, 235: 189-197.
- Schaelchli, U., 1993. *Die Kolmation von Fliessgewässersohlen Prozesse und Berechnungsgrundlagen*, Report, Zürich, 274 S. pp.
- Schaelchli, U., 2002. *Kolmation- Methoden zur Erkennung und Bewertung*, Schälchli, Abegg+Hunzinger.
- Schiemer, F. and Zalewski, M., 1992. The importance of riparian ecotones for diversity and productivity of riverine fish communities. *Netherland Journal of Zoology*, 42(2-3): 323-335.
- Schmidli, J., Schmutz, C., Frei, C., Wanner, H. and Schar, C., 2002. Mesoscale precipitation variability in the region of the European Alps during the 20th century. *International Journal of Climatology*, 22(9): 1049-1074.
- Schotterer, U. et al., 2000. *Das Schweizer Isotopenmessnetz*. *Gas-Wasser-Abwasser*, 80(10): 3-11.
- Schuerch, M. and Vuataz, F., 2000a. Natural Tracers to quantify seasonal variations of groundwater mixing in a complex alluvial aquifer (Pfywald, Switzerland), *TraM'2000*, Liège Belgium.
- Schuerch, M. and Vuataz, F.D., 2000b. Groundwater components in the alluvial aquifer of the alpine phone River valley, Bois de Finges area, Wallis Canton, Switzerland. *Hydrogeology Journal*, 8(5): 549-563.
- Shankman, D. and Smith, L.J., 2004. Stream channelization and swamp formation in the US Coastal Plain. *Physical Geography*, 25(1): 22-38.
- Sheets, R.A., Darner, R.A. and Whitteberry, B.L., 2002. Lag times of bank filtration at a well field, Cincinnati, Ohio, USA. *Journal of Hydrology*, 266(3-4): 162-174.
- Siegenthaler, U., Oeschger, H., 1980. Correlation of $\delta^{18}\text{O}$ in precipitation with temperature and altitude. *Nature*, 285.

- Silliman, S.E. and Booth, D.F., 1993. Analysis of time-series measurements of sediment temperature for identification of gaining vs losing portions of Juday-Creek, Indiana. *Journal of Hydrology*, 146(1-4): 131-148.
- Stanford, J.A. et al., 1996. A general protocol for restoration of regulated rivers. *Regulated Rivers-Research & Management*, 12(4-5): 391-413.
- Stichler, W., Maloszewski, P. and Moser, H., 1986. Modeling of river water infiltration using O-18 data. *Journal of Hydrology*, 83(3-4): 355-365.
- Stuyfzand, P.J., 1989. Hydrology and water-quality aspects of Rhine bank groundwater in the Netherlands. *Journal of Hydrology*, 106(3-4): 341-363.
- Taylor, S., Feng, X., Williams, M. and McNamara, J., 2002. How isotopic fractionation of snowmelt affects hydrograph separation, 59th Eastern Snow Conference, Stowe, Vermont USA, pp. 285-293.
- Tockner, K., Karaus, U., Paetzold, A. and Blaser, S., 2004. Ökologischer Zustand der Rhone: benthische Evertebraten und Uferfauna. *Wasser Energie Luft*, 96(11/12): 315-317.
- Truffer, B. et al., 2003. Green Hydropower: The contribution of aquatic science research to the promotion of sustainable electricity. *Aquatic Sciences*, 65(2): 99-110.
- Truffer, B., Markard, J., Bratrach, C. and Wehrli, B., 2001. Green electricity from Alpine hydropower plants. *Mountain Research and Development*, 21(1): 19-24.
- Utrecht, E., 1906. Die Ablation der Rhone in ihrem Walliser Einzugsgebiete im Jahre 1904/05, Report, Bern, 66 S. pp.
- Vannote, R.L., Minshall, G.W., Cummins, K.W., Sedell, J.R. and Cushing, C.E., 1980. River Continuum Concept. *Canadian Journal of Fisheries and Aquatic Sciences*, 37(1): 130-137.
- Vorosmarty, C.J. et al., 1997. The storage and aging of continental runoff in large reservoir systems of the world. *Ambio*, 26(4): 210-219.
- Walther, A., 2002. Comparison of the groundwater fauna of two contrasting reaches of the Upper Rhone River. Diploma Thesis Thesis, EAWAG/ ETHZ, Kastanienbaum.
- Ward, J.V., 1989. The 4-dimensional nature of lotic ecosystems. *Journal of the North American Benthological Society*, 8(1): 2-8.
- Weber, C. and Peter, A., in preparation. Where have all the fishes gone? Deficit analysis in a degraded river.
- Werner, R.A. and Brand, W.A., 2001. Referencing strategies and techniques in stable isotope ratio analysis. *Rapid Communications in Mass Spectrometry*, 15(7): 501-519.
- Wett, B., Jarosch, H. and Ingerle, K., 2002. Flood induced infiltration affecting a bank filtrate well at the River Enns, Austria. *Journal of Hydrology*, 266(3-4): 222-234.
- Whiting, P.J., 2002. Streamflow necessary for environmental maintenance. *Annual Review of Earth and Planetary Sciences*, 30: 181-206.
- Willi, H.P., 2001. Synergism between flood protection and stream ecology. *EAWAG news*, 51e: 26-28.
- Wueest, A., 2002. Alpine hydroelectric power plants and their "long-range effects" on downstream waters. *EAWAG news*, 55e: 18-20.
- Yehdegho, B., Rozanski, K., Zojer, H. and Stichler, W., 1997. Interaction of dredging lakes with the adjacent groundwater field: An isotope study. *Journal of Hydrology*, 192(1-4): 247-270.

C Curriculum Vitae

Markus W. Fette

Born 12th of September 1973 in Stuttgart, Germany

Education

2001 – 2005	Ph.D. Thesis in the Department of Environmental Sciences, Swiss Federal Institute of Technology (ETH) Zürich, and in the Department of Surface Water, Swiss Federal Institute for Environmental Science and Technology (EAWAG) in Kastanienbaum/ Luzern.
1994 – 2000	Study of Environmental Engineering at the University of Stuttgart (Germany).

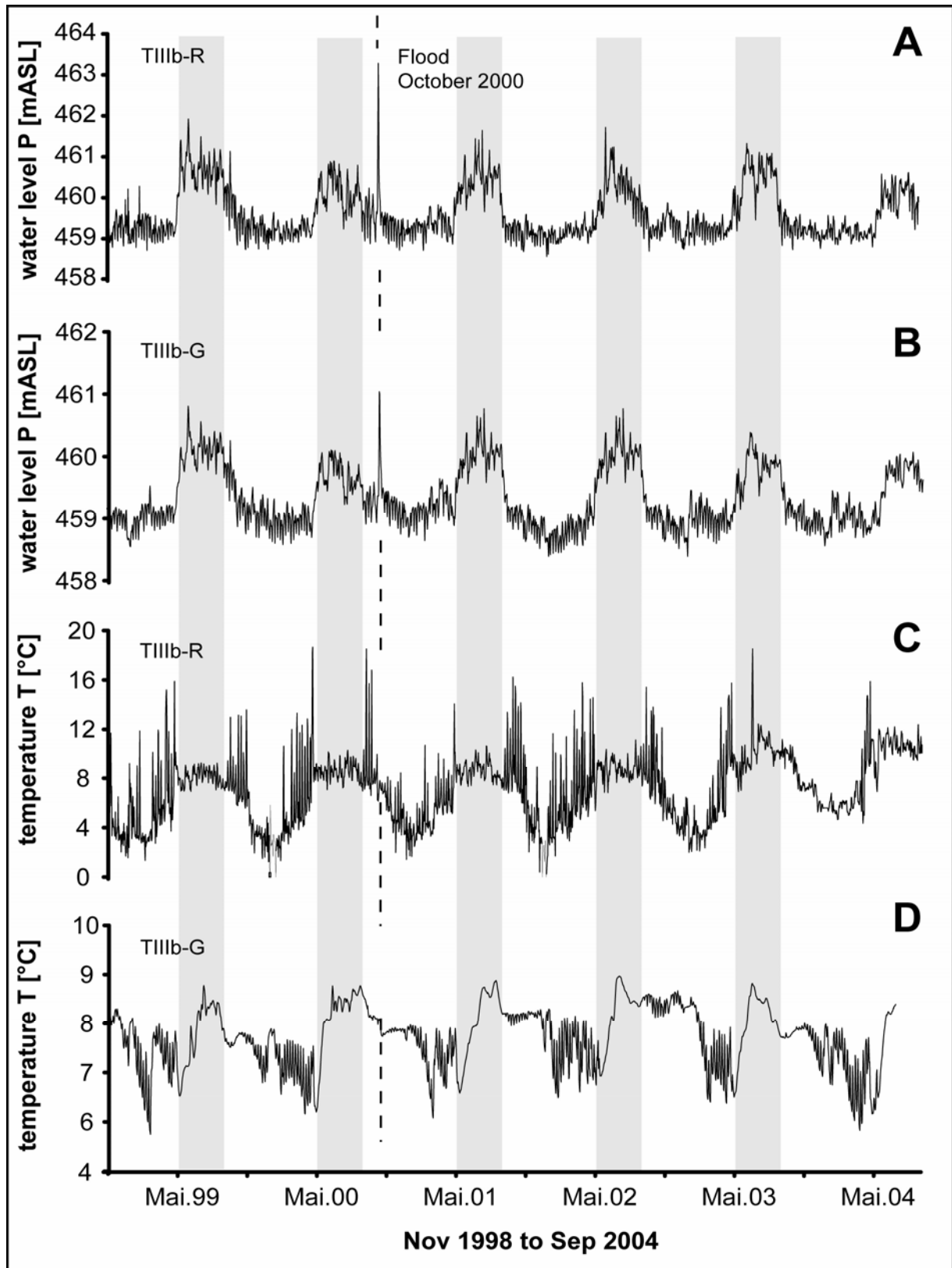
Work Experience

1999 – 2000	Assistant, Centre for Water Research (CWR), University of Western Australia (Perth/ Australia)
1998 – 1999	Assistant, Research Facility for Subsurface Remediation (VEGAS) , University of Stuttgart (Stuttgart, Germany)
1998	Intern, Environmental Protection Authority (SCPE) in Neuchâtel (Neuchâtel, Switzerland)
1997 – 1998	Intern, wastewater treatment plant CERS in Montréal (Québec/ Canada)
1996	Internship in the environmental section of the Airport Frankfurt/ Main (Frankfort, Germany)

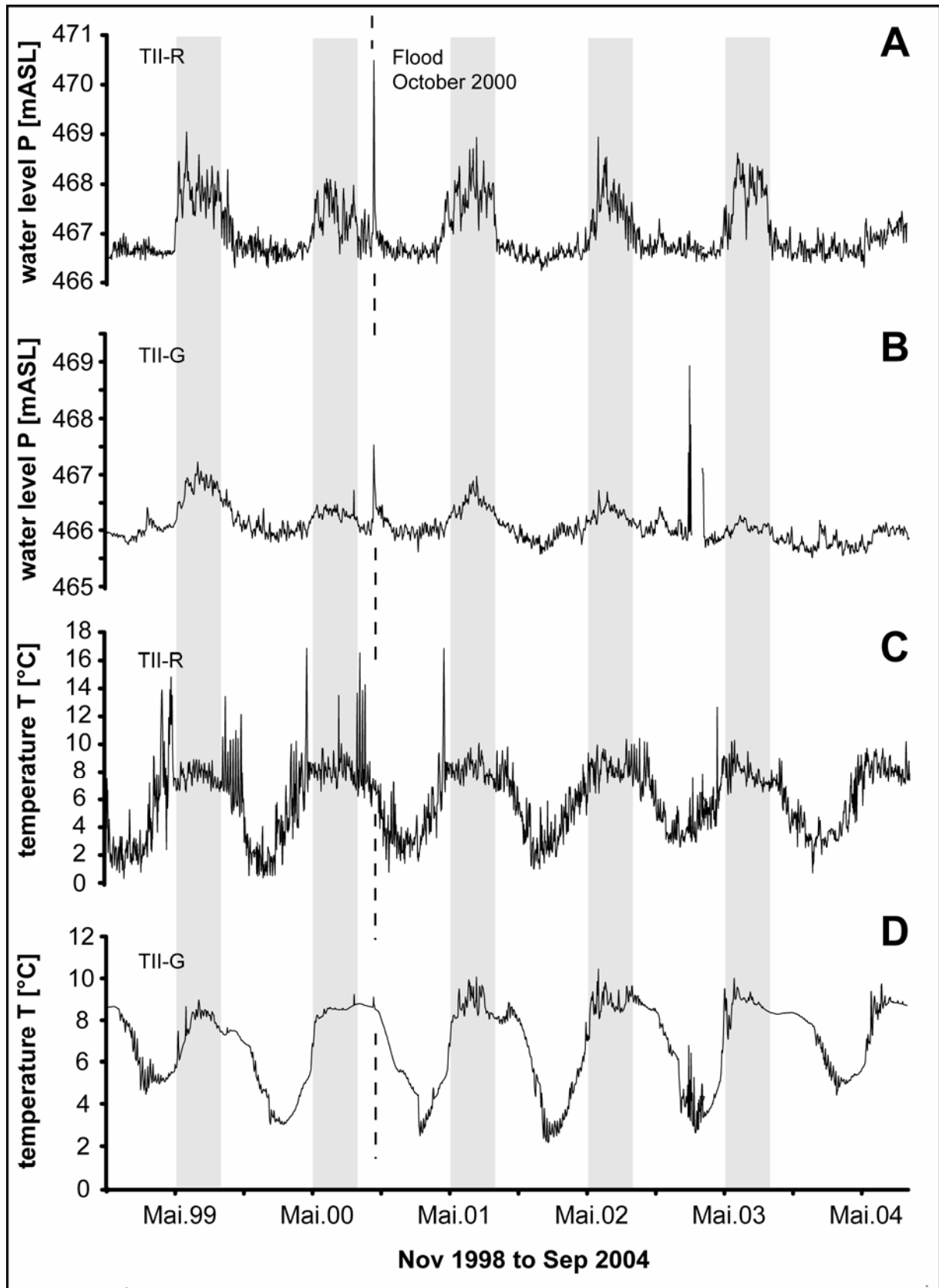
A Annexes

	Summer 5 th to 6 th July 2001			Winter 9 th to 11 th Dec. 2001		
	Flow [m ³ s ⁻¹]	c(SO ₄ ²⁻) [mM]	Flux [moles s ⁻¹]	Flow [m ³ s ⁻¹]	c(SO ₄ ²⁻) [mM]	Flux [moles s ⁻¹]
Rhone						
Sion	301.3	0.21	64.0	39.9	1.1	41.0
Branson	330.9	0.26	84.7	69.6	0.9	52.0
Tributaries						
Printse	--	--	--	0.24	1.30	0.3
Morge	--	--	--	0.14	0.46	0.07
Lizerne	--	--	--	0.14	1.72	0.23
Fare	--	--	--	0.25	3.25	0.81
Losentse	--	--	--	0.04	0.92	0.04
Salentse	--	--	--	0.03	0.82	0.03
Drainage						
Grand Canal	--	--	--	0.81	2.31	1.88
Hydropower						
Grande Dixence	--	--	--	15.7	0.08	1.32
Mauvoisin	--	--	--	9.9	0.07	0.71

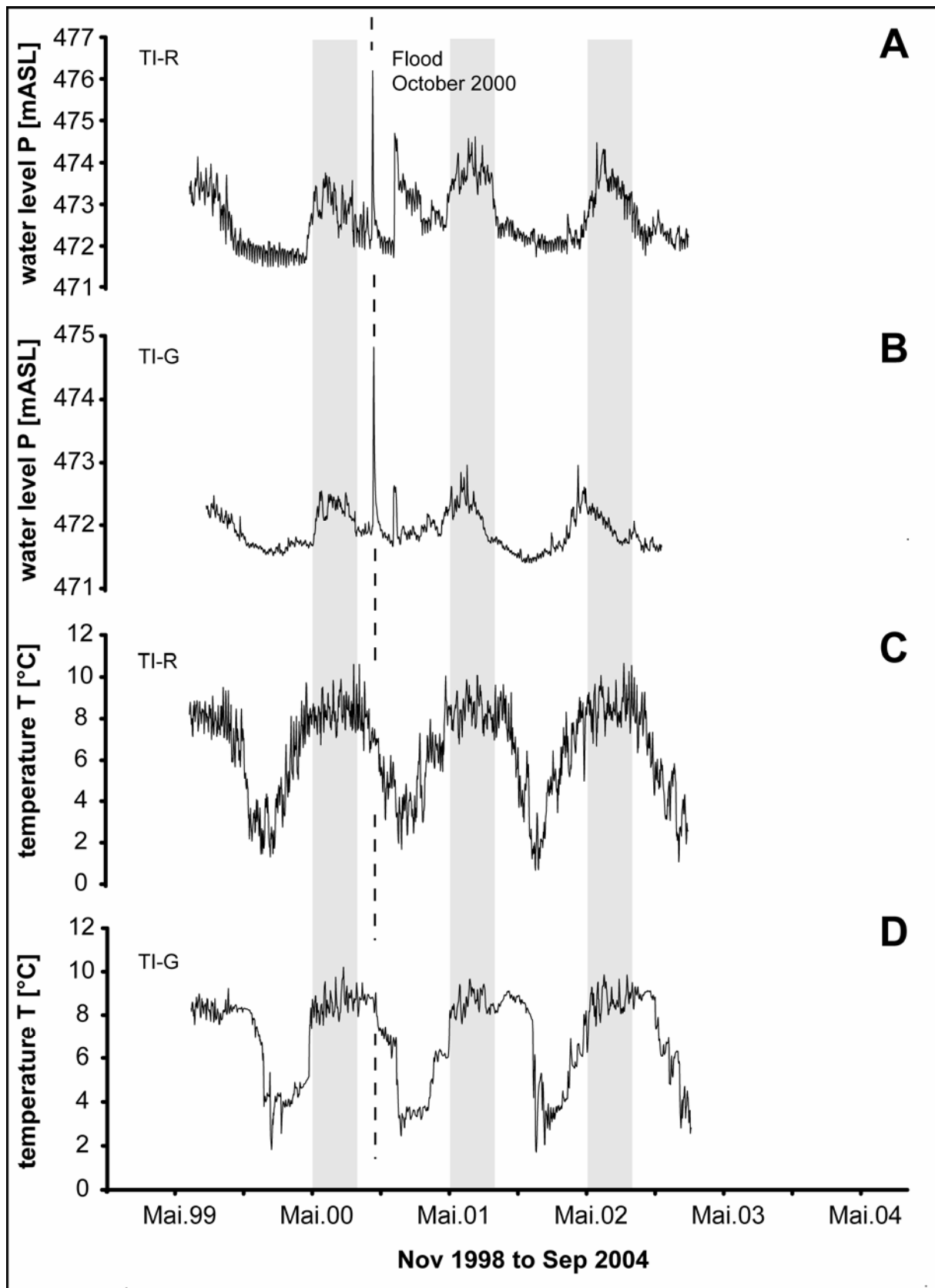
Annexe 1: Source data for the calculation of sulphate flux in the Rhone River and the tributaries. Samples were taken in ~3 hour intervals during 24 hours in summer (5th-7th July 2001) and in ~6 hour intervals during 42 hours in winter (9th -11th December 2001). In summer, only the location Sion and Branson were measured. The results given in the table are averaged values over the whole sampling period. Attention: the indicated flux in the table is not equal to the product of the average discharge times the average sulphate concentration listed in the table. This is due to the fact that the product of averages is unequal to the average of products of the single measurements.



Annexe 2: Time series of daily averaged levels and temperatures in TIIIb-R and TIIIb-G between October 1998 and September 2004. The graphs are almost identical to Figure 15. Due to low water levels in the river during winter time, the loggers in the Rhone River regularly measured air temperature instead of water temperature. For that reason, only the data set during the high water period from May to August (grey boxes) of each transect could be used for calculations (see text for further explanation).



Annexe 3: Time series of daily averaged levels and temperatures in TII-R and TII-G between October 1998 and September 2004. Due to low water levels in the river during winter time, the loggers in the Rhone River regularly measured air temperature instead of water temperature. For that reason, only the data set during the high water period from May to August (grey boxes) of each transect could be used for calculations (see text for further explanation).



Annexe 4: Time series of daily averaged levels and temperatures in TI-R and TI-G between June 1999 and September 2003. Due to low water levels in the river during winter time, the loggers in the Rhone River regularly measured air temperature instead of water temperature. For that reason, only the data set during the high water period from May to August (grey boxes) of each transect could be used for calculations (see text for further explanation).

